NASA TECHNICAL NOTE

NASA TN D-3181

NASA TN D-3181

MANNED MARS LANDING MISSION BY MEANS OF HIGH-THRUST ROCKETS

by Roger W. Luidens, Richard R. Burley, Joseph D. Eisenberg, Jay M. Kappraff, Brent A. Miller, Michael D. Shovlin, and Edward A. Willis, Jr.

Lewis Research Center
Cleveland, Ohio

NATIONAL AERONAUTICS AND SPACE ADMINISTRATION • WASHINGTON, D. C. • JANUARY 1966

NASA TN D-3181

MANNED MARS LANDING MISSION BY MEANS OF HIGH-THRUST ROCKETS

By Roger W. Luidens, Richard R. Burley, Joseph D. Eisenberg,
Jay M. Kappraff, Brent A. Miller, Michael D. Shovlin,
and Edward A. Willis, Jr.

Lewis Research Center
Cleveland, Ohio

NATIONAL AERONAUTICS AND SPACE ADMINISTRATION

For sale by the Clearinghouse for Federal Scientific and Technical Information
Springfield, Virginia 22151 – Price $4.00

CONTENTS

	Page
SUMMARY	1
INTRODUCTION	2
INPUTS TO THE ANALYSIS	3
Mission Payloads	5
Real payloads	7
Earth return mission payloads	7
Mars exploration weights	11
Mission Propulsion Systems	14
Propellant and tankage	14
Thrustor performance	15
Space vehicle staging	15
Guidance and control	16
Mission Trajectories	16
INITIAL WEIGHT IN EARTH ORBIT	30
Operations at Earth Return	31
Atmospheric braking	31
Choice of deceleration propulsion system	33
Variation of effect of atmospheric entry velocity with mission duration	35
Effect of Mission Duration on Initial Weight in Earth Orbit	36
Radiation Shielding	38
Propellant for radiation shielding	39
Effect of allowable crew dose	41
Orbital Operations at Mars	44
Mars parking orbit	44
Mars takeoff profile	49
Possibility of attaining parallel eliptic parking orbital performance	50
Effect of mission duration on parking orbit effect	52
Comments on assumptions	53
Atmospheric Braking at Mars	53
Effect of parking orbit	54
Effect of structure plus heat protection weight	55
Effect of mission duration	55
Direct Landing on Mars	57
Other Propellant Sources	58
Propellant collection at Mars	58
Other propellant sources	58

Two-Phase Mission Profiles 59
Elliptical orbit pickup at Earth return 59
Hyperbolic rendezvous at Earth return 60
Hyperbolic rendezvous at Mars departure 63
Two-phase Earth departure 63
Perturbed Trajectories 64
Perihelion propulsion 65
Propulsion at Mercury 69
Venus swingby 69
Lunar swingby 72
Other Mission Profiles 73
Two option stay time 73
Phobos or Diemos landing 73
Convoy mode 74
Chemical Space Propulsion 74
Aborts 76
Sensitivity of Initial Weight in Earth Orbit to Inputs 80
Effect of mission payloads 81
Effect of propulsion system performance 83
CONCLUDING REMARKS 87
Technical Areas for Research 88
Criteria for Selecting a Mission Profile 88
Earth surface to orbit launch weight 88
Advanced development 88
Compatibility with overall space program 88
Data acquired 88
Timing 88
Crew safety 88
Probability of mission success 88
Suggested Mission Profile 88
APPENDIXES
A - SYMBOLS 91
B - BIOLOGICAL SHIELDING 93
Radiation Sources 93
Shield Characteristics 95
Allowable Dose 96
Shield Weights 97
C - MARS LANDING AND TAKEOFF MANEUVERS 98
REFERENCES 100

MANNED MARS LANDING MISSION BY MEANS OF HIGH-THRUST ROCKETS

by Roger W. Luidens, Richard R. Burley, Joseph D. Eisenberg, Jay M. Kappraff, Brent A. Miller, Michael D. Shovlin, and Edward A. Willis, Jr.

Lewis Research Center

SUMMARY

An examination of a wide variety of Mars manned landing missions with 1- to 3-year durations that use high-thrust nuclear and chemical propulsion for the 1979-80 synodic period gave the following principal results.

The use of atmospheric braking for Earth return at velocities up to 52 000 fps is an effective way to reduce the initial weight in Earth orbit (IWIEO). Using the Earth deceleration propellant for space radiation shielding can reduce the IWIEO about 20 percent. Propulsive braking to a high circular or an elliptic parking orbit at Mars yields significantly lower weights than a low circular parking orbit. If the spaceship is parked in a high circular orbit, dispatching a tanker to a low circular orbit to refuel the takeoff vehicle gives lower weights than a single-stage takeoff mode of operation. Atmospheric braking to an elliptic parking orbit at Mars yields additional weight reductions. A direct landing of the entire spaceship on the Mars surface by means of atmospheric braking gives very large weights unless a source of propellant is available on the Mars surface.

Propulsive deceleration of a small capsule containing the crew and data to an elliptic orbit at Earth return can yield an IWIEO competitive with atmospheric braking from a 52 000 fps velocity. Hyperbolic rendezvous of the Earth deceleration system at Mars departure reduces both the passenger phase and the total IWIEO.

In 1980 a Mars round trip using a Venus swingby, propulsive braking at Mars, and atmospheric braking at Earth yields about the same weight for a 37 000 fps entry velocity as an unperturbed profile (one not using a Venus swingby) with a 52 000 fps entry velocity. The Venus swingby with atmospheric braking at Mars and Earth yields the lowest weight of any system considered. Trip durations of about 950 days yield stay times of 450 days for weights comparable with those for the 400- to 500-day trips with a 40-day stay.

The IWIEO is sensitive to the input assumptions. The accumulated effect of reducing the propulsion system performance (i.e., specific impulse, engine weight, and tank fraction) can double the IWIEO. Doubling mission payloads would also approximately double the IWIEO. Chemical space propulsion for the Mars mission can yield an IWIEO that may be acceptable for the mission profiles which use elliptic parking orbits or atmospheric braking at Mars and atmospheric braking or elliptical orbit pickup at Earth return.

INTRODUCTION

After the successful exploration of the Moon, a subsequent major step in man's conquest of space will be the exploration of the nearby planets of Mars and Venus. The manned Mars landing mission is perhaps a decade or two in the future. In view of the great difficulty of this mission, it is appropriate to examine many possible approaches to the mission with the general objective of finding those that are feasible and advantageous and to indicate necessary and fruitful areas for research.

Some early detailed studies of fast Mars and Venus missions are reported in references 1 and 2. One of the first studies to report the influence of solar-flare shielding and atmospheric braking at Earth and Mars on the landing mission was reference 3. More recently the NASA EMPIRE contracts have resulted in reports on manned flyby and stopover missions (refs. 4 to 6). These studies were made for the most part for the time period of the early 1970's because this period appears to be the most favorable in terms of energy requirements.

A second round of mission studies was made for the more difficult 1975 to 1985 time period (refs. 7 to 13), and more detailed studies were made of some phases of the mission (refs. 14 and 15). Although each investigator studied some variations in mission profile, a comprehensive comparison of mission profiles was not made; also, while different contractors considered different mission profiles, their basic inputs were not always consistent.

This report presents an analysis of a broad range of alternative mission profiles that use internally consistent inputs. The present study was made for 1980, one of the more difficult years. If reasonable solutions to the mission problems existing in that year can be found, then the mission can be accomplished in the easier years with, for example, increased payloads.

Information in many technical areas is required to make a mission study. The available information was reviewed, and many problems were restudied or the existing analyses extended. Some of the areas investigated were the following: corpuscular radiation shielding, atmospheric entry, structures, solar-flare protection, chemical and nuclear engines, trajectories, and life-support systems. In the course of this study, the interactions between various subsystems were examined to assess the associated weight penalties or gains and particularly to find those that can be made to serve multiple purposes.

Mars manned landing missions of 1 to 3 years in duration that use high-thrust nuclear and chemical propulsion are discussed. Some of the more important mission profile elements evaluated are the following: atmospheric braking at Earth and Mars, elliptic orbits at Mars, two-phase and direct landing missions, perihelion propulsion, and Venus swingby trajectories. The criteria of merit used are the stay time at Mars, the initial

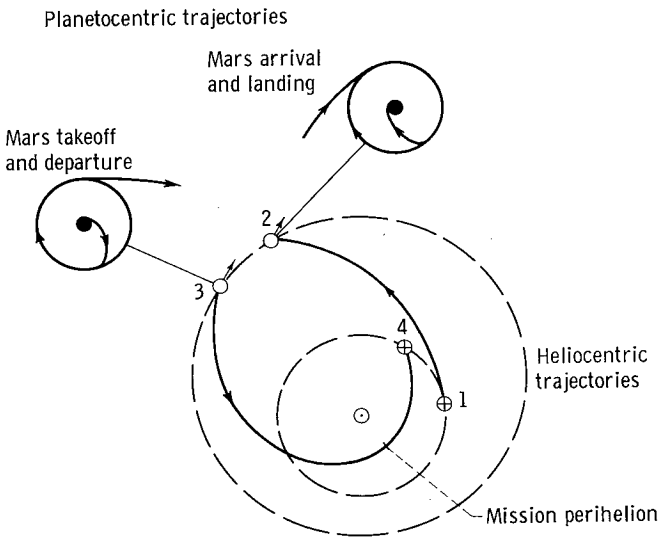

Figure 1. - Typical mission profile for Mars manned landing.

weight in Earth orbit, and the time the crew is absent from Earth. While some of the effects of total trip time, such as the variation of life-support system weight, are accounted for in the initial weight, other factors, such as reliability and psychological effects on the crew, have not been quantitatively evaluated.

INPUTS TO THE ANALYSES

The primary objective of this report is to examine and compare a number of mission profiles for landing men on Mars and returning them safely to Earth. The term mission profile here refers to trajectories and techniques employed to deliver the mission payloads to the required places in the mission. A manned Mars landing can be accomplished by any of several mission profiles. A typical profile is shown in figure 1. The mission begins with the vehicle system in a low orbit about Earth (point 1). On an appropriate launch date, the vehicle and crew are accelerated by high-thrust propulsion onto an Earth-Mars transfer trajectory. At Mars (point 2) the vehicle is decelerated into a parking orbit. The vehicle stays at Mars 40 days, during which time part of the crew descends to the Martian surface. Upon their return to the mother vehicle, it is accelerated (point 3) onto a Mars-Earth transfer trajectory. The vehicle is finally decelerated at Earth (point 4).

One of the criteria used to evaluate the various mission profiles is the initial weight in Earth orbit (IWIEO). This weight depends, in addition to the general mission profile, primarily on three inputs to the weight estimation:

(1) Mission payloads, fixed weights delivered to various points in the mission profiles

(2) Mission propulsion systems, that is, the engine and propellant systems

(3) Mission trajectories, which determine the required propulsive velocity increments and may affect some of the mission payloads

In the following sections the concepts and numerical values used for each of the three inputs are described. The values presented are based on detailed studies which for the sake of brevity are not presented here. As a test of the reasonableness of the numbers, the reader may compare the present values with those of other investigators (refs. 7 to 15) as presented in table I. The lack of a consistent and precise definition of terms by the various authors precludes accurate comparisons. In general, the present analysis values appear to be within the range of values estimated by others. Also, the effect of

TABLE I. - COMPARISON OF INPUTS FOR PRESENT ANALYSIS WITH THOSE OF OTHER ANALYSES

Input	Present analysis	Contractor					
		Douglas	General Dynamics Astronautics	General Dynamics Fort Worth	General Electric	Lockheed	Philco (Ford)
		Reference source					
		7	8	9	11	12, 14	15
Crew size	7	6	8	6	4	3	------
Mission duration, days	500	460	500	500	450	600	------
Command module (storm shelter) weight, lb:							
Structure	4 500	------	-------	------	1 000	------	------
Astrionics	3 500	------	-------	[a]1 000	2 650	------	------
External equipment	1 000	------	-------	------	------	------	------
Shielding	15 000 (typical)	------	11 800	17 550	------	------	------
Total	24 000	------	-------	------	10 500	13 300	------
Living module (service module) weight, lb:							
Structure	5 700	------	-------	------	4 400	------	------
Centrifuge	700	760	-------	------	------	------	------
Internal equipment	2 600	------	-------	------	800	------	------
Radiation shielding	7 900	------	-------	------	------	------	------
Total	16 900	------	-------	------	6 000	6 460	------
Combined command and living module (excludes life-support consumables) weight, lb:							
Without radiation shield	18 000	20 900	[b]26 200	18 950	------	------	------
With radiation shield	40 900	------	38 000	------	18 500	19 760	------
Life-support system (food, water, air) weight, lb	26 000	15 000	41 500	22 800	11 500	15 200	------
Earth entry vehicle weight, lb:							
37 000 to 40 000 fps	11 000	13 030	9 400	------	------	------	------
52 000 fps or greater	13 850	[b]28 230	-------	12 800	------	13 800 (6 men; 65 000 fps)	--------

[a]Communications.
[b]Maximum value.

TABLE I. - Concluded. COMPARISON OF INPUTS FOR PRESENT ANALYSIS WITH THOSE OF OTHER ANALYSES

Input	Present analysis	Contractor					
		Douglas	General Dynamics Astonautics	General Dynamics Fort Worth	General Electric	Lockheed	Philco (Ford)
		Reference source					
		7	8	9	11	12, 14	15
Power supply	3 000	[b]24 000	5 000	5 400	6 000	1 490	-------
Mars excursion module:							
Landed crew	4	------	------	3	2	-----	3
Crew capsule	------	------	------	------	------	-----	------
Landed equipment	------	------	------	------	------	-----	------
Initial weight in Mars orbit, lb	76 000	55 000	------	70 000	36 250	-----	58 070
Mars orbital weight, lb	6 500	------	------	------	------	-----	------
Tank fraction	0. 125	------	------	0. 075	0. 18	-----	------
Nuclear engine:							
Specific impulse, sec	850	850	------	------	------	-----	------
Engine thrust to engine weight ratio:							
Unshielded	10	15	------	------	------	-----	------
With thermal shield	8	------	------	------	------	-----	------
With biological and thermal shield	3	------	------	------	------	-----	------
Assumed minimum weights, lb:	16 000; 8 000	14 300	------	------	------	-----	------
Chemical engine:							
Specific impulse, sec (BeH_2/H_2O_2)	430	480	------	------	------	-----	------
Engine thrust to engine weight ratio	67	75	------	------	------	-----	------
Specific impulse, sec (H_2/F_2)	460	------	------	------	------	-----	------

[a]Communications.
[b]Maximum value.

changing the present input values is shown in the Sensitivity of Initial Weight in Earth Orbit to Inputs section (p. 80).

Mission Payloads

The mission payloads fall into two general categories:

TABLE II. - EARTH RETURN MISSION PAYLOADS

Item	Weight, lb
Command module (exclusive of radiation shielding)	9 000
Living module and centrifuge (exclusive of radiation and meteoroid protection	9 000
Earth deceleration system (includes 37 000 lb of chemical propellant that serves also as radiation and meteoroid shielding for the command and living modules)	54 000
Life-support system (fixed part only)	3 500
Space-power-generation system	3 000
Attachments and miscellaneous	1 500
Total	80 000

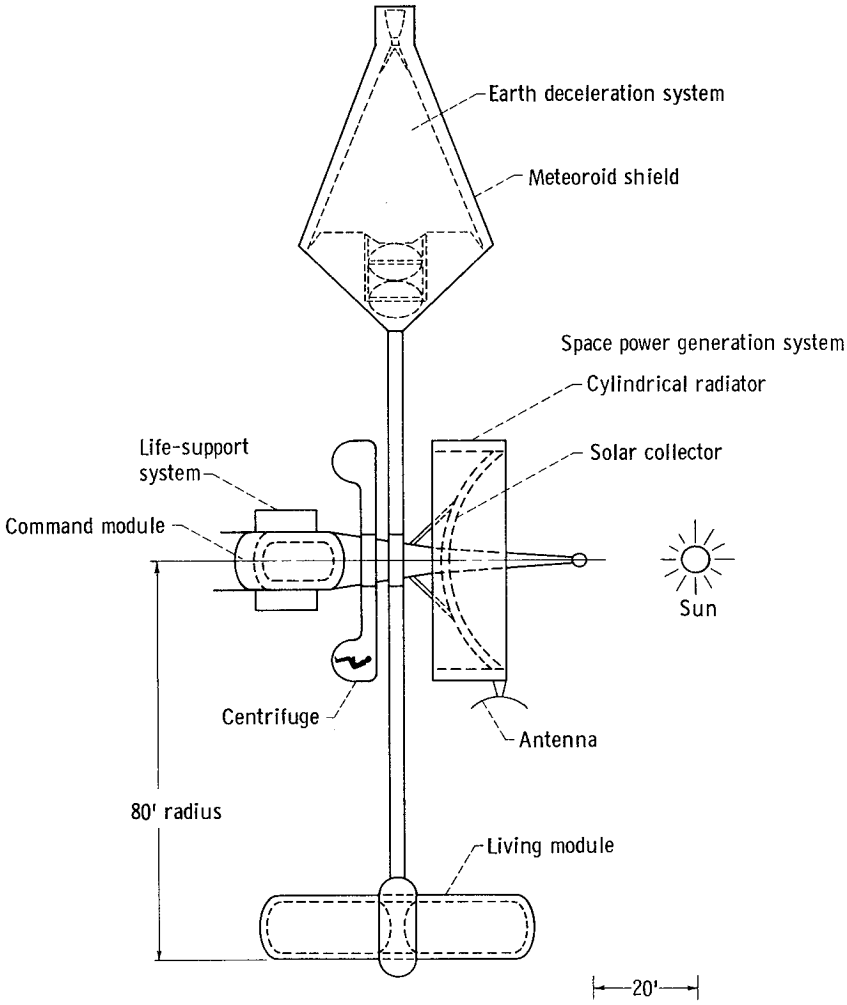

Figure 2. - Earth return mission payloads deployed for space flight.

(1) Those carried around the entire mission and returned to the vicinity of Earth

(2) Those carried to and left at Mars

The mission payloads, in turn, depend on the real payloads.

Real payloads. - The real payload of the mission is the crew and the samples and data acquired during the trip. The total crew consists of seven men of which either four or all seven make the excursion to the Mars surface. These numbers were selected based on the following general consideration. The primary purpose of the mission is the manned exploration of the Martian surface; hence, a large fraction of the men carried to Mars should land on the surface. The success of the mission should not depend on one man operating alone; hence, the smallest grouping is pairs. One of the more hazardous phases of the trip is the landing and takeoff from Mars. For the fast trips four men (in pairs) make the excursion to the surface in two vehicles, each of which is capable of returning the four explorers to the spaceship. Three crewmen are considered the minimum for emergency operation of the spaceship; this is required in the event the surface expedition is lost.

A minimum of six men is required for a normal duty cycle based on pairs of men operating one-third of the time on spaceship operational duty, one-third of the time sleeping, and one-third of the time in recreation, personal chores, and scientific duties and studies. The previous considerations lead to the selection of a seven-man crew, which is consistent with the size used by other investigators (table I). One thousand pounds of samples and the stored data are assumed to be acquired at Mars and during the trip, and this weight is also part of the real payload. The total real payload weight is about 2400 pounds. The purpose of the Mars spaceship is to carry these real payloads, which in turn determine the mission payloads that must be known to determine the initial weight in Earth orbit.

Earth return mission payloads - The fixed weights returned to the vicinity of Earth consist of the items listed in table II. The weights given are for a typical 420-day mission. The items of table II arranged for coasting interplanetary flight are shown in figure 2 and are now described.

Command module: The command module, which is shown in more detail in figure 3 serves two purposes. First of all, it is the control center for operation of the spaceship, and second, it is a shelter from high energy corpuscular radiation. The volume of the module is 450 cubic feet of which 50 cubic feet are occupied by radiation sensitive operating equipment. A crew of two or three occupies the command center during normal operation. All seven of the crew can be accommodated, with four men in the standing position, for the short periods (e. g., 1 day) when high energy radiation is expected. The major weight of this item is generally the radiation shielding surrounding the interior volume.

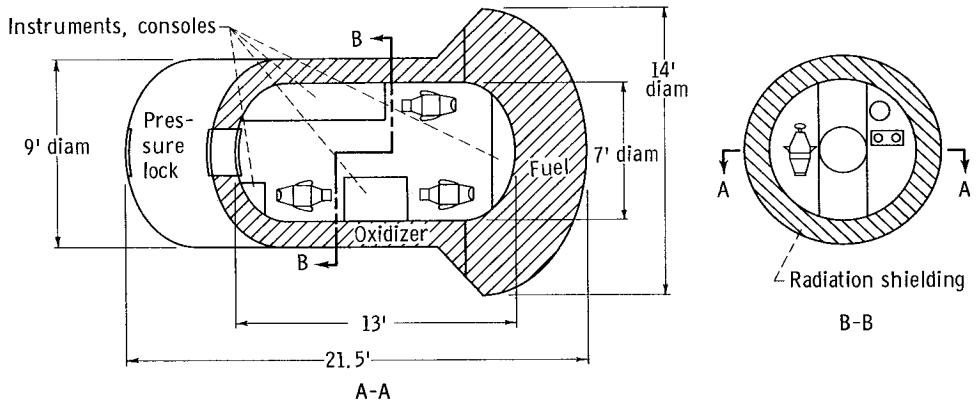

Figure 3. - Command module shown with chemical propellant radiation shielding.

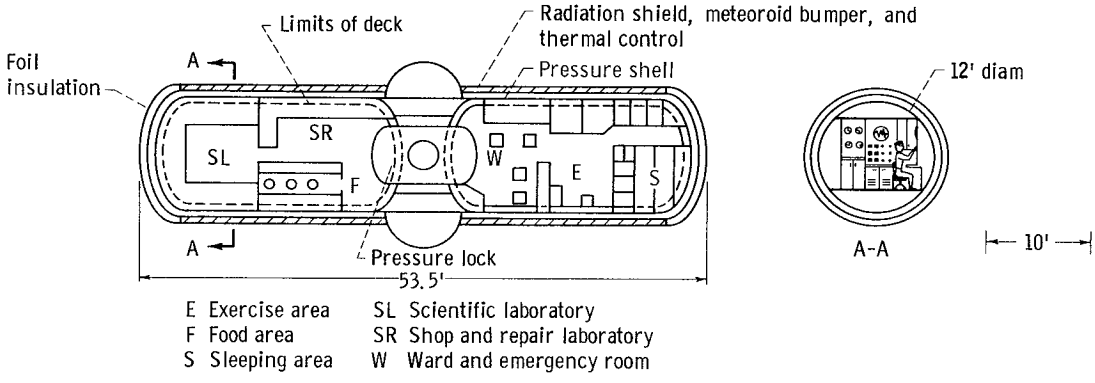

(a) Plan view.

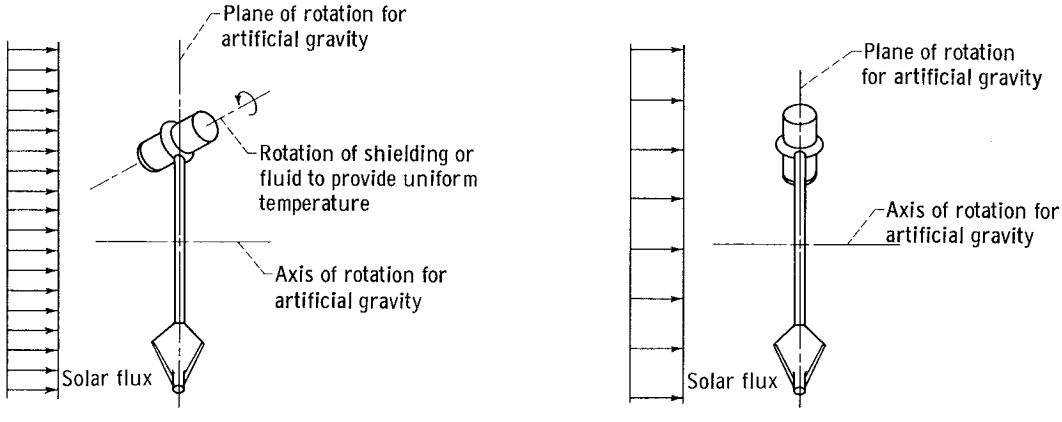

(b) Living module orientation at perihelion.

(c) Living module orientation at aphelion.

Figure 4. - Living module.

Living module: The living module should contain the normal living equipment for eating, sleeping and recreation, and laboratory and medical facilities. It should be designed to provide a liveable environment in terms of atmosphere, volume, gravity, temperature, and safety from meteoroid and radiation hazards. One conceptual design satisfying these requirements is shown in figure 4. The living module has a volume of 5500 cubic feet and an internal atmospheric pressure of 7 pounds per square inch absolute. It is connected to the Earth entry vehicle by a boom (see fig. 2). An artificial gravity of 0.3 g is provided by the rotation of the living module Earth entry vehicle system, with the Earth entry vehicle plus some retrorocket propellant serving as a counterweight. The angular momentum is balanced by a counter rotating centrifuge, which provides up to 10 g's to exercise the crew's G tolerance. The centrifuge mass may consist of men, retrorocket propellant, or life-support items. The combined systems are accelerated angularly by electric power or manpower and decelerated by a friction brake.

Protection from daily and weekly solar flares and meteoroids is provided by 6 pounds per square foot of mass in the outer shell. During the higher energy radiation of the monthly solar flares and class 3+ flares, the crew occupies the command module.

The Sun heats only one side of the outer shell of the living module. A uniform temperature is maintained by rotating the meteoroid shield around the vehicle or by circulating fluid in the outer shell. The circulating fluid functions as a radiation and meteoroid protection and is contained in multiple independent loops. A meteoroid puncture would require the patching and refilling of the damaged tubes. The desired level of temperature is maintained by adjusting the aspect of the module with respect to the Sun and by surface coatings. To improve reliability, the living module is divided into two pressure independent units. The full-duty cycle of the scientific crew members may be in this module.

Earth deceleration system: The Earth deceleration system (fig. 5) is also part of the weight that arrives in the vicinity of Earth. It consists, in general, of the Earth atmospheric entry vehicle and a retrorocket. The payload for the entry vehicle is the real mission payload (i.e., the crew, data, and samples) of 2400 pounds.

The Earth atmosphere entry vehicle weight varies from 11 000 to 16 500 pounds for atmospheric entry from 26 000 and 65 000 feet per second, respectively (refs. 16 and 17). As a matter of judgement, 52 000 fps was taken as the maximum atmospheric entry velocity, although higher entry speeds may be thermodynamically feasible (ref. 16). The vehicle has a lift-drag ratio of 1. It is sized to give 5.5 feet of unobstructed interior depth to accommodate the seated crewmen. The corresponding volume is 1400 cubic feet. The vehicle is shaped to minimize hot gas radiation. It has leading edges swept 60°, a small radius nose, and a maximum attack angle of 23° (refs. 16 and 18). The high convective heating rates at the nose might be accommodated by extruding ablation material or transpiration cooling. For a maximum G load of 10 g's the entry corridor depth is about 30 miles (ref. 18), which is adequate for the anticipated guidance capabilities

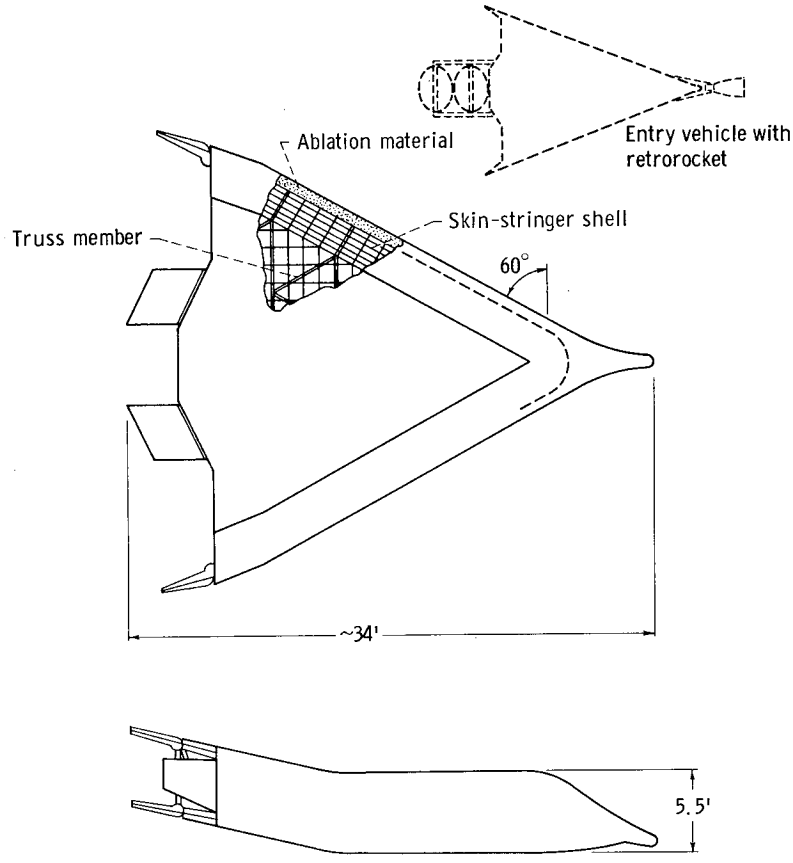

Figure 5. - Vehicle for Earth atmospheric entry from 52 000 fps.

(refs. 19 and 20).

The atmospheric flight path during the deceleration subsequent to the entry maneuver is characterized by a constant 8 G deceleration at supercircular speeds and 4 G at subcircular speeds. Downrange control is obtained by gliding up out of the atmosphere at circular velocity when increased range is required (ref. 21).

The Earth return retrorocket may vary from a substantial nuclear propulsion stage to a chemical stage to no stage at all, depending on the allowable atmospheric entry velocity and Earth approach velocity associated with each mission profile.

Life-support system: The life-support system selected for the interplanetary vehicle uses an open food and oxygen cycle but a closed water cycle (fig. 6). Food, water, and oxygen are consumed by crewmen at the rate of 2. 3, 4. 0, and 2. 1 pounds per man-day, respectively (ref. 22). In addition, 20 pounds per man-day of recycled water is allowed for utility purposes. Cabin air leakage is assumed to be 1. 5 pounds per day, and complete air changes are made at 3-month intervals. Potable water is recovered from the perspired and respired moisture in the atmosphere and by the vapor compression distillation of urine. The total life-support system requirements for seven men are 3500 pounds plus 45 pounds per day, plus 260 watts of power.

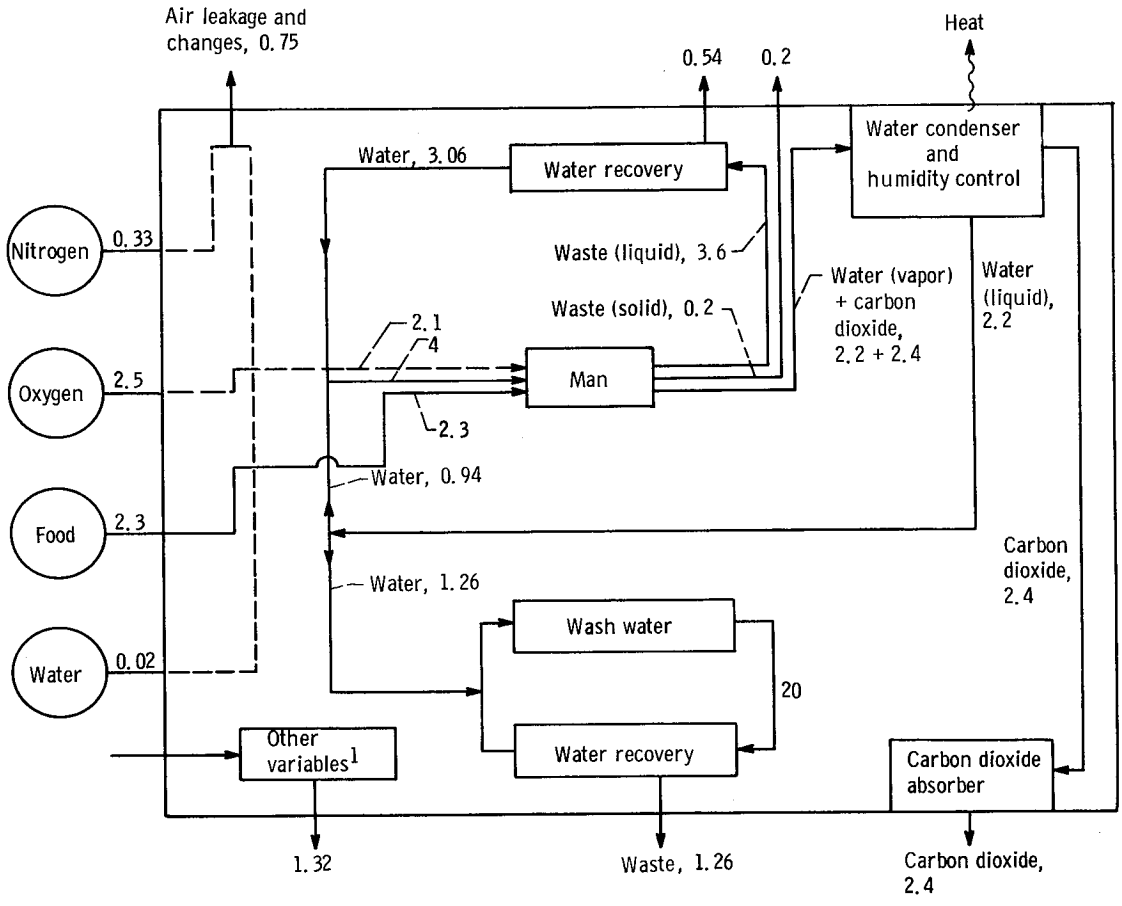

[1]Tankage, packing, bladders, sponges, and chemicals for water recovery system.

Figure 6. - Schematic of life-support system. (All weights in pounds per man per day.)

Space-power system: An estimated 7.5 kilowatts of power were required for the interplanetary vehicle. A solar Rankine system was selected to generate the power. This system was selected over a nuclear dynamic system to eliminate the radiation shield weight and dose associated with a nuclear system, and because the solar system offers a greater repair opportunity since its components are not radioactive. This system was estimated to weigh 200 pounds per kilowatt (ref. 23), and a spare unit was carried giving a total weight of 3000 pounds for the 7.5-kilowatt requirements. Solar cells are also a potentially lightweight and reliable power source.

Mars exploration weights. - In addition to the mission payload carried back to Earth (80 000 lb), there is a nearly equal weight carried to but left at Mars. This weight may be divided into the categories shown in table III. The typical lander weights shown are for a low circular parking orbit and a 40-day stay.

Orbital payloads: The total orbital payload weight is 6500 pounds for all mission profiles and provides for several functions:

(1) Landing probe to survey possible landing sites and to study sites not of sufficient

TABLE III. - MARS EXPLORATION WEIGHTS

Item	Weight, lb
Orbital payload	6 500
Manned landers (two-man landers)	60 000
Equipment landers with equipment (2)	14 000
Meteoroid protection, attachments, and miscellaneous	1 500
Total	82 000

interest to warrant manned landings

(2) Atmospheric static probes to check atmospheric composition, winds, and temperatures; dynamic probes to check heat protection performance and the characteristics of entry trajectories

(3) Space probes to monitor the magnetic and particulate radiation and the meteoroid fluxes in the vicinity of Mars and to serve as communication relays

(4) Probes to the moons of Mars

(5) Telescopic, infrared, ultraviolet, and radar systems for the study of the Mars surface and atmosphere from orbit

Manned landers: The weight required to land the men on the Mars surface and return them to the orbiting spaceship is the largest of the weights carried to and left at Mars. A major fraction of this weight is the propellant to boost the crew vehicle from the Mars surface to orbit. The weight of this system is hence sensitive to the propulsion system performance and to the mother ship parking orbit and takeoff trajectory profile, which are discussed in the Orbital Operations at Mars section. The landing from and takeoff to a low circular orbit to be described is typical of the landing operation (fig. 7).

The lander shown on the spaceship surrounded by meteoroid and space thermal protection in figure 7(a) corresponds to point A of the trajectory profile shown in figure 7(b). The lander is separated from the spaceship and the retrorocket is fired at point B to establish the atmospheric entry trajectory, which gives a 10° path angle at maximum G load (point D). Most of the landing vehicle velocity is absorbed by atmospheric braking (points C to F). This is possible even for Mars surface densities of one one-hundredth of the Earth's surface density. Heat protection during the atmospheric entry is provided by an ablation material (although radiation cooling is also possible). At point F the vehicle is at such a velocity and altitude that a 2 G deceleration by the retrorocket will bring it to rest just above the Mars surface. Two minutes of fuel is allowed for hover and translation to the planned landing site. The small landing impact is absorbed by shock absorbers (fig. 7(c)).

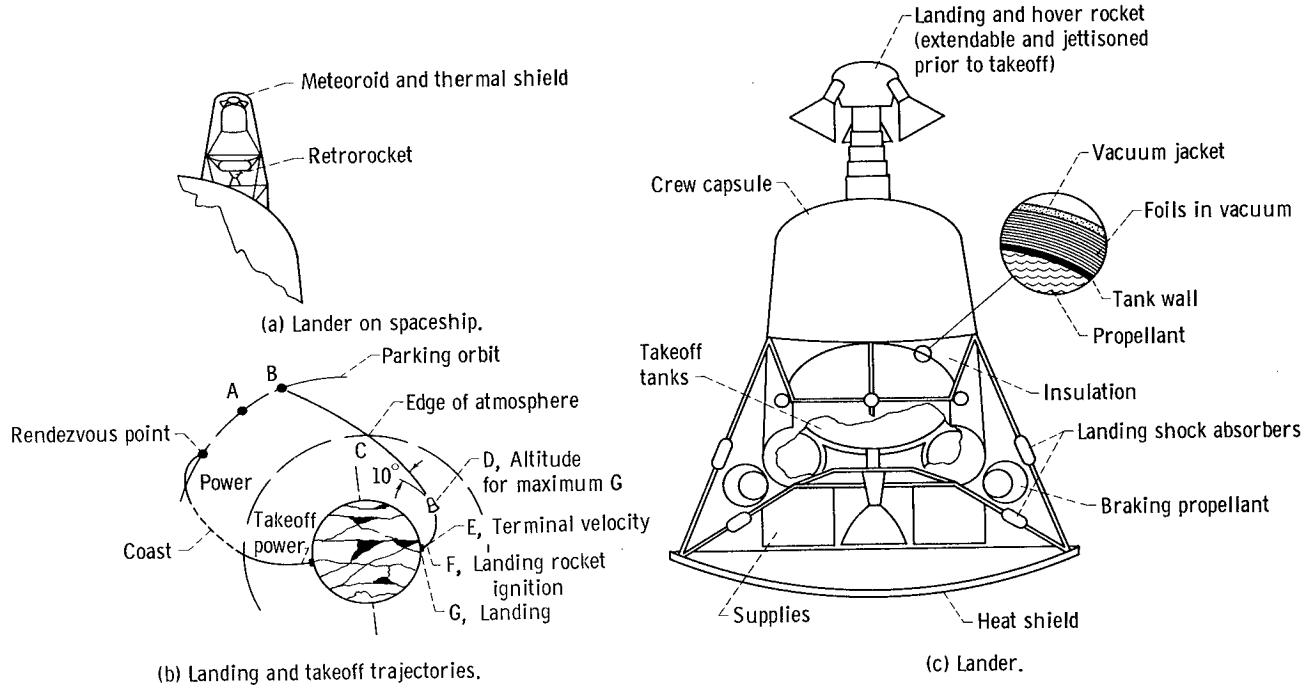

Figure 7. - Manned Mars landing and takeoff vehicle and trajectories.

During the stay on the surface the takeoff propellant is protected thermally by foils in a vacuum jacket around the tanks. Vacuum jacketing is feasible because of the low Mars atmospheric pressure. The crew life support and electrical power are provided by a completely open system for missions with a 40-day stay. For missions with a longer stay time, the life-support system is the same kind as that used for the spaceship.

Prior to takeoff, the lander is stripped or detached from all unnecessary weights, that is, tank insulation, landing and hover rocket systems, and heat shield and landing system. The boost to orbit is accomplished by a single-stage rocket operating along a minimum ΔV trajectory. After reaching orbit, two more brief propulsion periods result in a rendezvous with the spaceship.

The payload for the takeoff vehicle is the crew capsule, which weighs 3400 pounds and includes a crew of two and 500 pounds of samples and data. In the missions studied there are two two-man landers. In the event of a failure in one of the landers, the faultless vehicle can be arranged to accommodate four crewmen at the expense of the Mars samples.

For both nuclear and chemical space propulsion, a specific impulse of 430 seconds was assumed for the Mars takeoff propulsion system, which corresponds to a chemical combination such as $B_2H_6 + OF_2$.

Equipment lander: Most of the equipment is landed on separate vehicles. In the present analysis two equipment landers are used. The total landed equipment weight is 8000 pounds and may consist of a land roving vehicle and its propellant and scientific

equipment. The weight in orbit of the two landers is about 14 000 pounds. Because these vehicles do not return to orbit and only a small retrorocket is required for deorbit and landing, their weight is not very sensitive to the spaceship parking orbit or to the retrorocket propulsion system performance.

In some mission profiles it may be more convenient to combine the manned and equipment landers into a single vehicle. To a first approximation this will result in no change in the system weights.

Mission Propulsion Systems

In addition to the mission payloads, the initial weight in Earth orbit depends also on the mission propulsion system. The propulsion system in the broadest sense consists of the propellant and related tankage and structure and the thrustors and their associated weights. Both high-thrust nuclear and chemical propulsion systems are considered.

Propellant and tankage. - For the nuclear propulsion system hydrogen is the logical propellant choice. The quantity of hydrogen required is determined during the course of the calculation of the IWIEO. The weight of a number of propulsion system items is related to the propellant consumed by the engine. These items are the propellant tank shell which contains the internal pressure and transmits loads, the meteoroid and thermal protection, the boiloff, the tank pressurization system, and the outage. The weight of the tank and structure required to contain the propellant was estimated by considering a number of factors. The tankage was designed strong enough to contain an internal pressure of 10 psi and to allow boost from the Earth surface to Earth orbit with fully loaded tanks for a booster peak acceleration of 6.0 g's. The mission payloads are not supported by the spaceship tanks during boost. The tankage is also designed to sustain a space flight acceleration of 1.0 g with the mission payloads in place.

Meteoroid protection of the bumper type was designed to give a probability of no puncture of 0.999 based on 1964 flux and penetration data (refs. 24 and 25). Weight allowances have been made for leak detection and patching. With the patching of one leak, the probability of mission success is still 0.999 for a flux 100 times as severe as that when no patching is assumed.

Because of its low liquid temperature the thermal protection of the hydrogen is an important consideration (ref. 26). During space flight and in the Mars parking orbit the interplanetary vehicle is assumed oriented to minimize the area exposed to the Sun and so that the solar collector shades the tanks. In the planetary parking orbit the vehicle is assumed randomly oriented with respect to Mars about the spaceship axis through the Sun. Thermal protection from the solar and planetary fluxes is provided by multiple foils. The heat that does penetrate to the propellant is absorbed by boiloff, which is

vented to maintain a constant tank pressure of 10 psi. A hot gas bleed system has been assumed for tank pressurization during propulsion.

An allowance has also been made for both ullage and liquid outage. In the aggregate, the previous propellant-related weight items yield the same IWIEO as some equivalent value of the ratio of propellant tank to useful propellant, which is called the effective tank weight fraction (defined as the deadweight divided by the propellant weight). Based on the previously mentioned studies, an effective tank weight fraction of 0.125 was used in the present analysis for nuclear stages. This fraction in reality varies somewhat with mission profile, stage size, and mission maneuver, and it also depends on such factors as whether the meteoroid and thermal protection weights are shed prior to firing of the stage and whether tanks are staged during firing.

For chemical space propulsion a hydrogen-fluorine system was assumed with an effective tank weight fraction of 0.05. A separate allowance was made for the weight of thrust structure, 0.01 of the thrust, and for the weight of interstage structure, 0.01 of the force transmitted.

Thrustor performance. - Nuclear engines without shielding were assumed to have a thrust-to-weight ratio of 10 and a specific impulse of 850 seconds (ref. 27). All engines are required to have thermal shielding to reduce propellant boiloff during firing. This reduces the thrust-to-weight ratio to 8.0. In the present study when a nuclear stage is used for decelerating the Earth entry vehicle at Earth return, it must have biological as well as thermal shielding to reduce the radiation dose to the crew. The overall thrust-to-weight ratio in this case is 3. For nuclear engine firings other than at Earth return, crew protection from nuclear reactor radiation is provided by the tanks of liquid hydrogen and the separation distance, in addition to protection afforded by the command module solar radiation shielding.

Minimum sizes and weights for available nuclear engine systems were also assumed for the Earth deceleration stage. Arbitrary values of 8 000 and 16 000 pounds were assumed for the minimum weight of a nuclear engine plus biological and thermal shielding.

An engine thrust-to-weight ratio of 67 and a specific impulse at 460 seconds were used for the hydrogen-fluorine chemical system (ref. 28).

Space vehicle staging. - For the present study separate engine and tank systems were used for each major propulsive maneuver. This is sometimes referred to as tandem staging. A possible space vehicle configuration consistent with this assumption is shown in figure 8. Analyses, not presented here, show that other spaceship arrangements, such as a single engine with only tank staging or a system of parallel staging of tanks and engines, can give approximately the same mission weights as the system selected. The results of the mission profile analyses are thus only slightly dependent on the assumption of the type of staging for the space vehicle.

For stages other than the Earth deceleration stage, the initial accelerations for each major maneuver is 0.2 g's for nuclear stages and 0.4 for chemical stages. This presumes

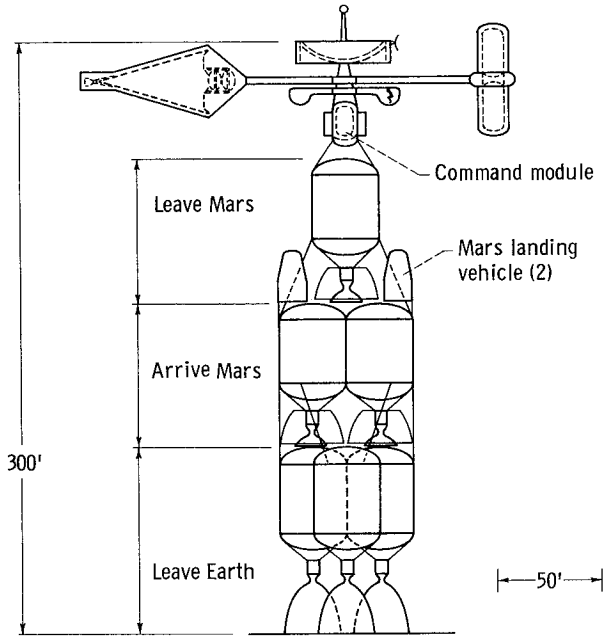

Figure 8. - Assembled Mars space vehicle in Earth orbit. Earth return mission payloads shown deployed for space flight.

that engines of the required thrust level are available, or that the desired thrust level can be achieved by clustering smaller engines.

Guidance and control. - Interplanetary trajectory guidance corrections were provided by separate chemical stages for all cases. The specific impulse was 430 seconds, the engine thrust-to-weight ratio 67, and the acceleration 0.01 g. The midcourse correction ΔV's were estimated from references 4 and 5 and are shown in tables IV and V.

Mission Trajectories

In addition to the mission payloads and propulsion system, the third major factor determining mission weights is the trajectory. The trajectory is characterized by its launch date, leg and stay times, mission perihelions, maximum communication distance, propulsive ΔV's, and atmospheric entry velocities. These characteristics are given for a spectrum of trips in tables IV to XI. The following discussion classifies the types of trajectories considered.

The trajectories used in the present study are referred to as medium thrust trajectories. The propulsive ΔV's are determined by assuming impulsive thrust maneuvers (ref. 29). These ΔV's are then appropriately increased to account for the propulsive efficiency (frequently referred to as "gravity losses") associated with operation in planetary gravitational fields at practical thrust levels (refs. 30 and 31).

Fast mission profiles are characterized by trip times of less than 600 days (figs. 9 and 10(a) and table IV) and short stay times, for example, 40 days. (The data of fig. 9 assume low circular parking orbits at Earth and Mars.) The mission $\sum \Delta V$ increases with increasing stay time (fig. 9), the mission perihelions are inside the Earth orbit (fig. 10(a)), and the mission aphelions are at Mars. The fast trips show a local minimum in the ΔV sum for trips times of about 500 days.

The intermediate mission profiles occur for mission durations between about 640 and 850 days (fig. 9). The stay time for minimum propulsive ΔV is zero, and the propulsive ΔV increases with increasing stay time. However, at 800 days the change in propulsive ΔV is slight for increases in stay time up to about 150 days. For the intermediate trips, the mission aphelions are outside the Mars orbit, the mission perihelions are at Earth (fig. 10(b)), and the Mars approach velocities are higher than for the slow trips (table IV).

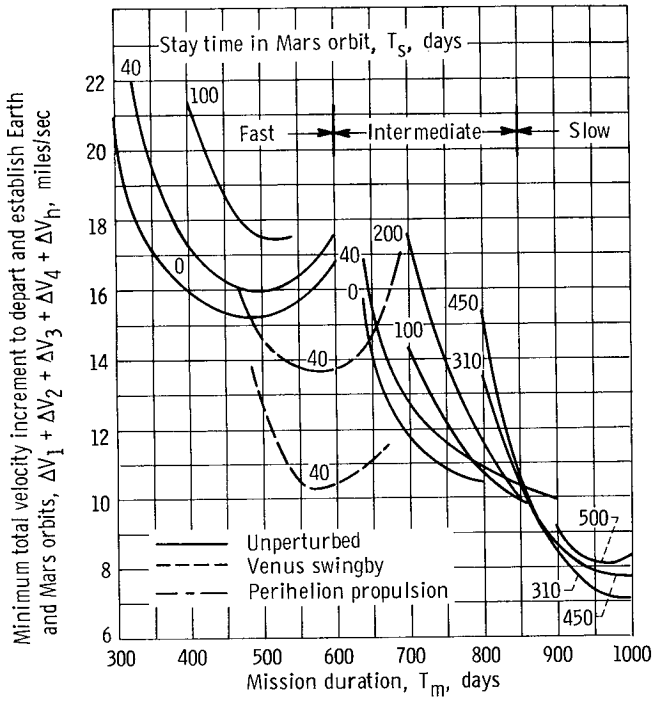

Figure 9. - Minimum total velocity increments required for stopover round trips to Mars. Departure date, 1979-80.

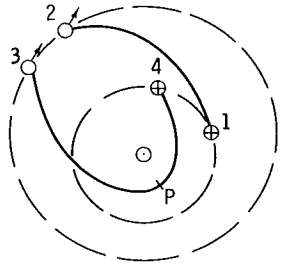

(a) Mission duration, 420 days; stay time, 40 days; launch year, 1979-80; profile, short-long.

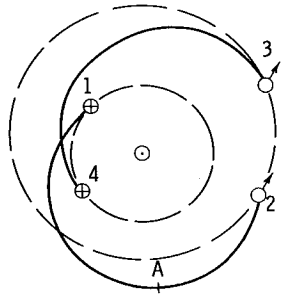

(b) Mission duration, 800 days; stay time, 100 days; launch year, 1979-80.

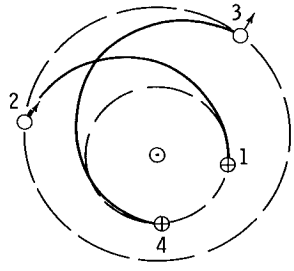

(c) Mission duration, 1000 days; stay time, 450 days; launch year, 1979-80; profile, "double Hohmann".

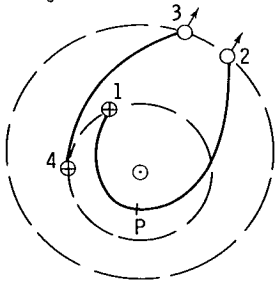

(d) Mission duration, 420 days; stay time, 40 days; launch year, 1979-80; profile, long-short.

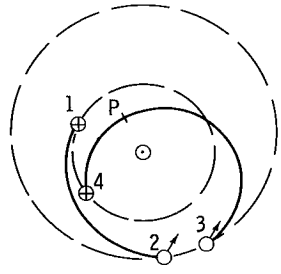

(e) Mission duration, 420 days; stay time, 40 days; launch year, 1970-71; profile, short-long.

P Mission perihelion
A Mission aphelion
⊕ Earth
♂ Mars
⊙ Sun

Figure 10. - Types of unperturbed Mars stopover round-trip trajectories.

TABLE IV. - TRAJECTORY PARAMETERS FOR ALL-PROPULSIVE MARS STOPOVER ROUND TRIPS IN 1979-80

[Circular Mars parking orbit, 1.1 radii.]

(a) Fast, short-long trajectory profile (see fig. 10)

Mission duration, days	300	360	420	500	600
Departure date, Julian day, 2444 -	250	240	220	190	100
Perihelion radius (min), astromonical unit	0.658	0.581	0.501	0.401	0.382
Maximum transmission distance, astronomical unit	0.265	1.341	1.635	1.920	1.996
Minimum $\sum\Delta V$, miles/sec	25.7	19.6	16.8	16.2	17.6
Earth departure:					
V_{H1}, miles/sec	22.10	21.73	20.91	20.56	19.95
α_1, deg	14.90	10.76	5.81	.50	-13.73
ΔV_1, miles/sec	4.38	3.49	2.56	2.21	3.41
Earth-Mars transit:					
$\theta_{1,2}$, deg	64.0	84.3	122.9	177.0	270.0
$\Delta T_{1,2}$, days	100	120	180	260	360
ΔV_{MC}, miles/sec	0.084	0.084	0.084	0.084	0.084
Mars arrival:					
V_{H2}, miles/sec	14.40	13.87	12.90	13.07	12.87
α_2, deg	27.90	23.05	10.24	-.0017	-9.02
ΔV_2, miles/deg	5.86	4.79	2.58	1.50	1.56
Mars stay:					
$\Delta T_{2,3}$, days	40	40	40	40	40
Mars departure:					
V_{H3}, miles/sec	15.0	11.88	11.08	10.05	9.85
α_3, deg	-38.4	-25.02	-21.61	-14.34	-12.44
ΔV_3, miles/sec	7.06	3.88	3.75	4.20	4.29
Mars-Earth transit:					
$\theta_{3,4}$, deg	206.0	252.2	273.7	298.3	302.8
$\Delta T_{3,4}$ days	160	200	200	200	200
ΔV_{MC}, miles/sec	0.095	0.095	0.095	0.095	0.095
Earth arrival:					
V_{H4}, miles/sec	222.3	20.31	19.51	18.23	17.96
α_4, deg	29.8	29.63	32.85	36.28	36.95
ΔV_4, miles/sec	8.46	7.42	7.82	8.30	8.38

TABLE IV. - Concluded. TRAJECTORY PARAMETERS FOR ALL-PROPULSIVE MARS STOPOVER ROUND TRIPS IN 1979-80

[Circular Mars parking orbit, 1.1 radii.]

(b) Intermediate and slow trajectory profiles (see fig. 10)

	Trajectory profile			
	Intermediate		Slow	
Mission duration, days	700	800	900	1000
Departure date, Julian day, 2444 -	400	340	210	200
Perihelion radius (min), astronomical unit	1.0	1.0	1.0	1.0
Maximum transmission distance, astronomical unit	2.0	2.5	2.5	2.5
Minimum $\sum\Delta V$, miles/sec	12.87	10.71	8.62	7.65
Earth departure:				
V_{H1}, miles/sec	21.06	20.93	20.59	20.36
α_1, deg	6.17	4.55	3.50	-5.25
ΔV_1, miles/sec	2.84	2.47	2.26	2.17
Earth-Mars transit:				
$\theta_{1,2}$, deg	211.7	219.9	207.25	228.8
$\Delta T_{1,2}$, days	480	440	240	260
ΔV_{MC}, miles/sec	0.084	0.084	0.084	0.084
Mars arrival:				
V_{H2}, miles/sec	13.89	14.57	14.50	13.96
α_2, deg	-1.99	-1.66	-1.11	-9.14
ΔV_2, miles/sec	4.20	4.33	1.51	1.44
Mars stay:				
$\Delta T_{2,3}$, days	40	100	450	450
Mars departure:				
V_{H3}, miles/sec	11.85	12.70	12.59	13.46
α_3, deg	-3.30	1.73	3.98	8.21
ΔV_3, miles/sec	1.69	1.29	1.38	1.45
Mars-Earth transit:				
$\theta_{3,4}$, deg	100.8	157.4	142.9	215.0
$\Delta T_{3,4}$, days	180	260	210	290
ΔV_{MC}, miles/sec	0.095	0.095	0.095	0.095
Earth arrival				
V_{H4}, miles/sec	20.07	20.28	20.19	20.32
α_4, deg	-15.88	-5.33	-9.52	0.80
ΔV_4, miles/sec	4.14	2.62	3.47	2.59

TABLE V. - TRAJECTORY PARAMETERS FOR MARS STOPOVER ROUND TRIPS IN 1979-80 USING ATMOSPHERIC BRAKING AT MARS ARRIVAL AND ATMOSPHERIC BRAKING AT EARTH RETURN FROM 52 000 fps

[Circular Mars parking orbit, 1.1 radii.]

(a) Fast, short-long trajectory profile (see fig. 10)

Mission duration, days	300	360	420	500
Departure date, Julian day, 2444 -	260	240	200	140
Perihelion radius (min), astronomical unit	0.643	0.581	0.548	0.499
Maximum transmission distance, astronomical unit	1.378	1.341	1.365	1.520
Minimum $\Sigma\Delta V$, miles/sec	15.55	9.91	8.01	8.90
Earth departure:				
V_{H1}, miles/sec	21.39	21.73	21.69	20.60
α_1, deg	19.70	10.76	-1.05	-8.50
ΔV_σ, miles/sec	5.10	3.50	2.52	2.95
Earth-Mars transit:				
$\theta_{1,2}$, deg	64.0	84.3	125.0	194.5
$\Delta T_{1,2}$, days	100	120	160	240
ΔV_{MC}, miles/sec	0.084	0.084	0.084	0.084
Mars arrival:				
V_{H2}, miles/sec	13.35	13.87	13.92	12.70
α_2, deg	25.53	23.05	20.68	10.8
V_σ, miles/sec	7.36	6.93	6.43	4.25
Mars stay time:				
$\Delta T_{2,3}$, days	40	40	40	40
Mars departure:				
V_{H3}, miles/sec	14.88	11.88	10.80	10.39
α_3, deg	-38.56	-25.02	-16.28	-13.58
ΔV_3, miles/sec	7.10	3.88	3.09	3.20
Mars-Earth transit:				
$\theta_{3,4}$, deg	211.6	252.2	272.5	283.4
$\Delta T_{3,4}$, days	160	200	220	220
ΔV_{MC}, miles/sec	0.095	0.095	0.095	0.095
Earth arrival:				
V_{H4}, miles/sec	22.12	20.31	19.70	19.29
α_4, deg	30.87	29.63	30.35	32.29
ΔV_4, miles/sec	3.35	2.53	2.52	2.75

TABLE V. - Concluded. TRAJECTORY PARAMETERS FOR MARS STOPOVER ROUND TRIPS IN 1979-80 USING ATMOSPHERIC BRAKING AT MARS ARRIVAL AND ATMOSPHERIC BRAKING AT EARTH RETURN FROM 52 000 fps

[Circular Mars parking orbit, 1.1 radii.]

(b) Fast, short-long, intermediate, and slow trajectory profiles (see fig. 10)

	Trajectory profile				
	Fast, short-long	Intermediate		Slow	
Mission duration, days	600	700	800	900	1000
Departure date, Julian day, 2444 -	100	400	340	210	200
Perihelion radius (min), astronomical unit	0.382	1.0	1.0	1.0	1.0
Maximum transmission distance, astronomical unit	1.996	2.5	2.5	2.5	2.5
Minimum $\Sigma\Delta V$, miles/sec	11.08	4.53	3.76	3.64	3.62
Earth departure:					
V_{H1}, miles/sec	19.95	21.06	20.93	20.59	20.36
α_1, deg	-13.73	6.17	4.55	3.50	-5.25
ΔV_1, miles/sec	3.41	2.84	2.47	2.26	2.17
Earth-Mars transit:					
$\theta_{1,2}$, deg	270	211.7	219.9	207.3	228.8
$\Delta T_{1,2}$, days	360	480	440	240	260
ΔV_{MC}, miles/sec	0.084	0.084	0.084	0.084	0.084
Mars arrival:					
V_{H2}, miles/sec	12.87	13.89	14.57	14.50	13.96
α_2, deg	-9.03	-1.99	-1.66	-1.11	-9.14
V_∞, miles/sec	3.70	6.34	6.47	3.93	3.48
Mars stay time:					
$\Delta T_{2,3}$, days	40	40	100	450	450
Mars departure:					
V_{H3}, miles/sec	9.85	11.85	12.70	12.59	13.46
α_3, deg	-12.44	-3.30	1.73	3.98	8.21
ΔV_3, miles/sec	4.29	1.69	1.29	0.38	1.44
Mars-Earth transit:					
$\theta_{3,4}$, deg	302.8	100.8	157.4	142.9	215.0
$\Delta T_{3,4}$, days	200	180	260	210	290
ΔV_{MC}, miles/sec	0.095	0.095	0.095	0.095	0.095
Earth arrival:					
V_{H4}, miles/sec	17.96	20.07	20.28	20.19	20.32
α_4, deg	36.95	-15.88	-5.33	-9.52	0.80
ΔV_4, miles/sec	3.38	0	0	0	0

TABLE VI. - PROPULSIVE VELOCITY INCREMENT FROM PROPELLANT SOURCE TO ACQUIRE TRAJECTORY TO MARS

Mission duration, $T_{m'}$ days	Propulsive velocity increment, ΔV, miles/sec		
	Propellant source		
	Earth surface	Collected in orbit about Earth	Moon surface
300	10.08	4.38	5.73
360	9.19	3.49	4.46
420	8.26	2.56	2.84
500	7.91	2.21	2.08
600	9.11	3.41	4.36
700	8.54	2.84	3.39
800	8.17	2.47	2.66
900	7.96	2.26	2.21
1000	7.87	2.17	1.99

TABLE VII. - PROPULSIVE VELOCITY INCREMENT CONSIDERATIONS FOR RENDEZVOUS AT EARTH RETURN AND AT MARS DEPARTURE

Mission duration, T_m, days	Total propulsive velocity increment to approach Earth by means of Mars, $\sum_{1}^{3}\Delta V$, miles/sec		Propulsive velocity increment for rendezvous with spaceship near Earth return, miles/sec		Propulsive velocity increment for rendezvous with spaceship at Mars departure with matched inbound trajectories and time separation between phases (see fig. 30(b))	
	Propulsive braking into a low circular parking orbit at Mars ($\bar{r}_c = 1.1$)	Propulsive braking into an elliptic parking orbit at Mars ($\bar{r}_a = 27$, $\bar{r}_p = 1.1$)	At $\bar{r}_\oplus = 1.1$ $\Delta V_a = \Delta V_b$ (see fig. 30(a))	At $\bar{r}_\oplus = 10$ $\Delta V_a = \Delta V_b$ (see fig. 30(a))	Time after manned phase launch, days	Propulsive velocity increment for rendezvous, miles/sec
300	17.30	15.67	8.46	11.48	---	----
360	12.16	10.53	7.42	10.19	-40	7.20
420	8.89	7.26	7.82	10.74	20	5.38
500	7.91	6.28	8.30	11.29	25	5.83
600	9.26	7.63	8.38	11.37	125	6.19
700	8.73	7.10	4.14	6.12	---	----
800	8.09	6.46	2.62	3.67	0 to -60; or -930	2.25
900	5.15	3.52	3.47	5.11	0 to -60; or -800	2.25
1000	5.06	3.43	2.59	3.58	0 to -60; or -790	2.25

TABLE VIII. - COMPARISON OF TRAJECTORY PARAMETERS FOR UNPERTURBED AND PERTURBED MARS STOPOVER ROUND TRIPS

[Atmospheric entry velocity at Earth is $V_{\oplus} \sim 4.9 + \Delta V_4$ miles/sec and at Mars is $V_{\sigma'} \sim 2.1 + \Delta V_2$ miles/sec.]

	Unperturbed short-long trajectory	Perihelion Propulsion		Venus swingby on outbound leg	
		Braking on inbound leg of short-long trajectory	Acceleration on outbound leg long-short trajectory		
Mission duration, days	500	556	542	550	Mission duration, days
Mission perihelion	0.40	0.375	0.33	0.33	Mission perhelion
Earth departure date, Julian day, 2444 -	190	180	885	840	Earth departure date, Julian day, 2443 -
Propulsive velocity increment leaving Earth, ΔV_1, miles/sec	2.21	2.35	2.42	2.37	Propulsive velocity increment arriving Earth, ΔV_4, miles/sec
Earth-Mars transit time, days	260	240	240	230	Mars-Earth transit time, days
Earth-Mars heliocentric travel angle, $\theta_{1,2}$, deg	177	174	159	---	Mars-Earth heliocentric travel angle, $\theta_{3,4}$, deg
Propulsive velocity increment arriving Mars, ΔV_2, miles/sec	1.50	1.95	1.67	1.76	Propulsive velocity increment leaving Mars, ΔV_3, miles/sec
Mars stay time, days	40	40	40	40	Mars stay time, days
Propulsive velocity increment leaving Mars, ΔV_3, miles/sec	4.20	4.15	4.60	3.61	Propulsive velocity increment arriving Mars, ΔV_2, miles/sec
Mars perihelion transit time, days	----	163	169	124	Mars perihelion (Venus) transit time, days
Perihelion propulsion, ΔV_h, miles/sec	----	1.72	1.71	----	Perihelion propulsion, ΔV_h, miles/sec
Perihelion Earth transit time, days	----	113	93	156	Perihelion (Venus) Earth transit time, days
Mars-Earth transit time, days	200	276	262	280	Earth-Mars transit time, days
Mars-Earth heliocentric travel angle, $\theta_{3,4}$, deg	298	360	360	370	Earth-Mars heliocentric travel angle, $\theta_{3,2}$, deg
Propulsive velocity increment arriving Earth, ΔV_4, miles/sec	8.30	3.60	3.88	2.68	Propulsive velocity increment leaving Earth, ΔV_1, miles/sec
All propulsive, $\sum_1^4 \Delta V + \Delta V_h$	16.21	13.77	14.28	10.42	All propulsive, $\sum_1^4 \Delta V + \Delta V_h$
Atmospheric braking at Earth, $\sum_1^3 \Delta V + \Delta V_h$	7.91	10.17	11.86	8.05	Atmospheric braking at Earth, $\sum_1^3 \Delta V + \Delta V_h$
Atmospheric braking at Earth and Mars, $\Delta V_1 + \Delta V_3 + \Delta V_h$	6.41	8.22	7.26	4.44	Atmospheric braking at Earth and Mars, $\Delta V_1 + \Delta V_3 + \Delta V_h$

TABLE IX. - TRAJECTORY PARAMETERS FOR PERIHELION BRAKING ON INBOUND LEG OF A SHORT-LONG MARS STOPOVER ROUND TRIP

[Atmospheric entry velocity at Earth is $V_{\oplus} \approx 4.9 + \Delta V_4$ miles/sec and at Mars is $V_{\sigma'} \approx 2.1 + \Delta V_2$ miles/sec.]

	Mission duration, T_m, days					
	476	496	556	596	656	676
Mission perihelion	0.375	0.375	0.375	0.375	0.375	0.375
Earth departure date, Julian day, 2444 -	260	240	180	140	080	060
Propulsive velocity increment leaving Earth, ΔV_1, miles/sec	4.4	3.25	2.35	2.59	3.91	4.86
Earth-Mars transit time, days	160	180	240	280	340	360
Earth-Mars heliocentric travel angle, $\theta_{1,2}$, deg	91.5	112	174	212	270	289
Propulsive velocity increment arriving Mars, ΔV_2, miles/sec	2.2	2.05	1.95	1.67	1.57	2.01
Mars stay time, days	40	40	40	40	40	40
Propulsive velocity increment leaving Mars, ΔV_3, miles/sec	4.15	4.15	4.15	4.15	4.15	4.15
Mars perihelion transit time, days	163	163	163	163	163	163
Perihelion velocity, ΔV_h, miles/sec	1.72	1.72	1.72	1.72	1.72	1.72
Perihelion Earth transit time, days	113	113	113	113	113	113
Mars-Earth transit time, days	276	276	276	276	276	276
Mars-Earth heliocentric travel angle, $\theta_{3,4}$, deg	360	360	360	360	360	360
Propulsive velocity increment arriving Earth, ΔV_4, miles/sec	3.60	3.60	3.60	3.60	3.60	3.60
All propulsive, $\sum_{1}^{4} \Delta V + \Delta V_h$	16.07	14.77	13.77	13.73	14.97	16.34
Atmospheric braking at Earth, $\sum_{1}^{3} \Delta V + \Delta V_h$	12.47	11.17	10.17	10.13	11.37	12.74
Atmospheric braking at Earth and Mars, $\Delta V_1 + \Delta V_3 + \Delta V_h$	10.27	9.12	8.22	8.46	9.80	10.73

TABLE X. - TRAJECTORY PARAMETERS FOR PERIHELION THRUSTING ON OUTBOUND LEG OF A LONG-SHORT MARS STOPOVER ROUND TRIP

[Atmospheric entry velocity at Earth is $V_{\oplus} \sim 4.9 + \Delta V_4$ miles/sec and at Mars is $V_{\sigma^{\prime}} \sim 2.1 + \Delta V_2$ miles/sec.]

	Mission duration, T_m, days			
	502	542	602	642
Mission perihelion	0.33	0.33	0.33	0.33
Earth departure date, Julian day, 2443 -	885	885	885	885
Propulsive velocity increment leaving Earth, ΔV_1, miles/sec	3.88	3.88	3.88	3.88
Earth perihelion transit time, days	93	93	93	93
Perihelion velocity, ΔV_h, miles/sec	1.71	1.71	1.71	1.71
Perihelion Mars transit time, days	169	169	169	169
Earth-Mars transit time, days	262	262	262	262
Earth-Mars heliocentric travel angle, $\theta_{1,2}$, deg	360	360	360	360
Propulsive velocity increment arriving Mars, ΔV_2, miles/sec	4.60	4.60	4.60	4.60
Mars stay time, days	40	40	40	40
Propulsive velocity increment leaving Mars, ΔV_3, miles/sec	1.70	1.67	1.55	1.47
Mars-Earth transit time, days	200	240	300	340
Mars-Earth heliocentric travel angle, $\theta_{3,4}$, deg	121	159	216	255
Propulsive velocity increment arriving Earth, ΔV_4, miles/sec	3.27	2.42	2.60	3.38
All propulsive, $\sum_{1}^{4} \Delta V + \Delta V_h$	15.18	14.28	14.34	15.04
Atmospheric braking at Earth, $\sum_{1}^{3} \Delta V + \Delta V_h$	11.89	11.86	11.74	11.66
Atmospheric braking at Earth and Mars, $\Delta V_1 + \Delta V_3 + \Delta V_h$	7.29	7.26	7.14	7.06

TABLE XI. - TRAJECTORY PARAMETERS FOR A VENUS SWINGBY ON OUTBOUND LEG OF A LONG-SHORT MARS STOPOVER ROUND TRIP

[Atmospheric entry velocity at Earth is $V_{\oplus} \approx 4.9 + \Delta V_4$ miles/sec and at Mars is $V_{\sigma'} \approx 2.1 + \Delta V_2$ miles/sec.]

	Mission duration, T_m, days				
	480	500	550	600	650
Earth departure date, Julian day, 2443 -	840	840	840	840	840
Propulsive velocity increment leaving Earth, ΔV_1, miles/sec	2.66	2.66	2.66	2.66	2.66
Earth-Venus transit time, days	156	156	156	156	156
Venus-Mars transit time, days	124	124	124	124	124
Earth-Mars transit time, days	280	280	280	280	280
Earth-Mars heliocentric travel angle, $\theta_{1,2}$, deg	370	370	370	370	370
Propulsive velocity increment arriving Mars, ΔV_2, miles/sec	3.61	3.61	3.61	3.61	3.61
Mars stay time, days	40	40	40	40	40
Propulsive velocity increment leaving Mars, ΔV_3, miles/sec	2.20	1.87	1.76	1.72	1.42
Mars-Earth transit time, days	160	180	230	280	330
Mars-Earth heliocentric travel angle, $\theta_{3,4}$, deg	86.45	106.18	154.61	202.34	250.41
Propulsive velocity increment arriving Earth, ΔV_4, miles/sec	5.22	3.82	2.37	2.53	3.36
All propulsive $\sum_{1}^{4} \Delta V$	13.76	11.96	10.50	10.52	11.05
Atmospheric braking at Earth, $\sum_{1}^{3} \Delta V$	8.47	8.14	8.13	7.99	7.69
Atmospheric braking at Earth and Mars, $\Delta V_1 + \Delta V_3$	4.86	4.53	4.54	4.38	4.08

Slow mission profiles (fig. 10(c)) have trip times greater than about 850 days, stay times for minimum ΔV at about 310 days, mission perihelions at 1 astronomical unit, and aphelions at Mars (fig. 10(c) and table IV). A 450-day stay time was chosen for the 900- and 1000-day trips because it offers a longer stay time while retaining near-minimum ΔV when atmospheric braking is used at Earth. It is interesting to note that the actual travel time can be comparable for the fast and slow trips; for example, for a 500-day trip with a 40-day stay the travel time is 460 days while for a 900-day trip with a 450-day stay it is 450 days. The intermediate and slow trips show a general decrease in ΔV with increasing trip time up to about 1000 days, which is a global minimum (approximately the so-called double Hohmann trip).

Short-long profiles for the fast trips are characterized by outbound legs that are direct trajectories (i. e., pass through neither an aphelion or perihelion), shorter in terms of the travel angle θ measured at the Sun, and generally shorter in terms of travel time ΔT than the return leg (fig. 10(a) and tables IV and V). The return leg is a perihelion trajectory and the mission perihelion occurs on the return leg. The short-long profiles give a low ΔV to leave Earth and a high approach velocity at Earth return. The long-short mission profiles (fig. 10(d)) have the converse characteristics. Because the short-long profiles have high Earth return velocities, the initial gross weights for this profile are especially responsive to the use of atmospheric braking at Earth. Thus short-long profiles are of particular interest.

The previous trajectories all use single conic sections for their heliocentric segments. Perihelion propulsion or a Venus swingby can be used to produce new classes of trajectories called perturbed trajectories, which are generally of the fast type. As can be seen from figure 9 they yield attractive ΔV's and trip times. These trajectories are described more fully in the section Perturbed Trajectories (p. 64).

Because of the eccentricity of the Mars orbit, the propulsive ΔV for fast trips can vary considerably with the synodic period in which the trip is made. A trip in 1979-80 arrives at Mars when Mars is near its aphelion (fig. 10(a)). A trip in 1970-71 or 1986 arrives at Mars when it is near its perihelion (fig. 10(e)). At intermediate launch dates Mars is at intermediate positions. The effect of this on the propulsion requirements is illustrated in figure 11 (for low circular parking orbits at Earth and Mars) for a 420-day trip with a 40-day stay time. These curves are not continuous, and each symbol represents a discrete local minimum as illustrated by the "typical data." For the all propulsive case there is a marked change in $\sum \Delta V$ with launch year. The low $\sum \Delta V$'s occur in 1971 and again in 1986. The highest $\sum \Delta V$ occurs in 1977 and 1979. The present mission analysis was done for 1979-80 because it is one of the more difficult years. Missions with lower $\sum \Delta V$ requirements can usually be made for lower weights.

When atmospheric braking is used at Earth (middle curve) there is less variation of $\sum \Delta V$ with launch year and the level of the $\sum \Delta V$ is much reduced. The difference

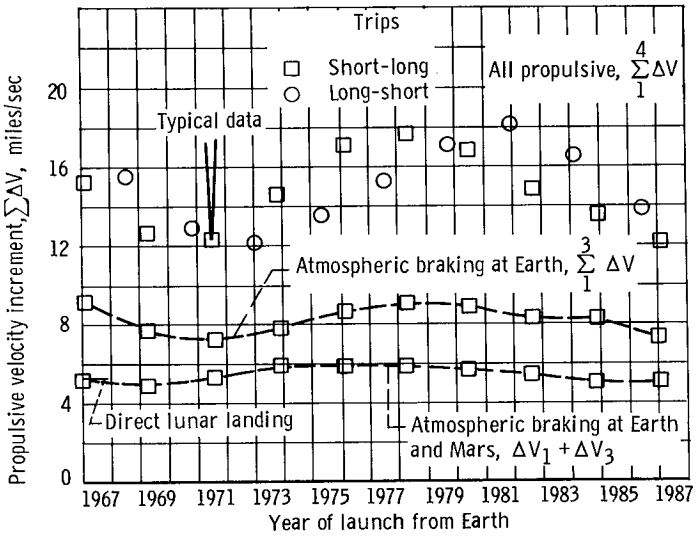

Figure 11. - Launch year effect on propulsive velocity increment. Mission duration, 420 days; stay time, 40 days.

between the upper and middle curves is an indication of the atmospheric entry velocity at Earth. The year 1979 is now characterized as a difficult year primarily in terms of atmospheric entry velocity. When atmospheric braking at both Earth and Mars is used, the $\sum \Delta V$ is even lower and varies even less with launch year. The variation in $\sum_{1}^{4} \Delta V$ is now almost completely absorbed in the atmospheric entry velocities. The variation in the $\sum \Delta V$ with launch year for the slow trips is small.

Mission trajectories may be selected to minimize any one of a number of criteria such as the mission cost, weight, or $\sum \Delta V$. The present trajectories yield minimum $\sum \Delta V$. Trajectories selected to give a minimum weight generally give only a slightly lower weight than do minimum $\sum \Delta V$ trajectories.

With the mission payloads, the propulsive velocity increments, and the propulsion system characteristics described, the initial weight in Earth orbit may be calculated by successive use of the rocket equation to account for jettisoned weights and staging:

$$W_G = W_E\left(1 - e^{\frac{-1.03\,\Delta V}{Ig}}\right)$$

where W_G and W_E are the stage initial and empty weights, respectively, ΔV is the characteristic velocity increment required from the stage, and Ig is the rocket exhaust velocity. (All symbols are defined in appendix A.) Each stage is designed with a 3-percent ΔV reserve.

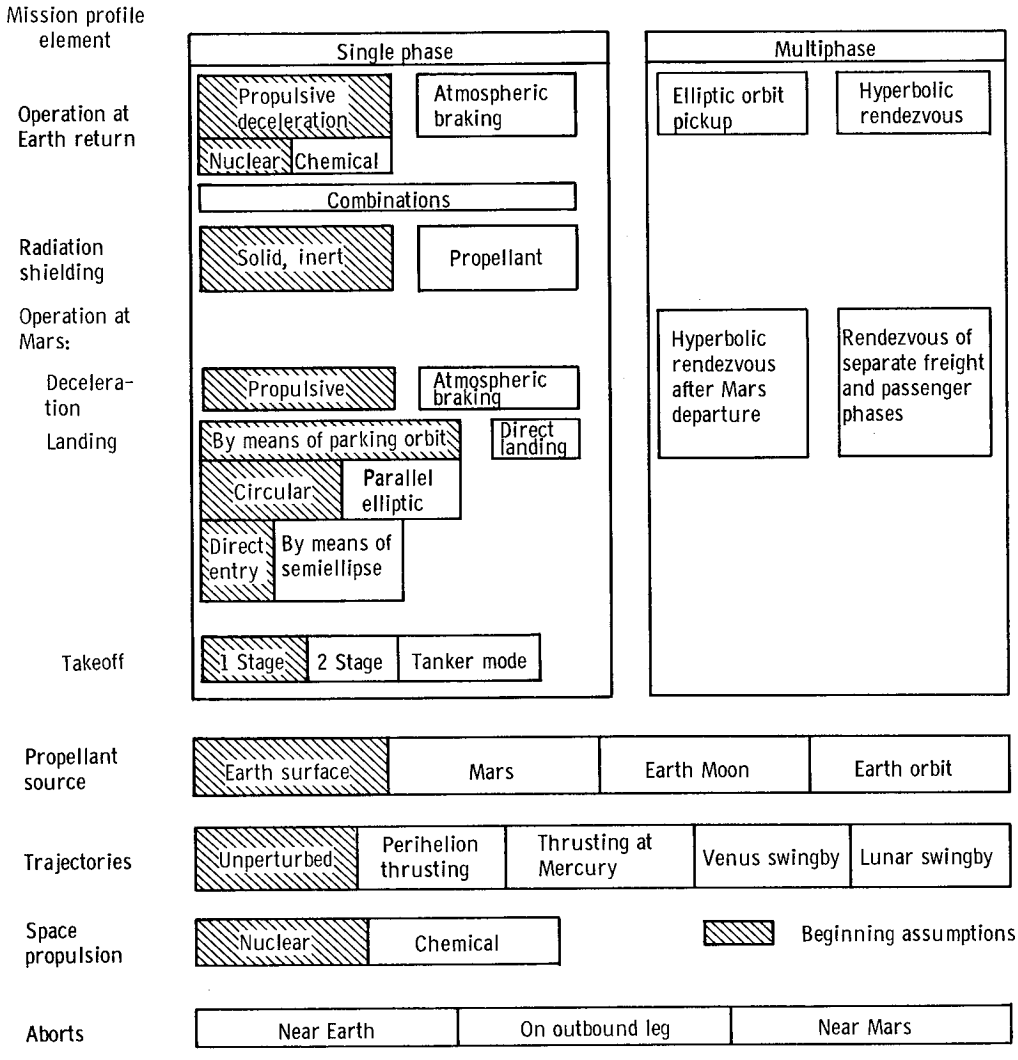

Figure 12. - Mission profile variations.

INITIAL WEIGHT IN EARTH ORBIT

The previously described inputs are used to study the mission profile variations depicted in figure 12 and as outlined in the table of contents. The mission profiles are divided into two broad categories, single- and multiphase profiles. For the single-phase profiles (e. g. , fig. 1, p. 3), all the mission components depart from Earth on the same date and traverse the same trajectory. For the multiphase missions there may be more than one launch date and the several mission components each travel a different trajectory.

The elements of a mission profile are given on the left and the options available for each element are given to the right. As in the procedure for calculating the vehicle weight, it is convenient to discuss the mission profile elements in the reverse of their temporal order. For the maneuver at Earth return, there is the choice of atmospheric braking, propulsive deceleration by chemical or nuclear systems, or combinations of

these. Next, the required space radiation shielding can be provided either by a solid inert material or by the propellants on board the spaceship. At Mars, the spaceship can be decelerated by either propulsion or atmospheric braking and can be either landed directly on the surface of Mars or parked in an orbit about Mars. In the latter case, a low or high circular orbit may be entered directly, the high circular orbits may be achieved by means of a semiellipse, or a parallel elliptic parking orbit may be used. When a parking orbit is used, the landing is conducted from the parking orbit. The take-off from the Mars surface to rendezvous with the spaceship in orbit may be accomplished by one- or two-stage vehicle or a system using an intermediate rendezvous with a tanker vehicle.

In the category of two-phase mission profiles, the mission payloads can be retrieved from an elliptic orbit about Earth at Earth return, or a separate Earth deceleration system can be accelerated to rendezvous with the spaceship as it approaches Earth at hyperbolic velocities. Alternatively the Earth deceleration system can rendezvous with the spaceship immediately after Mars departure. Rendezvous of separate freight and passenger ships at Mars is also possible. The previous profile variations use single conic trajectories with nuclear space propulsion and assume that the propellant source is located on the Earth's surface. Attention is next given to other sources of propellant, perturbed trajectories, chemical space propulsion, and aborts.

The discussion of the many mission profiles is begun by assuming nuclear space propulsion and a single-phase mission profile defined by the crosshatched blocks (fig. 12), and it then proceeds in the order of the previous discussion. Finally, the sensitivity of the IWIEO to the inputs to the analysis is shown and the results evaluated.

As was mentioned earlier, an important criterion for comparing the various profiles is the initial weight in Earth orbit. This parameter is presented as a function of mission duration for the various mission profiles.

Operations at Earth Return

Discussed herein are the effects of using atmospheric braking at Earth for a range of entry velocities and the effect of propulsion system choice, chemical or nuclear, to supplement the atmospheric braking. The Earth deceleration stage weight for a 420-day mission is considered first. This weight is then integrated into the mission to yield the IWIEO, and then the effect of the operations at Earth return is shown as a function of mission duration.

Atmospheric braking. - The incentive for atmospheric entry from high velocities is illustrated in figure 13. The calculations were made for the 420-day trip, which has a velocity approaching the Earth's atmosphere of 67 200 fps. The ordinate gives the total

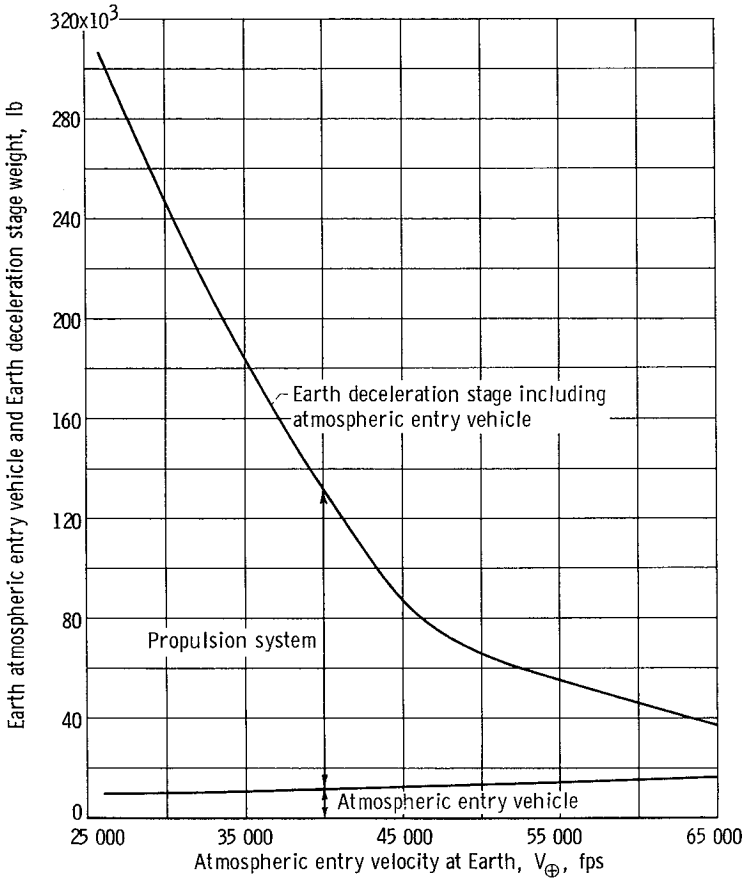

Figure 13. - Effect of Earth atmospheric entry velocity on Earth deceleration stage weights. Mission duration, 420 days; stay time, 40 days; Earth approach velocity, 67 000 fps.

weight of the Earth deceleration stage (Earth atmospheric entry vehicle plus propulsion system) using a nuclear retrorocket and also the weight of the associated atmospheric entry vehicle. The abscissa is the atmospheric entry velocity. The difference between the approach velocity (67 200 fps) and the atmospheric entry velocity is the ΔV provided by the retrorocket. (This distinction between the Earth approach velocity and Earth atmospheric entry velocity is retained throughout the report). This ΔV decreases directly as the atmospheric entry velocity increases. The total stage weight (upper curve) shows a very marked decrease in weight with increasing atmospheric entry velocity, and this is the reason high entry velocities are attractive.

The lower curve gives the increase in atmospheric entry vehicle weight with increasing entry velocity. The basic atmospheric entry vehicle with heat protection sufficient for deceleration from circular velocity weighs about 11 000 pounds. The weight of the heat protection increases with increasing entry velocity to give a total entry vehicle weight of about 16 500 pounds at 65 000 fps. The difference between the atmospheric entry vehicle weight and the total deceleration stage weight is the weight of the propulsion system: propellant, tank, structure, and engine weight. The weight of the propulsion system decreases much more rapidly than the entry vehicle weight increases, which results in the marked decrease in the overall stage weight with increasing entry velocity.

Although entry from, say, 65 000 fps appears feasible in terms of heat protection systems (e. g., ref. 16), there are other factors, all of which argue against ultrahigh-entry speeds, that must be considered:

(1) The entry corridor depths decrease sharply and thus burden the approach guidance and control system.

(2) The required maneuver rates increase and therefore tax the pilot and control systems.

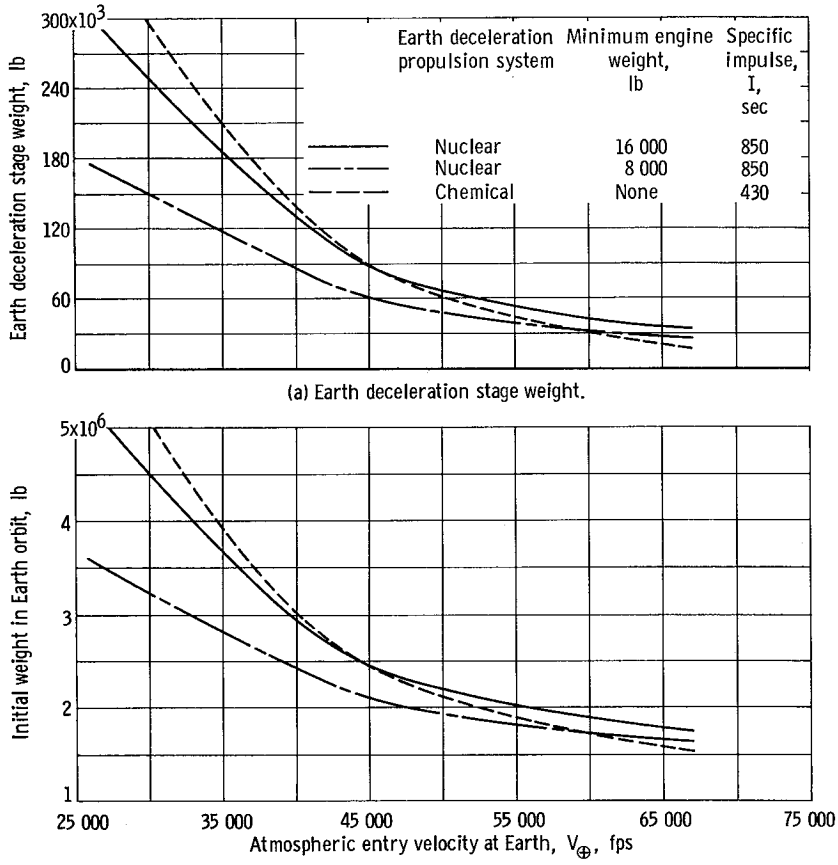

(a) Earth deceleration stage weight.

(b) Initial weight in Earth orbit; nuclear space propulsion.

Figure 14. - Effect of Earth atmospheric entry velocity and Earth deceleration propulsion on system weights. Mission duration, 420 days; stay time, 40 days; Earth approach velocity, 67 000 fps.

(3) The difficulty of development increases.

(4) As discussed subsequently, whatever radiation shielding weight is required on board the spaceship can be used also for retrorocket braking. Thus, the benefit to be gained from high-entry velocities is reduced. When these factors were considered, an entry velocity of 52 000 fps was chosen as a practical upper limit for this study.

Choice of deceleration propulsion system. - When the allowable atmospheric entry velocity is high (e. g., 52 000 fps), the required retro ΔV is comparatively low and chemical retropropulsion can be competitive with nuclear propulsion. A comparison of the application of these two propulsion systems to the Earth deceleration stage is made in figure 14(a) for the same mission as the previous figure. The solid curve is also taken from the previous figure and applies for nuclear propulsion. When nuclear propulsion is used in the Earth deceleration stage, the engine weight has an unusually large influence as the stage weight. Because it is the last propulsive stage, the engine weight must include weight for shielding the crew from the engine radiation. (The command module with its protective walls is abandoned prior to the Earth approach maneuver.) Without shielding on the engine the radiation dose from the engine rises precipitously as

the protective mass of the intervening propellant is consumed. Also thermal shielding of the propellants is required for this as well as for all maneuvers. The solid curve corresponds to the engine plus shield weight of 16 000 pounds. This is about the weight of a NERVA type engine without biological shielding. For comparison with this engine weight, recall that the stage payload, which is the Earth atmospheric entry vehicle, weighs between 11 000 and 16 000 pounds.

The dashed curve of figure 14(a) is for deceleration by a chemical propellant. For the chemical systems the engine weight is on the order of 500 pounds, more than an order of magnitude less than the weight of the nuclear engine or the weight of the entry vehicle. On the other hand, the specific impulse of the chemical system is 430 seconds compared with 850 seconds for the nuclear system.

As a consequence of the previously described engine characteristics, the curves for the stage weights of the nuclear and chemical system cross at an atmospheric entry velocity of 46 000 fps. Chemical propulsion gives lower weights for higher atmospheric entry velocities. Nuclear systems give lower weights for lower atmospheric entry velocities where the required propulsive ΔV's are correspondingly higher. With this nuclear engine, a chemical stage gives a lower weight than a nuclear stage for the assumed feasible atmospheric entry velocity of 52 000 fps.

The position of the nuclear system compared with the chemical system is improved if a nuclear engine plus shield of reduced weight is hypothesized. The dash-dot curve (fig. 14(a)) is for a nuclear engine with a minimum weight of 8000 pounds but with the same specific impulse as the heavier nuclear engine, 850 seconds. With this engine the stage weights are less than the chemical stages up to an entry velocity of 62 000 fps. At an atmospheric entry velocity of 52 000 fps the chemical stage is 20-percent heavier than the stage with the lighter nuclear engine.

If the Earth's atmospheric entry velocity were limited to 37 000 fps, then either nuclear system would give a lighter stage weight than the chemical system. The nuclear engine plus shield weighing 8000 pounds gives a stage weight of 105 000 pounds compared with 162 000 pounds for the 16 000-pound nuclear engine system. This last example illustrates the greatest importance of nuclear engine weight when nuclear propulsion is considered for the Earth deceleration maneuver. Engine weight is important because it is comparable in weight to the stage payload, which is the atmospheric entry vehicle.

The importance of the atmospheric entry velocity and deceleration propulsion system is best seen by looking at their effect on the initial weight in Earth orbit. The initial weight in Earth orbit is not directly proportional to the deceleration stage weight because the Earth deceleration stage weight is only part of the weight delivered to the vicinity of Earth and because a substantial weight is deposited at Mars. Figure 14(b) presents the initial weight in Earth orbit against the atmospheric entry velocity for the three Earth-return deceleration systems considered in figure 14(a); nuclear propulsion is assumed

for the prior space maneuvers.

The curves have the same general shape and intersect at the same values of entry velocity as those of figure 14(a). The use of atmospheric braking is seen to be a very powerful technique for reducing the IWIEO. For example, propulsive deceleration to circular velocity at Earth (26 000 fps) by using the heavier nuclear engine yields an IWIEO of 5.3 million pounds. If full-atmospheric braking (from 67 200 fps) is used, the weight is 1.75 million pounds, which is a weight reduction of 70 percent. A 60-percent weight reduction exists for chemical deceleration to 52 000 fps entry velocity, which is the assumed feasible value. The weight reduction for full-atmospheric braking compared with full propulsive deceleration is 60 percent if the lighter nuclear engine is available. At a 52 000 fps entry velocity, the use of the lighter nuclear engine in the Earth deceleration stage gives a IWIEO only 6 percent less than when chemical propulsion is used.

At this point the discussion on operations at Earth return is summarized. This phase of the study was made for a 420-day trip for which the Earth approach velocity is 67 200 fps. Atmospheric braking at Earth reduces the initial weight in Earth orbit 60 to 70 percent compared with propulsive braking to circular velocity. Atmospheric braking from 52 000 fps has been assumed a practical upper limit for this study. With this assumption a chemical deceleration stage yields lower gross weights than a nuclear stage using an engine plus shield of 16 000 pounds. Lighter nuclear engine-plus-shield weights are required and/or the limiting entry velocity must be lower for the nuclear stage to be superior to the chemical stage.

Variation of effect of atmospheric entry velocity with mission duration. - The effect of atmospheric braking varies with the mission duration primarily because the Earth approach velocities vary. The Earth approach velocities are shown in figure 15(a). For the fast trips the approach velocities vary only over the narrow range of 65 000 to 70 000 fps. The approach velocities for the slower trips are much lower, being for the most part less than 45 000 fps.

The variation of IWIEO for several values of atmospheric entry velocity is shown in figure 15(b). High atmospheric entry velocities (e.g., up to 52 000 fps) are an important factor in reducing weight for all the fast trips primarily because the Earth approach velocities are high and because the general ΔV level is higher for the fast trips, which makes the weights more sensitive to changes in ΔV. For the slow trips the use of atmospheric entry at velocities up to the approach velocities is helpful in reducing the weight, but high entry velocities, say above about 45 000 fps, are of no value in reducing weights. An entry velocity of 43 000 fps should be within post Apollo technology. Thus, the slow trips offer a comparatively easy atmospheric entry problem at Earth return.

In summary, when a lifting (hypersonic $L/D = 1.0$) atmospheric entry and landing vehicle is assumed, the use of atmospheric braking from speeds up to 52 000 fps is a very powerful way of reducing the IWIEO for trips of 600 days and less in duration. For

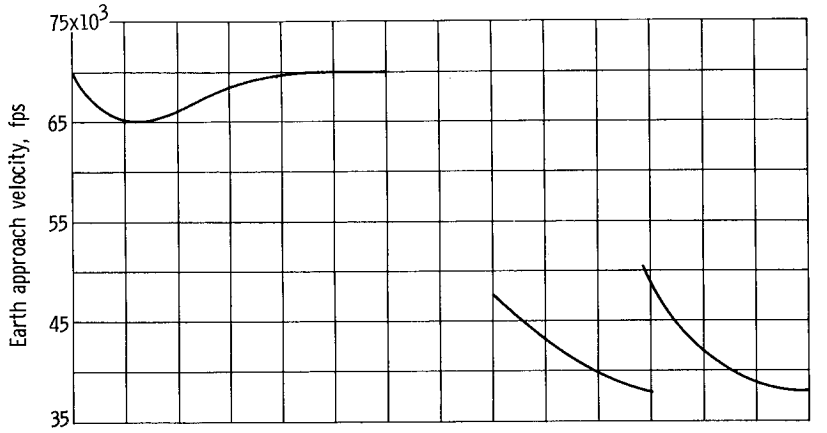

(a) Earth approach velocities.

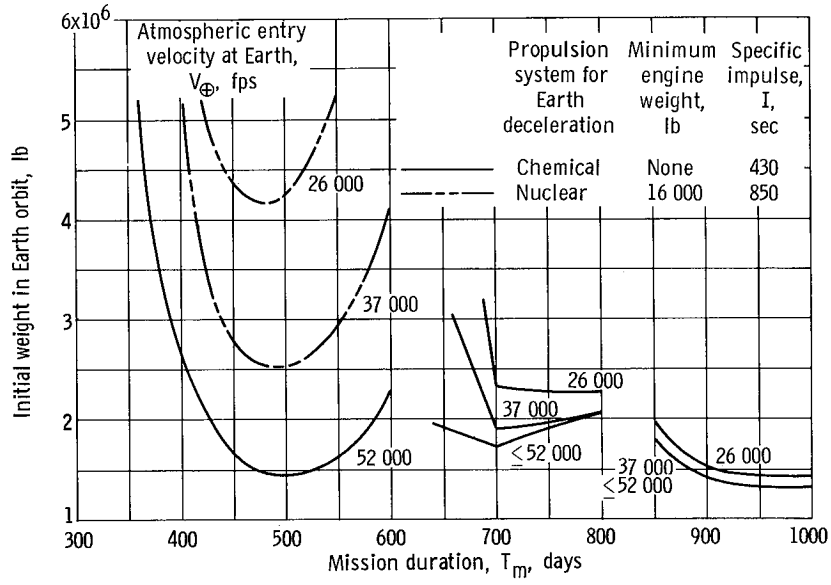

(b) Initial weight in Earth orbit.

Figure 15. - Effect of mission duration on Earth approach velocities and importance of atmospheric braking at Earth. Inert shielding, nuclear space propulsion.

trips longer than 700 days, atmospheric entry is less effective in reducing weight, entry velocities up to about 43 000 fps give most of the possible weight reduction, and higher entry velocities are not generally required.

Effect of Mission Duration on Initial Weight in Earth Orbit

At this point it is convenient to further discuss the variation of IWIEO with mission duration with respect to

(1) Some of the factors determining this variation

(2) The significance of the variation

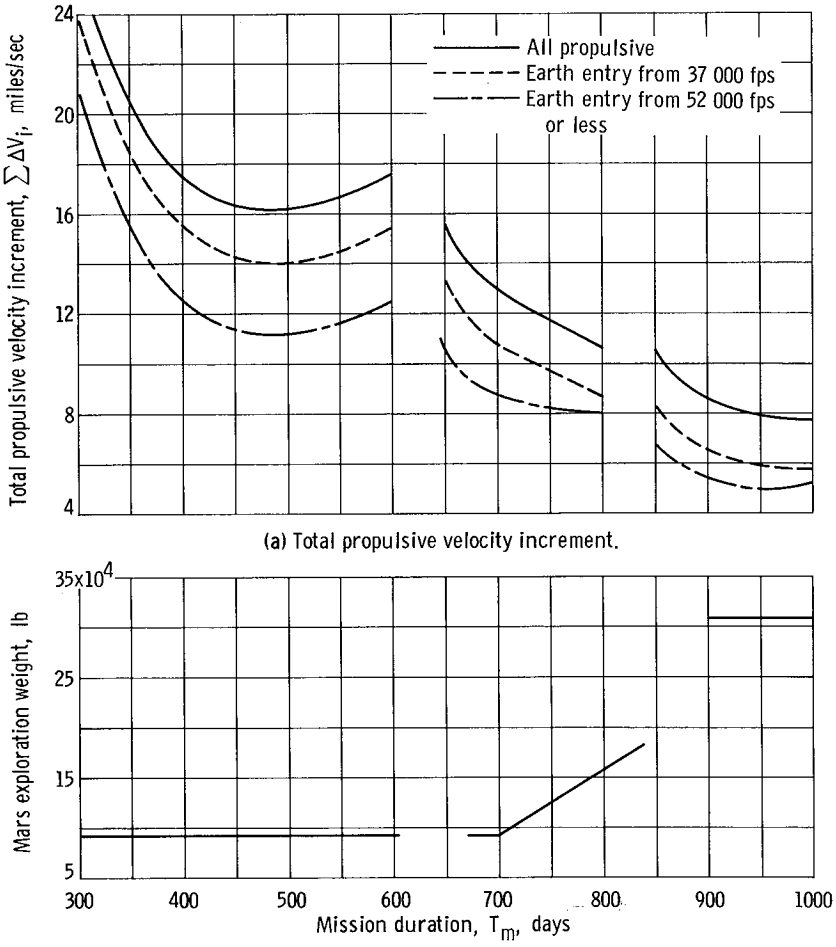

(a) Total propulsive velocity increment.

(b) Mars payload weight.

Figure 16. - Factors affecting variation of initial weight in Earth orbit with mission duration.

(3) Some factors affecting the choice of mission duration

It can be seen from figure 15(b) that the fast trips show local minimums in weight at a mission duration of about 490 days and decreasing weight with increasing atmospheric entry velocity. The lowest weight, however, occurs for mission durations of about 1000 days. The weights for these slow trips are, however, only slightly lower than those of the best fast trips.

The two factors largely responsible for the variation of IWIEO with mission duration are the propulsive ΔV and the weights delivered to Mars. These factors are presented against trip duration in figure 16. For the fast trips, the propulsive ΔV's show a local minimum near 490 days and decreasing values with increasing atmospheric entry velocity as did the IWIEO. In general, for the fast trips the IWIEO's faithfully follow the trends of the ΔV's.

The propulsive ΔV's for the slower trips are significantly lower than those for the fast trips, but the IWIEO's indicate this fact only weakly. This condition is due to the

variation of the weight delivered to Mars with mission duration (shown in fig. 16(b)). For trips of 700 days and less in duration, the stay time at Mars is 40 days and four of the seven-man crew descent from the spaceship in its circular parking orbit to the surface of Mars. For trip durations of 800, 900, and 1000 days the stay times are 100, 450, and 450 days, respectively, and all seven of the crew descend to the surface. The Mars landing system weights vary accordingly. The weight is about 80 000 pounds for trips of less than 700 days, but it increases to about 310 000 pounds for the 900- and 1000-day trips. The weight is larger for the longer missions both because more men descend to the surface and because more scientific and life-support equipment are landed to support the men for the longer stay time. The weight of equipment to be landed requires still further weight to perform the atmospheric entry and landing maneuver. Thus, in spite of the reduced ΔV's for the slower trips compared with the fast trips, the IWIEO's (fig. 15(b)) are only slightly less because of the increased Mars landing weights for the slow trips. The sharp minimum in IWIEO (fig. 15 (b)) at 700 days occurs because for shorter trips the $\sum \Delta V$ increases, while for longer trips the increase in Mars payload overrides the decrease in $\sum \Delta V$.

When the various trip durations are compared, it should be kept in mind that the fast trips permit a maximum of 160 man-days (four men for 40 days) on the Mars surface. The actual time on the surface may be somewhat less than 40 days because the time spent in landing and takeoff maneuvers. The 1000-day mission, on the other hand, has a larger weight of scientific equipment and permits about 3150 man-days on the surface (seven men for 450 days) or 20 times more than the fast trips. The slow trips thus offer the possibility of a much more extensive exploration of Mars.

A discussion of the significance of the segments of the curves which show increasing weight with increasing trip time, that is, fast trips to the right of the minimum weight trip time (fig. 15(b)), is also warranted. All the missions of figure 15(b) assume that the vehicle departs from Earth at the beginning of the trip time and comes back to Earth at the end of the trip time. This assumption is useful to find the trip time yielding minimum IWIEO. Having found the minimum, one can inquire as to what mission of 600-day duration will yield the lowest IWIEO. One answer is to first wait on the Earth's surface for 110 days and then do a 490-day mission. Alternatively, a terminal stay at Earth could be hypothesized. Thus the best 600-day trips should be constructed with initial or terminal waits at Earth. In general, regions of the curves (fig. 15(a)) where the weight increases with increasing mission duration are of little interest.

Radiation Shielding

The radiation shield weight is a weight carried throughout the mission to protect the

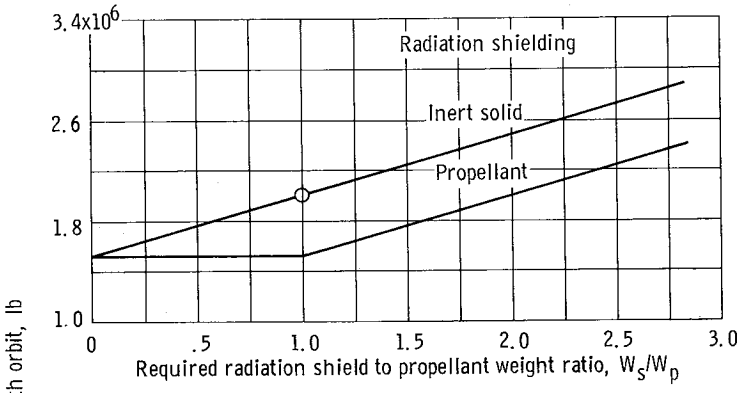

(a) Effect of required radiation shield weight. Mission duration, 420 days; propellant weight, 37 000 pounds.

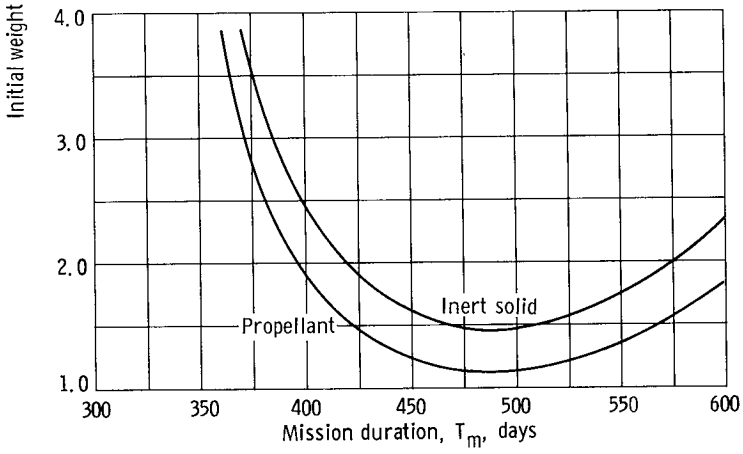

(b) Variation of initial weight in Earth orbit with mission duration. Weight of radiation shield equal to propellant weight, 37 000 pounds.

Figure 17. - Effect of using Earth deceleration stage propellant for radiation shielding. Atmospheric braking at Earth from 52 000 fps; nuclear propulsion.

crew from space radiation. In the previous figures 37 000 pounds of shielding was carried for the fast trips and 15 000 pounds for the slow trips for reasons subsequently discussed. This shielding served only the shielding function. In this section more detailed consideration will be given to the effect of two aspects of the shielding problem on the IWIEO:

(1) The use of propellant for shielding

(2) The effect of the allowable crew dose

Propellant for radiation shielding.- The propellant for deceleration at Earth is carried until the end of the trip. It can be used for radiation shielding, and the advantage for doing so is discussed with the aid of figure 17(a). The life-support system, the samples gathered at Mars, and other vehicle systems can also possibly contribute to radiation shielding. Their effect is generally less than the effect of using the propellant for shielding and is not considered herein. The IWIEO is presented against the ratio of required radiation shielding weight to the weight of propellant approaching Earth, for inert shielding and propellant shielding.

The propellant weight for the Earth deceleration in this illustration is 37 000 pounds, which corresponds to the 420-day mission with an atmospheric entry velocity of 52 000 fps. The previous calculations correspond to the circled point, that is, to inert shielding that serves only the shielding function and with a shield weight equal to the propellant weight required for deceleration, $W_s/W_p = 1.0$. For the case of inert shielding (upper curve), the IWIEO increases or decreases linearly from the circled point with increases or decreases in the required shield weight. If the required shield weight is zero ($W_s/W_p = 0$), the IWIEO is 24 percent less than that for the circled point.

If propellant is used for shielding (lower curve), then the IWIEO is independent of the shield weight as long as the required shielding weight is less than the propellant weight;

that is, $W_s/W_p < 1.0$. Also the IWIEO is at a level 24 percent below the case of inert shielding (circled point). For a still larger shield weight ($W_s/W_p > 1.0$), the IWIEO again increases with increasing shield weight. It can be seen from these curves that the greatest percent reduction in IWIEO for using propellant for shielding occurs when the shield and propellant weights coincide ($W_s/W_p = 1.0$). If the shield weight is small or large compared with the propellant, the advantage of propellant shielding is diminished.

Another implication of these calculations is that there is no reduction in IWIEO for higher atmospheric entry velocities if the shield weight is equal to the propellant weight for an Earth atmospheric entry velocity of 52 000 fps. In terms of figure 15(b) (p. 36), which is for inert shielding, the reduction in IWIEO for increasing the entry velocity from 52 000 to 67 000 fps can also be achieved while retaining the 52 000-feet-per-second entry velocity by eliminating the inert shielding and using the Earth deceleration propellant for shielding.

The effect on IWIEO when using propellant shielding as compared with using inert shielding of 37 000 pounds is shown in figure 17(b) as a function of mission duration. Propellant shielding can reduce the IWIEO about 24 percent for the fast trips near minimum weight. This concept is of little importance for the slower trips ($T_m > 700$ days) because the atmospheric entry velocities are within the expected future technology, that is, less than 45 000 fps.

Some of the physical characteristics that are desirable for fluids when they serve as both radiation shielding and propellants are the following:

(1) High specific impulse to reduce the propellant weight

(2) Good radiation shielding characteristics, which means high percentage of hydrogen or low Z atoms; for example, the combinations $BeH_2 + H_2O_2$ and $B_2H_6 + OF_2$

(3) High density for low structural weights and high values of shield surface density (lb/sq ft) for a given weight

(4) Low sensitivity to radiation, that is, little or no decomposition or deterioration due to radiation

(5) Room temperature storability for compatibility with the crew environmental requirements

(6) Low toxicity in case of a leak

(7) Insensitive to meteoroid shocks

(8) Pumpable for transfer from command module shield to the Earth deceleration stage tanks

Candidate chemical propellants are $BeH_2 + H_2O_2$ (room temperature storables) and $B_2H_6 + OF_2$ (mild cryogenics). Hydrogen, which would be used with a nuclear propulsion system, has the disadvantages of low density and low temperature, which will cause system weight penalties that must be accounted for if hydrogen is to be considered for a radiation shield.

Effect of allowable crew dose. - Thus far somewhat arbitrary values have been taken for the radiation shield weight. The required shield weight is determined by the incident radiation flux, the shielded volume, the interposed shielding density, and the allowable dose to the crew. The present shielding analysis is discussed in detail in appendix B. Some of the important effects are reviewed herein. The two major categories of radiation dose are the background radiation and the class 3+ solar flares. The dose from both these categories varies with mission duration. Also the dose from the class 3+ flares varies with mission perihelion.

The background radiation is taken as the sum of the doses from the smaller solar flares, which have a frequency higher than one per month, and the dose from the galactic radiation. For the shield surface densities considered here, 300 pounds per square foot or less, the dose from galactic radiation is not attenuated but slightly increased because of the secondary radiation generated in the shielding. This dose is taken as independent of shielding weight. The dose from the frequent solar flares is assumed to be that in the living module, which has a shield surface density of 6 pounds per square foot.

The galactic radiation tends to vary inversely with the solar activity (because of the associated solar magnetic fields), while the dose from the smaller solar flares tends to vary directly with solar activity. The same type of compensation tends to occur with distance from the Sun. Hence, the dose due to background radiation is assumed to be essentially independent of launch year and trajectory, and it was taken as 1.4 rem per week. The accumulated background radiation dose thus depends only on mission duration.

For flares of once a month frequency, the crew is assumed to be in the command module where the total dose will be small, that is, less than 1 rem.

The giant solar flares of the 3+ class occur with an average frequency of about once in 4 years. The flux from these flares is assumed to be that of the envelope flare of reference 32 and to vary inversely with the square of the distance from the Sun. For shield design purposes, one such flare is assumed to occur at or near the mission perihelion although the probability of this occurring is rather remote. The mission perihelions against trip duration are shown in figure 18. For the slow and intermediate trips ($T_m > 700$ days), the mission perihelions are at Earth so the flux measured at Earth will be that felt by the vehicle and crew. For the fast trips ($T_m < 600$ days), the mission perihelions are as low as 0.36 astronomical unit for a 500-day trip. For the 420-day trip it is about 0.5 astronomical unit. In this case the flux would be four times that at Earth's distance. Giant solar flares at low perihelions can thus have an important influence on the required shield weights. The Earth's Van Allen belts contribute only a small dose, and Mars was considered to have no trapped radiation.

The previous sources expose the crew to primarily proton and neutron doses. Perhaps the least known of the factors affecting shield weight are the human body's ability to

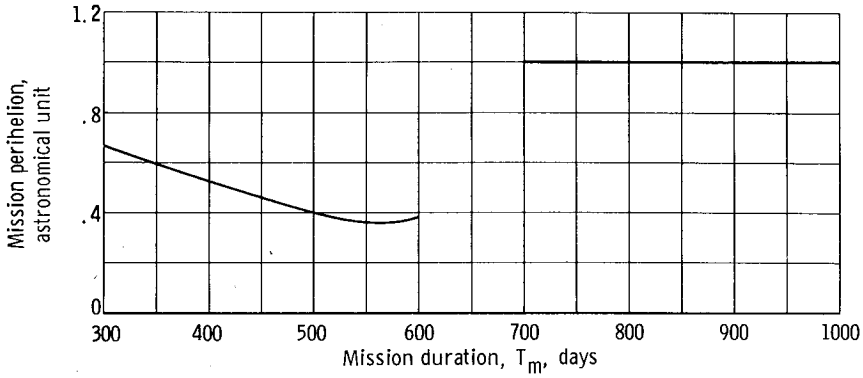

Figure 18. - Effect of mission duration on mission perihelion.

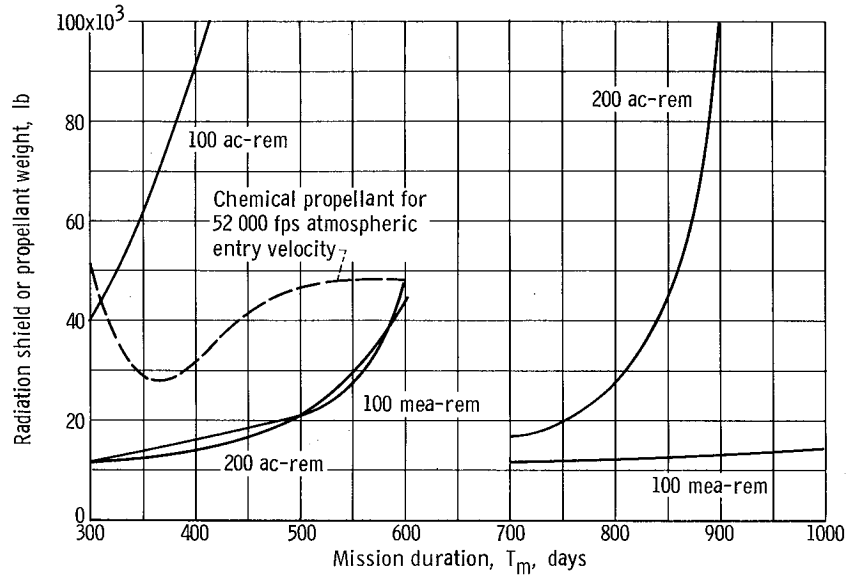

Figure 19. - Effect of crew dose and mission duration on radiation shield weights.

recover from proton and neutron doses received at various dose rates and the extent of permanent and/or temporary body damage that should be allowed. The effect of these two factors will be illustrated. As an example of the significance of the dose levels being considered, reference 33 states that for a 100-rem acute dose 10 percent of the crew will become ill but will not be permanently injured.

In figure 19 the solid curves present the shielding weight required around the command module to result in several values of dose to the crew. If it is assumed that the body does not recover from the radiation dose it receives, then the total accumulated during the trip should be limited. The upper solid curve to the left shows shield weights for 100-rem accumulated dose (the probability of not exceeding the doses given is 0.99). The shield weight rises sharply with increasing trip duration. The shield weights are below 100 000 pounds only for trips faster than 415 days. If the accumulated dose is allowed to go to 200 rem, the shield weights are less than 100 000 pounds for trips faster than 900 days. Now, for the fast trips ($T_m \leq 600$ days) the shield weights are

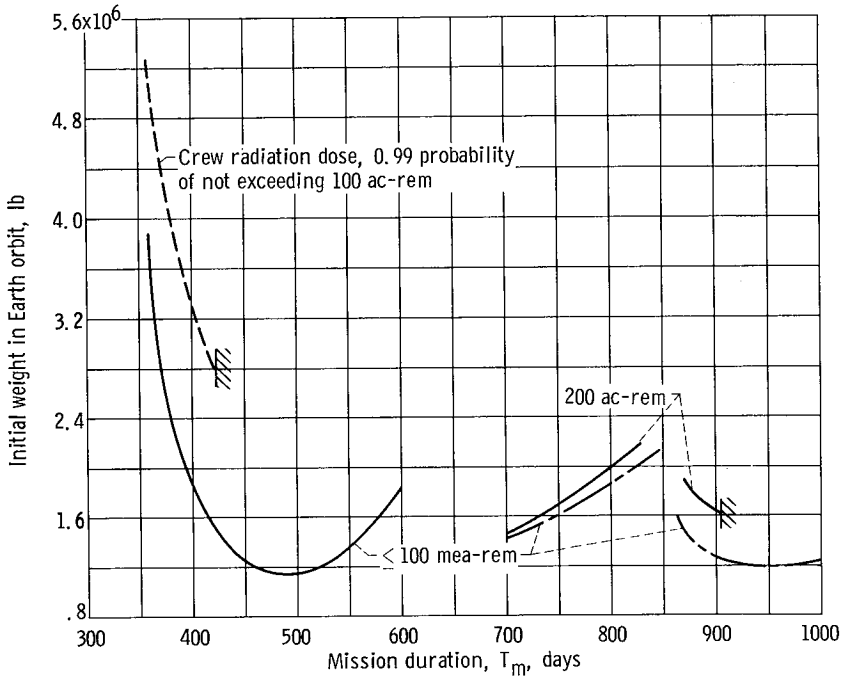

Figure 20. - Effect of crew radiation dose and mission duration on initial weight in Earth orbit. Atmospheric braking at Earth from 52 000 fps; Earth deceleration propellant provides partial shielding for fast trips; nuclear space propulsion.

generally less than the 37 000 pounds previously assumed.

A significant fraction of the accumulated dose results from the background radiation. If it is assumed that the body partially recovers from this radiation (ref. 34) then the contribution of the background radiation to the equivalent acute dose is much reduced, and as a consequence, larger doses from the giant flares can be tolerated. This in turn leads to lower shield weights. The curves labeled 100 mea-rem refer to the maximum equivalent acute dose in terms of Roentgen equivalent man that occurs during the trip. This maximum occurs immediately following the giant flare assumed at the mission perihelion for fast trips. For the slow trips the maximum exists after the giant flare assumed to occur near the end of the trip. When recovery is assumed, the shield weights are less than 15 000 pounds for the slow trips and again below 37 000 pounds for the fast trips.

The dashed curve of figure 19 shows the chemical propellant required for deceleration from the Earth approach velocity (fig. 15(a) p. 36) to 52 000 fps. This propellant weight exceeds the shielding weight required if the body recovers from the background radiation dose and the maximum equivalent acute dose is 100 rem, or if the allowable accummulated dose is 200 rem. For the case of propellant shielding no specific shield weight would be required for the fast trips.

The effect of the radiation shielding assumptions on the initial weight in Earth orbit is shown in figure 20. Atmospheric braking at Earth from 52 000 fps is assumed, and propellant is used for shielding for the fast trips. If the dose is limited to 100 rem

accummulated dose (dashed curve), only trip duration of less than 415 days are possible and the IWIEO's are above 2.8 million pounds. At 415 days, the shield weight has reached 100 000 pounds (fig. 19) and further increases in shield weight do not significantly reduce the dose (see appendix B). If 200 rem accumulated dose is allowed, the weights given by the solid curve result. For the fast trip the minimum IWIEO is reduced from 2.8 to about 1.15 million pounds for a 490-day trip. The lowest weight for the slow trips, 1.6 million pounds at 900 days, is greater than that for the fast trips.

If 100 mea-rem is the limit, the weights for the fast trips are again (coincidentally) given by the solid curve (fig. 20). For the slow trips (dash-dot curve), the weights are reduced. The effect of reducing the shield weight from 100 000 to 14 000 pounds for the 900-day trip (fig. 17) reduces the IWIEO from 1.6 to 1.2 million pounds. The slow trips for this case are comparable in weight to the fast trips.

The section on radiation shielding can now be summarized. The use of the Earth deceleration propellant for radiation shielding can reduce the initial weight in Earth orbit about 24 percent when the shield weight is about 37 000 pounds and when the propellant requirements and shielding requirements are about equal in weight. The maximum radiation dose that the crew should be allowed to receive and the permissible probability of exceeding a specified dose are not well established. The assumptions about the allowable radiation dose can have a marked effect on what trip durations are possible and on the level of the initial weights in Earth orbit.

Calculations from here on will use atmospheric braking at Earth from 52 000 fps with propellant shielding for the fast trips and 15 000 pounds of shielding for the slow trips unless otherwise noted. The resulting radiation dose is arbitrarily assumed to be acceptable.

Orbital Operations at Mars

The IWIEO depends on both the weight of the mission payload delivered to Mars and on the interplanetary ΔV to arrive at and depart from Mars. Both of these factors are affected by the operations at Mars. Considered in this section are the various parking orbits at Mars and several operational profiles for takeoff from the Mars surface to rendezvous with the spaceship in orbit.

Mars parking orbit. - For most of this discussion the Mars parking orbit is assumed to be in that unique plane that contains Mars and the velocity vectors arriving and departing Mars. It is one of the functions of the guidance system to assure the attainment of this plane. It is further assumed that the landing operation take place in the plane of the parking orbit. The parking orbits analyzed and the maneuvers to arrive at and depart from these parking orbits are shown in figure 21. The parking orbits fall broadly into

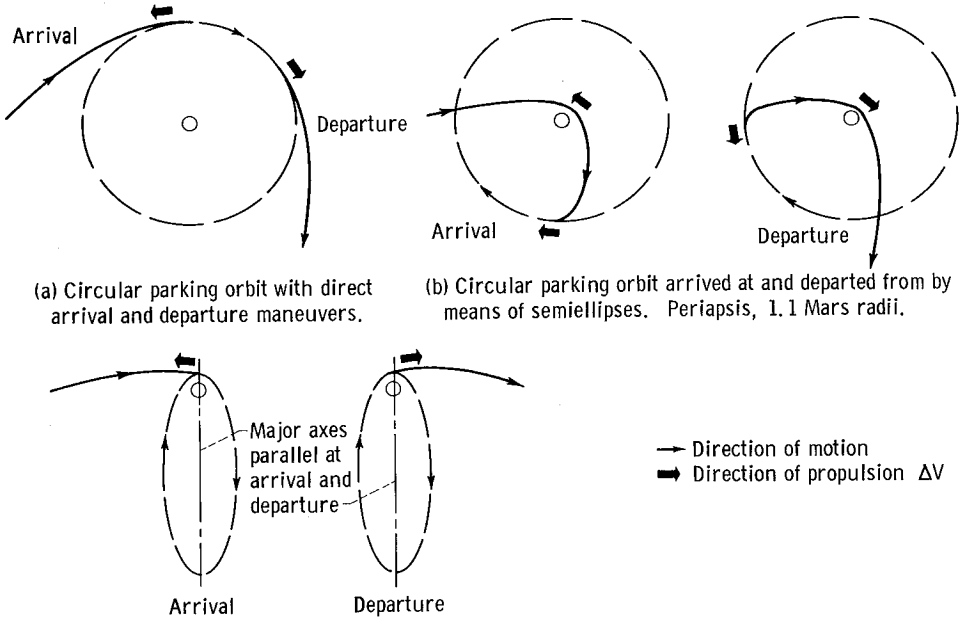

(a) Circular parking orbit with direct arrival and departure maneuvers.

(b) Circular parking orbit arrived at and departed from by means of semiellipses. Periapsis, 1.1 Mars radii.

(c) Parallel elliptic parking orbit. Periapsis, 1.1 Mars radii.

Figure 21. - Mars parking orbit and arrival and departure maneuvers.

two classes, circular and elliptic orbits. Figure 21(a) shows a circular orbit from which the spaceship enters and departs directly. The previous calculations have assumed such an orbit at 1.1 Mars radii. In general, the parking orbit radius could be any value, and the effect of parking orbit radius will be studied. Figure 21(b) shows a circular parking orbit that is attained at arrival by means of a semiellipse with a periapsis radius of 1.1 Mars radii and an apapsis at the circular parking orbit radius. The major deceleration maneuver occurs at the periapsis. A small posigrade thrust is required at apoapsis to circularize the elliptical trajectory. The departure maneuver is the reverse of that at arrival. Again a range of parking orbit radii will be considered, but the semiellipse periapsis is kept constant at 1.1 radii.

Figure 21(c) shows "parallel elliptic" parking orbits for which the major axes of the parking ellipse are parallel at arrival and departure. Arrival and departure from the elliptical parking orbit is assumed to take place from the periapsis with tangential thrusting. This is the most efficient manner for the propulsive maneuvers to occur. It is implied here that the resulting interplanetary trajectories are the required ones.

The relative merit of these orbits will be considered in terms of the following:

(1) Their compatibility with the interplanetary trajectory

(2) Their orbital period

(3) The ΔV savings afforded the interplanetary maneuvers

(4) The Mars landing system weight

(5) Their effect on the initial weight in Earth orbit

One of the advantages of the circular parking orbit (figs 21(a) and (b)) is that the ΔV's

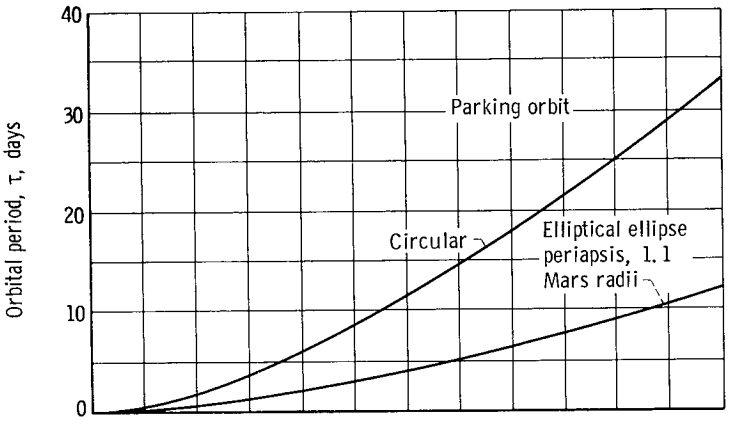

(a) Parking orbit periods.

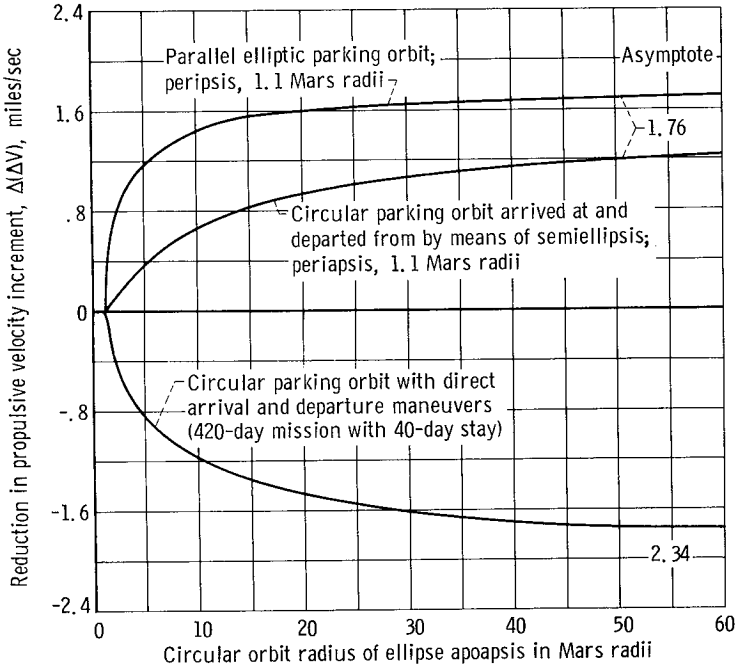

(b) Reduction in propulsive velocity increment.

Figure 22. - Mars parking orbit characteristics.

at Mars using this type of orbit are independent of the direction of the interplanetary arrival and departure velocity vectors; that is, any direction is permissible. This is not the case for the parallel elliptical parking orbit. The possibility of achieving an elliptical parking orbit is discussed later in this section.

The period in days of the circular and elliptical parking orbits is shown in figure 22(a) as a function of the circular orbit radius or ellipse apoapsis. The period increases with increasing parking orbit radius (or apoapsis) and is greater for the circular orbits than for the elliptical orbits. Several factors influence the period to be preferred. For example, if the Mars arrival and departure velocity vectors have the same direction, then the stay time must be an integral multiple of the orbital period. For a 40-day stay, the orbital period could be 40, 20, or 10 etc. days. If the possibility of an early or late departure is to be allowed, the smaller periods are preferred. A circular orbit with a period of 10 days (radius of 27 Mars surface radii) has been assumed for some of the subsequent calculations.

Another factor to be considered is the loss in time available for surface exploration. For instance, assume that the landing operation is initiated from the apoapsis of a parking ellipse and the stay time is defined to be that between the major arrival and departure maneuvers which occur at the periapsis of the parking ellipse. Then, the time lapse from arrival to a landing is the time from the ellipse periapsis to apoapsis where the landing maneuver is initiated plus approximately the same amount of time to travel from the apoapsis to the surface, or approximately the period of the vehicle in the ellipse. A similar time loss may occur for the takeoff and departure maneuver. For the previously mentioned apoapsis of 27 Mars radii the total lost surface time can be 7.4 days. This time

loss is the same for a circular parking orbit with a radius of 27 Mars radii when the circular orbit is arrived at and departed from by means of semiellipses. This time loss can, of course, be reduced by reducing the parking orbit radius (or apoapsis in the case of the ellipse).

There are also other possibilities for reducing the time loss on the surface while still retaining a long period parking orbit for the spaceship:

(1) The landing vehicle could rocket brake and enter the Mars atmosphere directly from the interplanetary trajectory rather than from the spaceship parking orbit. Rocket braking may even be unnecessary.

(2) The landing maneuver could be initiated near the initial periapsis of the ellipse (or semiellipse) and involve only a short period ellipse for the landing maneuver.

(3) Rendezvous for departure could take place near the parking ellipse (or departure semiellipse) periapsis rather than at the ellipse apoapsis.

Most of these possibilities would tend to give Mars landing and takeoff system weights slightly less than those to be shown.

As was previously mentioned, the prior calculations of IWIEO were made by using circular parking orbits at 1.1 Mars radii. The interplanetary ΔV data of figure 16 (p. 37) and tables IV (pp. 18 and 19) and V (pp. 20 and 21) are also for arriving and departing Mars from a 1.1 Mars radii circular parking orbit. Figure 22(b) shows the change in the interplanetary ΔV, $\Delta(\Delta V)$ (i.e., the sum of changes for arriving and departing Mars) with change in the parking orbit radius or apoapsis. The upper solid curve is the reduction in ΔV when a parallel elliptic parking orbit is used. For a given apoapsis (radius), the ΔV savings is greatest for this type of parking orbit. The ΔV savings rises sharply for increases of apoapsis up to about 10 Mars radii ($\overline{r}_a = 10$) and then increases more slowly for greater apoapsis. The asymptotic value ($\overline{r}_a \rightarrow \infty$) is 1.76 miles per second and is noted on the curve. At the previously suggested value of $\overline{r}_a = 27$, the $\Delta(\Delta V)$ is 1.64 miles per second reduction in ΔV. This value may be compared with the total mission ΔV of about 11 miles per second for a 490-day trip that uses atmospheric braking from 52 000 fps at Earth.

The middle solid curve is the reduction in ΔV when circular parking orbits arrived at and departed from by means of a semiellipse are used (fig. 21(b)). The ΔV savings increases considerably less rapidly with parking orbit radius even though the asymptotic value is the same as for the elliptical orbit case. At $\overline{r}_a = 27$ the ΔV savings is 1.03 miles per second.

In the form that these results are presented, the ΔV savings given by the upper two lines are equally distributed between the arrival and departure maneuver and are independent of mission duration (i.e., independent of the interplanetary trajectory and the required hyperbolic excess velocity). The lowest curve in figure 21(a) gives the increase in ΔV required to arrive and leave directly from circular parking orbits of various

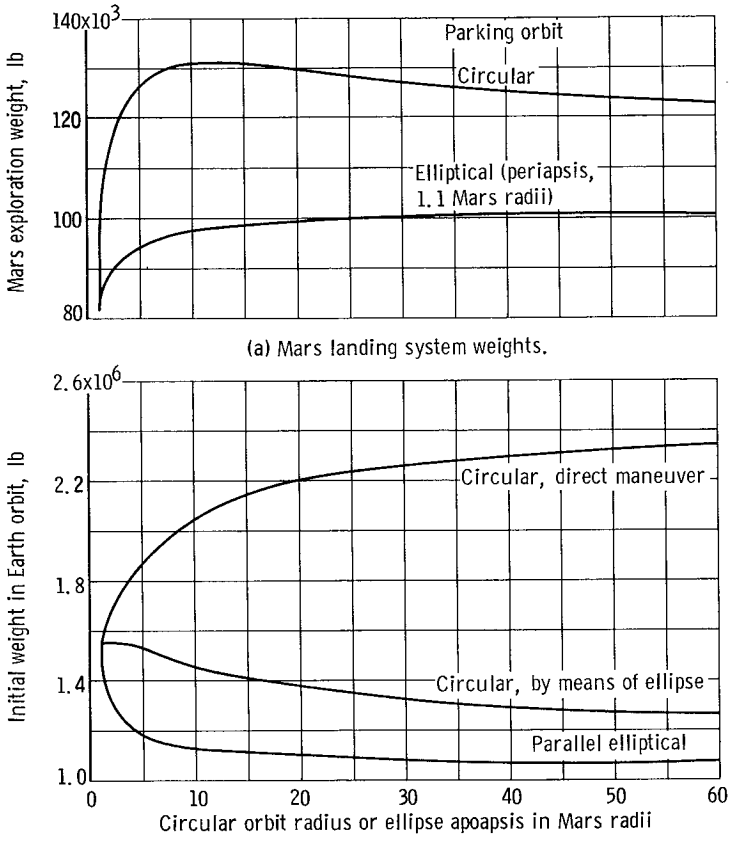

(a) Mars landing system weights.

(b) Initial weight in Earth orbit. Atmospheric braking at Earth from 52 000 fps; propellant shielding; nuclear space propulsion.

Figure 23. - Effect of Mars parking orbit on Mars landing system weights and initial weight in Earth orbit. Mission duration, 420 days; stay time, 40 days; single-stage Mars takeoff profile with 430-second specific impulse.

radii. This increase in the ΔV does depend on the mission time (i.e., the hyperbolic excesss velocity). The values shown are for the 420-day trip. For this type of maneuver (i.e., direct entry and leaving of a circular parking orbit) the low circular orbit gives the lowest ΔV.

Several of the parking orbits considered offer reductions in the interplanetary ΔV. However, these orbits are also associated with a corresponding increase in the ΔV required of the Mars landing system to takeoff from the Mars surface and rendezvous with the spaceship. (The landing and takeoff ΔV's are presented in appendix C.) This increase in the takeoff ΔV results in an increase in the landing system weight as indicated by the Mars exploration weights shown in figure 23(a). The Mars exploration weight is the landing system weight plus the orbital payload of 6500 pounds. These weights apply for missions with a 40-day stay that use a single-stage takeoff operational profile and chemical propulsion having a specific impulse of 430 seconds. The Mars landing system weight is about 82 000 pounds for a parking orbit with $\bar{r}_c = 1.1$. As the circular parking orbit radius increases, the weight increases to 131 000 pounds for $\bar{r}_c = 12$ and then decreases slightly to 127 000 pounds at $\bar{r}_c = 27$. For elliptic parking orbits the weights reach about 100 000 pounds at $\bar{r}_a = 27$.

Finally the landing system weights and interplanetary ΔV's for the various parking orbits are combined to yield the IWIEO as shown in figure 23(b). These calculations were made for the 420-day mission with a 40-day stay and use atmospheric braking at Earth from 52 000 fps and propellant for radiation shielding. The upper curve is for direct entry into circular parking orbits of various radii (fig. 21(a)). The lowest weight (1.55 million lb) occurs for a parking orbit of $\bar{r}_c = 1.1$, which is the parking orbit assumed in the previous calculations. Higher radii yield large weight penalties. Thus direct entry and departure from high circular orbits is not an attractive mode of operation.

The middle curve of figure 21(b) gives weights for a circular parking orbit using a

semiellipse for the arrival and departure maneuver. At $\bar{r}_c = 27$ the IWIEO is 1.34 million pounds as compared with 1.55 for $\bar{r}_c = 1.1$, which is a 14-percent reduction in weight. A slightly larger weight reduction is possible if higher parking orbit radii are acceptable. In this case, the increase in landing system weight (fig. 23(a)) is more than offset by the effect of the reduction in interplanetary ΔV (fig. 22(b)).

The parallel elliptic parking orbit gives the lowest weights. At $\bar{r}_a = 27$ the IWIEO is 1.09 million pounds, which is 30 percent less than that of $\bar{r}_c = 1.1$. There is little or no additional benefit for an ellipse with a higher apoapsis. Apoapsis values as low as 5 or 10 Mars radii still show attractive weight reductions.

The discussion of Mars parking orbits as compared with a low circular parking orbit can now be summarized. First of all, direct entry and departure from high circular orbits is not attractive. Entry and departure from a circular orbit at 27 Mars radii by means of a semiellipse maneuver offers about a 14-percent weight savings but requires two more engine restarts than the low circular orbit. The parallel elliptic parking orbit with an apoapsis of 27 radii offers a 30-percent weight savings.

Mars takeoff profile. - The previous discussion on the parking orbit assumed a single-stage takeoff vehicle. There are, however, other modes of operation that are attractive. The additional modes of operation considered here are a two-stage takeoff and a so-called tanker mode. These modes will affect the landing system weights but not the interplanetary ΔV's. In the two-stage mode of operation, the total required takeoff ΔV is equally divided between the two stages.

The tanker mode is best described by an example. The landing operation begins, for instance, in the high circular parking orbit of the spaceship. The manned landing vehicle is placed on a trajectory interesecting the atmosphere and lands by using atmospheric braking and a terminal retrorocket. A tanker is maneuvered by propulsion into a low circular parking orbit $\bar{r}_c = 1.1$. The manned lander contains enough propellant to take off and rendezvous with the tanker where it refuels and then accelerates again to rendezvous with the spaceship in its orbit. The landing system weights against parking orbit radius are shown in figure 24(a) again for an engine specific impulse of 430 seconds. For the tanker mode, these weights include the tanker weight. The general shapes of the curves are similar to those of figure 23(a) so the discussion will center on the effects at $\bar{r} = 27$. The solid curves apply for a landing and takeoff to a circular parking orbit. At $\bar{r}_c = 27$ the single-stage takeoff system weighs 127 000 pounds, a two-stage system weighs 117 000 pounds, and the tanker mode gives a weight of 97 000 pounds.

If the tanker mode of operation is applied to the elliptic parking orbit (dashed curves), the landing system weight is reduced to 83 000 pounds as compared with 100 000 pounds for a single-stage mode of operation. When the tanker mode is used with an elliptical parking orbit there is little increase in landing system weight with increasing ellipse apoapsis.

The corresponding changes in IWIEO are shown in figure 24(b). For circular parking

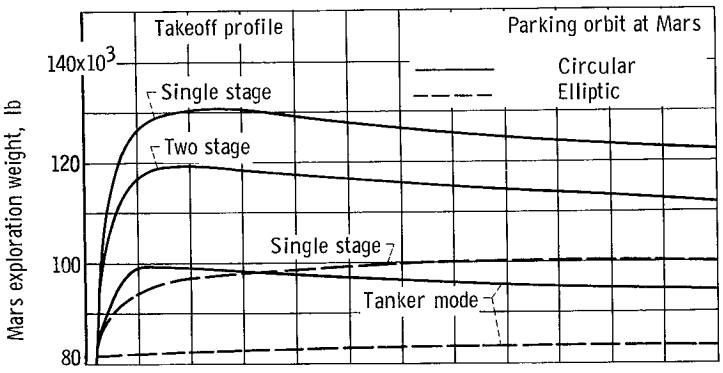

(a) Mars landing system weights.

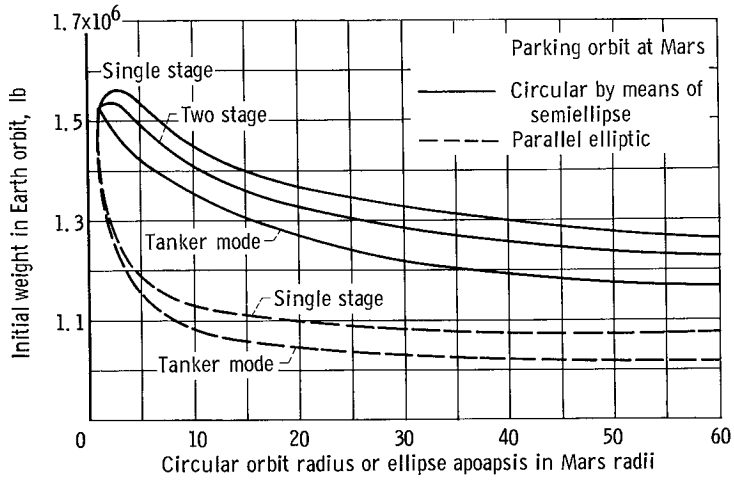

(b) Initial weight in Earth orbit. Atmospheric braking at Earth from 52 000 fps; propellant shielding; nuclear space propulsion.

Figure 24. - Effect of Mars takeoff profile on landing system weights and initial weight in Earth orbit. Mission duration, 420 days; stay time, 40 days; Mars takeoff specific impulse, 430 seconds.

orbits at $\bar{r}_c = 27$, the two-stage and tanker modes yield initial weights of 1.3 and 1.23 million pounds, respectively, as compared with 1.34 million pounds for the single-stage mode of takeoff. For elliptic orbits the tanker mode yields a weight of 1.04 as compared with 1.09 million for the single-stage mode. The tanker mode thus offers 8 and 5 percent savings in weight for circular and elliptic parking orbits respectively, at $\bar{r} = 27$.

Although the tanker mode of operation is more complex than a single-stage mode in that it involves an additional rendezvous, the rendezvous technique should be well established by the end of the Gemini and Apollo projects. Also, it can be anticipated that the tanker mode of operation will be less sensitive to specific impulse variations and structural weight fractions than the other modes of operation.

This discussion may be summarized by saying that the tanker mode of operation offers reduced weights when compared with either one- or two-stage takeoff profiles for high circular or elliptic spaceship parking orbits.

Possibility of attaining parallel elliptic parking orbit performance. - The previous discussion has shown that significant weight reductions accrue if a parallel elliptic parking orbit is used. Strictly speaking, to achieve the benefits shown, the interplanetary propulsion to arrive and leave from the ellipse must be applied at its periapsis and tangent to the direction of the motion. This can be done only if the trajectories at the Mars periapsis arriving from and returning to Earth are matched in direction. This is not generally the situation. Approaches to achieving elliptic parking orbit performance will be discussed briefly here.

First, one can search for interplanetary round trips that have cotangential arriving and leaving velocity vectors at Mars. One such class of trajectories is the nonstop (zero stay time) gravity turn round trips discussed, for example, in reference 35. The

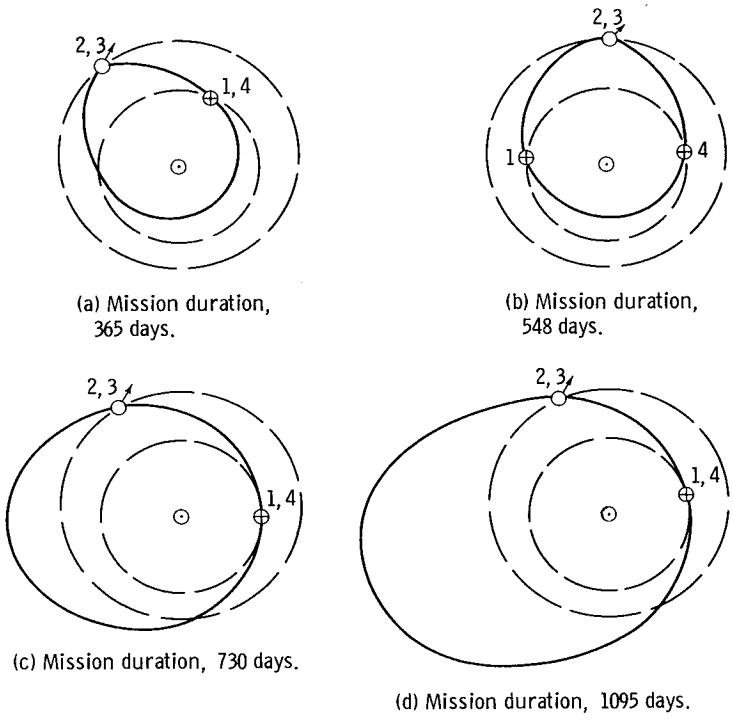

Figure 25. - Mars nonstop round-trip trajectories or zero stay time stopover trajectories with cotangential Mars arrival and departure velocity vectors. Launch year, 1979.

trajectories are continuous at Mars and hence cotangential. These trajectories occur in the vicinity of orbits that are synchronous with the Earth's orbit about the Sun, that is, near 365-, 550-, 730-, and 1100-day trip times. Such trajectories are illustrated in figure 25. In reference 35, gravity turns in 1979-80 were found near 380 days and over a range of trip times from 520 to 580 days. One would expect to find stopover trips with short stay times and with cotangential arrival and departure trajectories in the same vicinity. However, they are not necessarily minimum ΔV trips. Minimum ΔV trips with cotangential arriving and leaving vectors and a 40-day stay occur for trips of 485 and 610 days. Trips of these durations may thus be of interest. The 910-day trip with a short stay time is also a comparatively low-energy trip, though probably not one of interest.

Second, if the required turning angle at Mars is small, firing tangential to the velocity vector along the ellipse but at a position away from the periapsis of the ellipse will yield only a small ΔV penalty. For some range of turning angles this procedure will give lower ΔV's than going to a circular parking by means of the semiellipse. It was pointed out previously that the ΔV's associated with a circular parking orbit are independent of the interplanetary arrival and departure directions.

Third, if the vehicle thrust-to-weight ratio is small enough, appreciable turning during the deceleration and acceleration maneuvers at Mars will occur. For some acceleration levels, a parallel parking ellipse can be established. In this case there is a tradeoff between the ΔV savings for the elliptical parking orbit, the gravity losses during propulsion, and the engine weight. Also, by thrusting at an angle of attack, significant turning can be generated for little increase in the characteristic ΔV.

Fourth, when turning is required, it may be most efficient to do the turning at the Mars sphere of influence as was found in reference 35.

Fifth, if atmospheric braking from the hyperbolic approach velocity to orbit is used at Mars, the atmospheric maneuver can also be used to generate the required turning at Mars to establish an ellipse appropriately oriented for departure. The combined deceleration and turning will determine a vehicle lift-drag ratio.

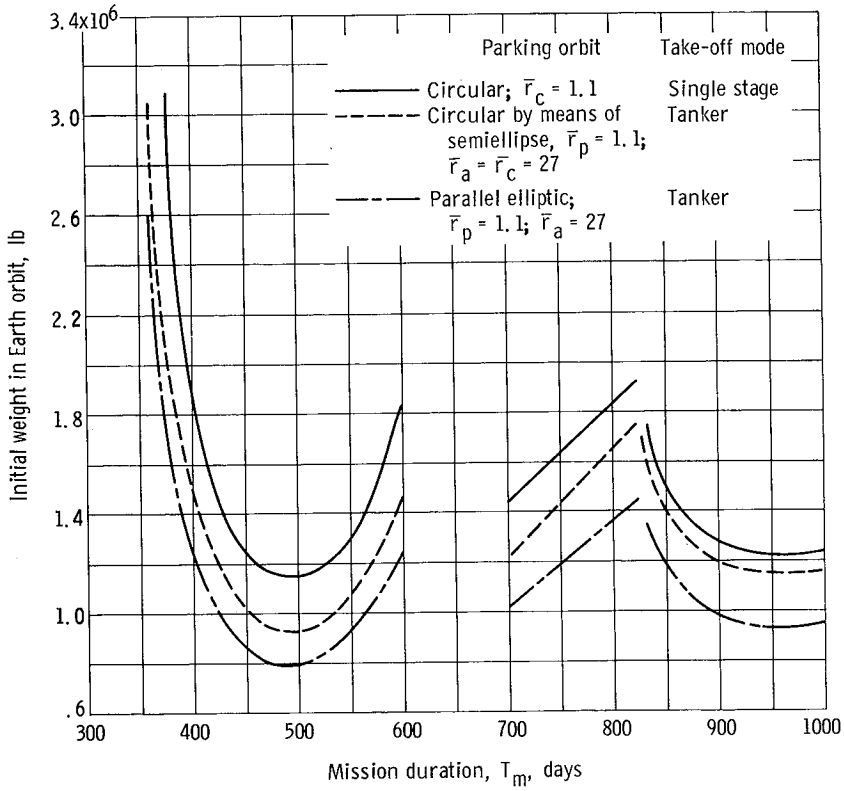

Figure 26. - Variation of Mars parking orbit effect with mission duration. Atmospheric braking at Earth from 52 000 fps; propellant shielding for fast trips; 15 000 pounds of inert shielding for slow trips; nuclear space propulsion.

Sixth, the rotation of the line of apsides due to the planet oblateness may help provide the required shift in the ellipse.

Seventh, the previous discussion has dealt with maneuvers in the plane of the interplanetary trajectory. Another interesting possibility is an elliptic parking orbit out of this plane. To acquire the desired outbound direction a plane change is made at the ellipse apoapsis. The required ΔV is small if the apoapsis is high. In practice, for example, an elliptical parking orbit with a 5 or 10 radii apoapsis could be used with a maneuver to a higher apoapsis and a plane change made only at departure time.

There are a number of approaches for attaining parallel elliptical parking orbit performance. This area warrants continued study. In general, the parallel elliptical parking orbit assumption yields a lower bound in IWIEO as a function of parking orbit choice. This bound can be approached by practical techniques.

Effect of mission duration on parking orbit effect. - The previous calculations were for a mission duration of 420 days. The effect of parking orbit selection at other mission durations is shown in figure 26. The initial weights in Earth orbit are compared for the low circular parking orbit, a circular parking orbit arrived at and departed from by means of a semiellipse, and a parallel elliptic parking orbit. The latter two parking

orbits have a radius (apoapsis) of 27 Mars radii, and the tanker mode of takeoff operation is used. The high circular and elliptic orbit give weight reductions at all mission durations. The minimum IWIEO occurs at about 480 days and is 0.79 million pounds. A second local minimum occurs at 950 days and 0.93 million pounds.

Comments on assumptions. - The Mars orbital operations have been discussed presuming Mars is spherical. Mars is actually oblate, which causes the parking orbital plane to change with time and the line of apsides of the parking orbit to rotate with time. The plane of the parking orbit at arrival must be selected so that it rotates to the desired departure plane during the stay time at Mars. Similarly, in designing trajectories for parallel elliptic parking orbits, account must be taken of the rotation of the line of apsides during the stay time. Both the plane rotation and the rotation of the line of apsides vary directly with the number of revolutions made by the space vehicle about Mars (ref. 36); thus, a parking orbit that makes only a few revolutions during the Mars stay will be little affected by the planet oblateness. This may be an advantage for the high circular and elliptic parking orbits which have long periods.

The Mars landing has been assumed to take place in the plane of the parking orbit. For a low circular parking orbit a large ΔV or a lifting landing vehicle would be required to achieve a landing appreciably outside the parking orbit plane. For a highly elliptic parking orbit, a landing outside the orbit plane can be achieved for little expense in ΔV to land or takeoff. This is still another advantage for the highly elliptic or high circular parking orbit.

Atmospheric Braking at Mars

It was previously shown that atmospheric braking at Earth could markedly reduce the IWIEO. This leads naturally to an interest in the effect of atmospheric braking of the entire spaceship at Mars. This effect is examined here as a function of the parking orbit at Mars, the structure plus heat protection weight of the Mars entry system, and the mission duration. In the previous mission profiles the complete spaceship was braked by propulsion from the hyperbolic approach velocity to a parking orbit about Mars. The vehicle which lands on the Mars surface from the parking orbit uses atmospheric braking in every case.

The interplanetary trajectories used in this case differ from those of the preceeding calculations. The launch date and outbound leg time for the preceeding calculations were selected to give a minimum $\sum_{1}^{4} \Delta V$ for a specified total mission duration and stay time where ΔV_4 at Earth return is that for decelerating to a low circular parking orbit for

which the circular velocity is 26 000 fps. When entry velocities at Earth from 37 000 and 52 000 fps were considered, the ΔV was reduced by the difference between those velocities and 26 000 fps, a constant amount for any launch date. Because the ΔV is changed by a constant amount, the optimum launch date and outbound leg time are not changed (as in calculus, the addition of a constant to a function does not affect the value of the independent variable at which the function has an extremum). The same argument applies when the ΔV's are reduced by changing the parking orbit at Mars for the cases of elliptic orbits and the circular orbits arrived at and departed from by means of semiellipses.

The situation is different for atmospheric braking at Mars. For the previous mission the Mars approach velocity can be quite low, that is, less than 37 000 fps, and the entire deceleration hence can be taken by atmospheric braking. Often the $\Delta V_1 + \Delta V_3$ can be reduced by selecting launch dates and outbound leg times that increase the Mars atmospheric entry velocities. The trajectories considered in this section yield a minimum $\Delta V_1 + \Delta V_3$ and are presented in table V (pp. 20 and 21).

The feasibility of atmospheric braking at Mars from hyperbolic velocities to orbit (or to a landing) depends on the density of the atmosphere at Mars. The density of the atmosphere at the surface is of particular importance. Preliminary calculations indicate that a surface density of one-hundredth the Earth's atmospheric surface density is sufficient to permit atmospheric braking of vehicles with a surface loading of 100 pounds per square foot or less.

Effect of parking orbit. - To study how the effect of atmospheric braking at Mars varies with parking orbit the 420-day mission was again selected. The Mars atmospheric entry velocity for this trip is 33 500 fps. The atmospheric braking will be used to decelerate the spaceship from its hyperbolic Mars approach velocity into parking ellipses of various apoapses. The elliptic parking orbit was chosen rather than the circular orbit arrived at by a semiellipse because the orientation desired for the parking ellipse can be achieved during the atmospheric braking maneuver. For the 420-day mission a vehicle with a lift-drag ratio of 1/2 is adequate, for instance. The parallel elliptical parking orbit results in the lowest propulsive requirements as was pointed out previously. If a parallel elliptic parking orbit cannot be achieved without some ΔV penalty for the case of propulsive deceleration at Mars, then the relative advantage of atmospheric braking compared with propulsive braking will be somewhat greater than that to be shown.

In figure 27 the IWIEO for atmospheric braking at Mars is compared with that for propulsive deceleration. Curves of weight for three values of $(W_S/W_G)_{\sigma'}$ (ratio of Mars entry vehicle structure plus heat protection plus atmosphere approach guidance and control system weight to gross weight) are given. The abscissa is the apoapsis of the parking ellipse. The periapsis is 1.1 Mars radii. The tanker mode of takeoff operation for the Mars landing system was used, and the weights for the landing system were given in figure 24(a) (p. 50). At $\bar{r}_a = 1.1$, a limiting case occurs in that the parking orbit is

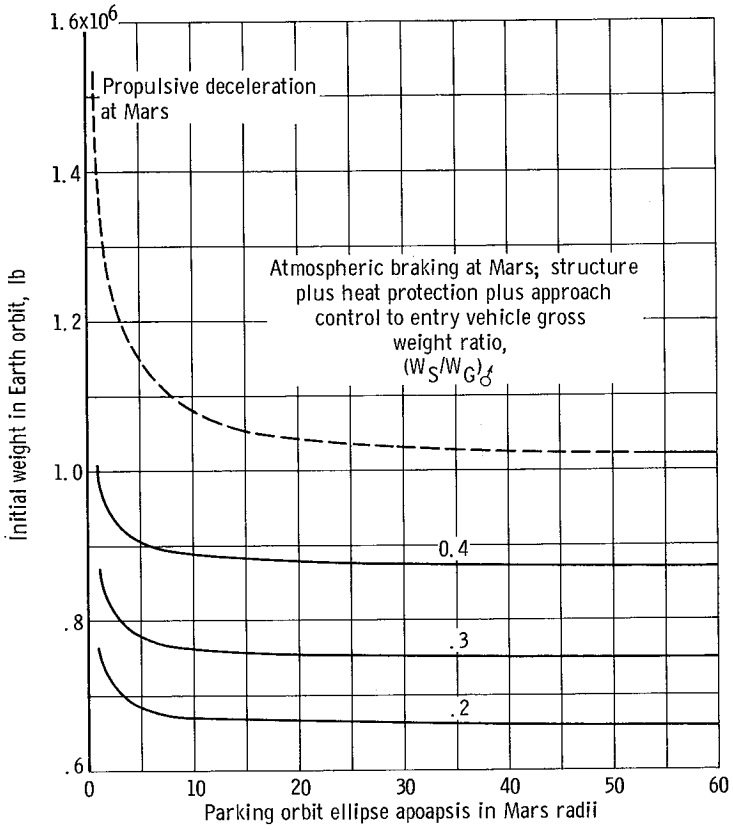

Figure 27. - Effect of atmospheric braking at Mars on initial weight in Earth orbit. Mission duration, 420 days; stay time, 40 days; parallel elliptic parking orbit with 1.1 Mars radii periapsis; atmospheric braking at Earth from 52 000 fps; nuclear space propulsion.

circular and the tanker weight zero.

The most salient point to be made with these curves is that there is a marked reduction in IWIEO for using atmospheric braking at Mars if the space vehicle is to be parked in a circular orbit at $\bar{r}_a = \bar{r}_c = 1.1$. The IWIEO is reduced from 1.54 to 0.87 million pounds, a 45-percent reduction, for $(W_S/W_G) = 0.3$ for the atmospheric braking vehicle. It is for this parking orbit that the largest velocity increment is absorbed in the atmospheric braking maneuver. The advantage of atmospheric braking is less but still substantial for larger values of $\bar{r}_a$; for example, at $\bar{r}_a = 27$ the IWIEO is reduced from 1.05 to 0.76 million pounds (27 percent), again for $(W_S/W_G)_{\sigma} = 0.3$.

Effect of structure plus heat protection weights. - A second effect illustrated by these curves is the effect of the structural plus heat protection fraction $(W_S/W_G)_{\sigma}$. At an $\bar{r}_a = 27$ doubling the structural fraction from 0.2 to 0.4 increases the IWIEO from 0.66 to 0.88 million pounds, an increase of 33 percent. Thus the structural plus heat protection fraction is an important parameter. But even for a value of the structural fraction that is believed conservative, 0.4, atmospheric braking is advantageous. The curves of the next figure are for $\bar{r}_a = 27$ and $(W_S/W_G)_{\sigma} = 0.3$ for those cases where atmospheric braking at Mars is used.

Effect of mission duration. - Figure 28 shows the Mars atmospheric entry velocities and the IWIEO as functions of mission duration. As was the case for atmospheric braking at Earth, the importance of atmospheric braking at Mars depends on the Mars approach velocities. These velocities are shown in figure 28(a). For trip durations of longer than 350 days the approach velocities are less than 37 000 fps, or less than Earth parabolic velocity. Hence, these velocities appear acceptable for atmospheric entry from a heat protection point of view. For the fast trips the entry velocities decrease from 37 000 fps for the 350-day trip to 20 000 fps for the 600-day trip. The entry velocities are about 34 000 fps for the trips of intermediate duration and drop to less than 24 000 fps for the slow trips.

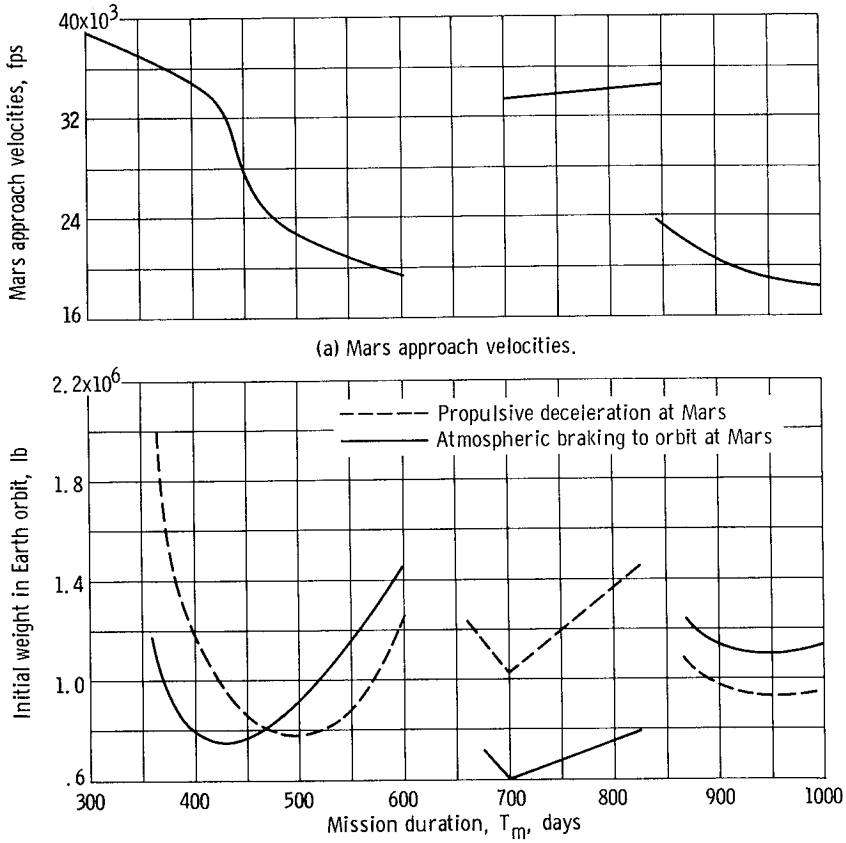

(a) Mars approach velocities.

(b) Initial weight in Earth orbit.

Figure 28. - Effect of mission duration on Mars atmospheric entry velocities and the importance of atmospheric braking at Mars. Atmospheric braking at Earth from 52 000 fps; propellant shielding for fast trips; 15 000 pounds shielding for slower trips; parallel elliptic parking orbit with 27 Mars radii apoapsis; structure plus heat protection for Mars atmospheric braking, 0.3 of entry gross weight; nuclear space propulsion.

The IWIEO for atmospheric braking at Mars are shown in figure 28(b) (solid curves). These weights are compared with those for propulsive braking (dashed curves). Parallel elliptic parking orbits with $\bar{r}_a = 27$ are assumed for both cases. For trip times less than 470 days atmospheric braking is an advantage. This is the region where the atmospheric entry velocities are high. The high entry velocities are an indication that atmospheric braking has given a large reduction in the required propulsive ΔV.

For the slow trips, $T_m > 850$ days, braking at Mars is a disadvantage in that it causes an increase in the IWIEO. Atmospheric braking increases the gross weight when the weight of structure and the heat protection for atmospheric braking exceed the propulsion system weight to accomplish the same deceleration.

A perhaps unexpected result shown in this figure is that the lowest IWIEO's occur for the intermediate trips. These low weights are readily understandable when the high Mars approach velocities for these trips are recalled (fig. 28(a)). It is also recalled that the Mars payload weights are less than those for the 900- to 1000-day trips (fig. 16(b), p. 37).

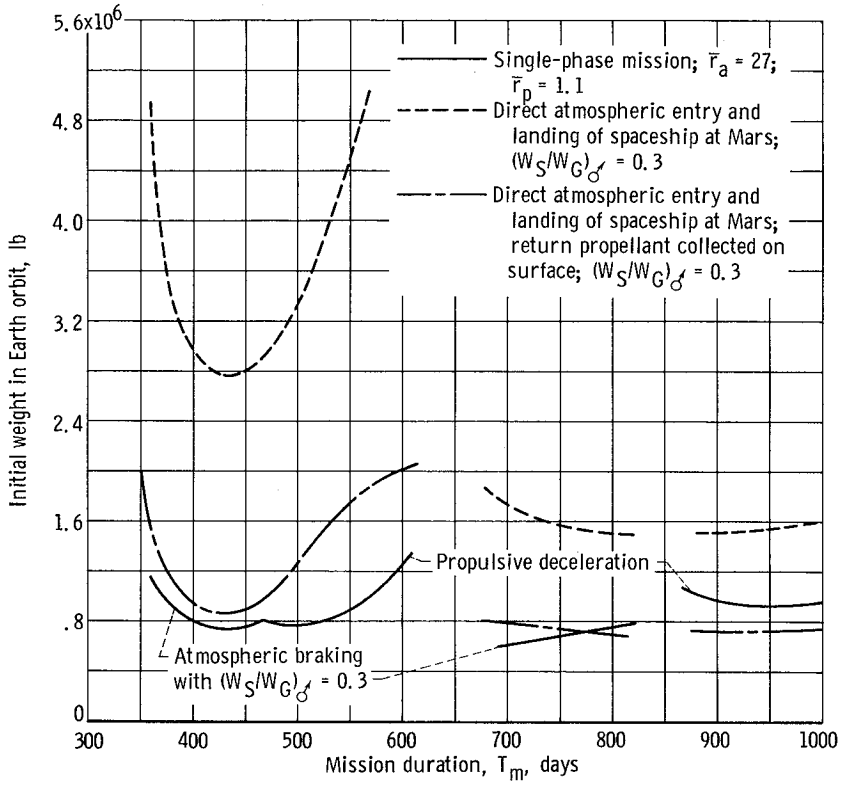

Figure 29. - Initial weight in Earth orbit for direct Mars landing with and without propellant collection at Mars for various mission durations. Atmospheric braking at Earth from 52 000 fps; propellant shielding for fast trips; 15 000 pounds of shielding for slow trips; nuclear space propulsion.

The lowest weight shown is 0.6 million pounds for the 700-day trip.

The discussion of atmospheric braking at Mars may be summarized by saying that atmospheric braking gives the greatest reductions in IWIEO when the greatest velocity increment is absorbed by atmospheric braking. Thus mission profiles using low circular parking orbits are benefited more than those using elliptic orbits. Also, missions with high Mars approach velocities benefit more than those with low approach velocities. High approach velocities occur for trips of intermediate durations, 700 to 800 days, and faster trips of less than about 470 days.

Direct Landing on Mars

It is recalled that the previous mission profiles all used a parking orbit at Mars. When atmospheric braking from the hyperbolic approach velocity to orbit is used at Mars one is led also to consider the possibility of atmospheric braking the entire spacecraft to a landing on the Mars surface, thus eliminating the parking orbit altogether. In particular, in this mode the propellant for the return to Earth and the Earth return mission payloads are carried to the Mars surface. Such a possibility is considered in figure 29,

which presents IWIEO against mission duration for several mission profiles. The solid line is the lowest IWIEO previously shown for using a parking orbit at Mars. The dashed line is for the direct landing of the complete spaceship. For the fast trips the weights for the direct landing mode are about three times those for the orbital mode. For the slow trips the factor is about 1.5. In general, the direct landing mode does not appear attractive on a weight basis although operationally it is the simplest.

Other Propellant Sources

For the previous mission profiles all the propellants and, of course, the hardware are assumed to originate on the Earth surface. Other sources of propellant such as at Mars, in Earth orbit, and on the Earth's Moon can be considered.

Propellant collection at Mars. - The import of propellant collection at Mars for the direct landing mode is shown in figure 29 (dash-dot curve). In this case, a source of hydrogen is assumed to exist on the Mars surface. No weight has been charged to the collection system, thus implying that either it is a very lightweight or it has been previously delivered. The weights for this mode of operation are comparable to the low weights achieved by the orbital modes. If the propellant collection system weight must be carried on the mission to Mars, its weight is most likely to be a small fraction of the collected propellant if it operates over a long period of time. Thus missions with a long stay time, that is, the mission durations of 800 to 1000 days are most likely to benefit from propellant collection.

Although not considered here, it may be anticipated that propellant collection in a Mars parking orbit would also yield reduction in IWIEO if a lightweight collection is hypothesized. In general, propellant collection at Mars is a possible way to achieve low IWIEO, but this mode is not a likely one for early missions.

Other propellant sources. - In addition to the Earth's surface and Mars there are several other possible sources of propellant that will be briefly considered, in Earth orbit and at the Earth's Moon.

Reference 37 describes a possible air collection system that orbits in the low density air at a high altitude about the Earth and uses a nuclear electric propulsion system to overcome the momentum of the collected air and the air drag. This system could collect oxygen from the atmosphere to be used in a chemical propulsion system for the Mars trip. Some indication of the potential advantage of such a scheme is given in table VI (p. 22) for trips of several durations. For a datum, the second column gives the ΔV required to launch propellant from the Earth's surface onto a trajectory to Mars, which is the conventional mode of operation. If the source of propellant is in an Earth orbit, the ΔV to acquire the Mars trajectory is reduced by a factor of from 2 to about 4. Not considering the weight of the collection system, this reduction in ΔV will result in a significant

reduction in the weight to be launched from the Earth's surface, although the initial weight in Earth orbit of the Mars mission vehicle itself would remain unaffected.

If the Moon is considered as a propellant source for the Mars mission, a base is needed on the Moon with a substantial electrical generating capacity and, for instance, a source of water either as ice or in chemical combination in the rocks. The water can be electrolyzed to yield hydrogen and oxygen for a chemical space propulsion system, or the hydrogen alone can be used as the expellant for the nuclear system. With the Moon as a propellant source the most efficient mode of operation appears to be to either rendezvous the propellant and spaceship during a close pass of the spaceship with the Moon (the subsequent discussion of a lunar swingby is appropriate), or to rendezvous the propellant and space vehicle at a point on the outbound leg to Mars beyond the Moon. In either case the ΔV to accelerate the propellant from the lunar surface to the outbound leg of the Mars trip is about the same and is given in the last column of table VI. Again there is a reduction factor of from 2 to 4 in the ΔV compared with the launch of propellant from the Earth's surface. (A rendezvous in a lunar orbit would require that the spaceship from Earth undergo the additional ΔV's of arriving at and leaving from the lunar rendezvous orbit.)

While each of the propellant collection and/or generation systems offers a significant potential ΔV advantage, the total system in turn implies a significant technological development and much added complexity. Propellant sources other than the Earth's surface are hence not attractive for the early manned Mars mission, although they are of interest for possible subsequent transportation systems.

Two-Phase Mission Profiles

The previous mission profiles were all single-phase profiles; that is, there was only one depart-from-Earth-orbit launch period (which occurred at the beginning of the mission) and all the components of the mission travelled together along the same trajectory. Considered here are a number of two-phase mission profiles; that is, missions that entail two or more launch periods.

Elliptical orbit pickup at Earth return. - In this mode the crew is enclosed in a lightweight capsule and propulsively decelerated into an elliptic parking orbit at Earth return. A recovery vehicle is then accelerated from Earth orbit to rendezvous with the Mars capsule and return the crew to the Earth's surface. A second Earth surface to orbit launch is thus required at the end of the mission to orbit the recovery system.

The application of the elliptic orbital pickup to the fast mission profiles is considered. Let all of the maneuvers through the chemical deceleration to 52 000 fps velocity relative to Earth occur as before. Then there are 13 850 pounds available for deceleration from

52 000 fps to an elliptic velocity, that is, a velocity less than 37 000 fps. In the previous cases, the 13 850 pounds were for an atmospheric entry vehicle that carried the crew through the deceleration from 52 000 fps to a landing on the Earth's surface. Based on the earlier discussion of Earth deceleration operations, a chemical stage is preferable to a nuclear one for the small payload to be decelerated for the profile under consideration. With a specific impulse of 430 seconds a total capsule weight of 3500 pounds can be decelerated to 36 800 fps. Of the total capsule weight about 2400 must be allowed for the real payload (i. e., crew, data, and samples). Thus 1100 pounds are available for a pressure capsule, a life support, and a communication system. This capsule is not subject to high g's and is not required to perform an atmospheric entry or landing so a light weight is possible.

If the previous capsule weight is acceptable, then the IWIEO shown on the previous figures for the fast trips with atmospheric entry from 52 000 fps applies also for the first phase of the elliptic orbital pickup mode.

The total weight required in Earth orbit is increased by the weight of the recovery system, which is estimated to be about 70 000 pounds. This weight, however, is launched near the end of the mission and does not require the use of the launch pad at mission launch time.

The elliptic orbital pickup mode would be relatively more attractive if for some reason the Earth atmospheric braking vehicle weights were larger than estimated or if the chemical rocket specific impulse were higher than assumed.

The two-phase elliptical orbital pickup mission profile is a possible alternative to the single-phase mission using atmospheric braking at Earth return, and this profile avoids the necessity of developing an Earth entry capability for velocities above 37 000 fps.

Hyperbolic rendezvous at Earth return. - This two-phase mission profile also applies primarily to fast trips. As was illustrated in the earlier discussion of atmospheric braking at Earth, the IWIEO at mission launch is quite sensitive to the Earth deceleration system weight. In the limit this system need not be carried on the Mars trajectory at all; instead, the Earth deceleration system can rendezvous with the Mars vehicle near Earth at Earth return as shown in figure 30(a). The recovery vehicle is first accelerated from the low circular parking orbit about Earth into a highly elliptical trajectory. On the inbound leg of the ellipse the recovery vehicle is accelerated a second time to match the velocity vector and position of the spaceship returning from Mars. The Mars crew then transfers to the Earth deceleration vehicle, and the Earth deceleration is accomplished, for example, by a propulsive deceleration from the approach velocity (if above 52 000 fps) to 52 000 fps followed by an atmospheric entry.

The propulsive velocity increments that must be applied to the recovery system are shown in table VII (p. 23) for several mission profiles and trip times. Columns 2 and 3 give the total ΔV that must be applied to the Earth deceleration system if it is carried

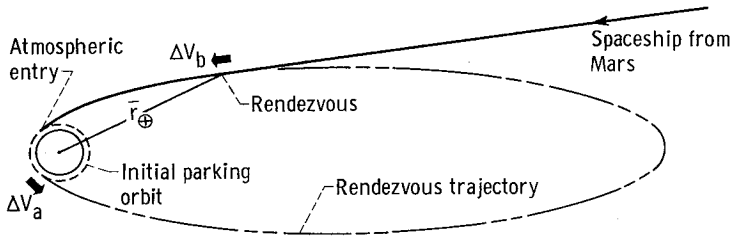

(a) Hyperbolic rendezvous at Earth return.

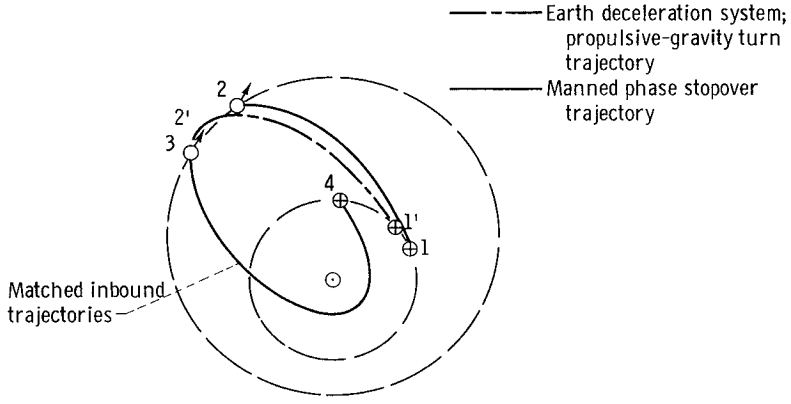

(b) Hyperbolic rendezvous at Mars departure.

Figure 30. - Trajectories for two-phase missions.

on the trajectory to Mars and accelerated back toward Earth. Column 2 assumes a low circular parking orbit and column 3 an elliptic parking orbit at Mars. Columns 4 and 5 apply for rendezvous of the recovery system with the spaceship near Earth. Column 4 is a limiting case where rendezvous takes place at 1. 1 Earth radii. Column 5 is the more practical case where rendezvous takes place at a distance of 10 Earth radii. When columns 2 and 3 are compared with 5 it is interesting to note that for trip times between 360 and 600 days, for instance, the propulsive ΔV to get the Earth deceleration system to the mission Earth approach velocity is about the same or lower for carrying the Earth deceleration system to Mars and back than for maneuvering near Earth. As a consequence, when compared with the single-phase profile, the profile with hyperbolic rendezvous at Earth will reduce the IWIEO at mission launch, but the total IWIEO, the sum of the weights for the mission and for the crew recovery system, will be greater. This is shown in figure 31 for the case of inert radiation shielding, a low circular parking orbit at Mars, and an atmospheric entry velocity at Earth not exceeding 52 000 fps. The solid line gives the IWIEO for the single-phase profile for which the Earth deceleration stage is carried to Mars and back and uses atmospheric braking from 52 000 fps. The solid curve is also the weight of the manned mission phase of the two-phase mission using elliptical orbit pickup at Earth return. The lowest curve (dashed) is the IWIEO for the

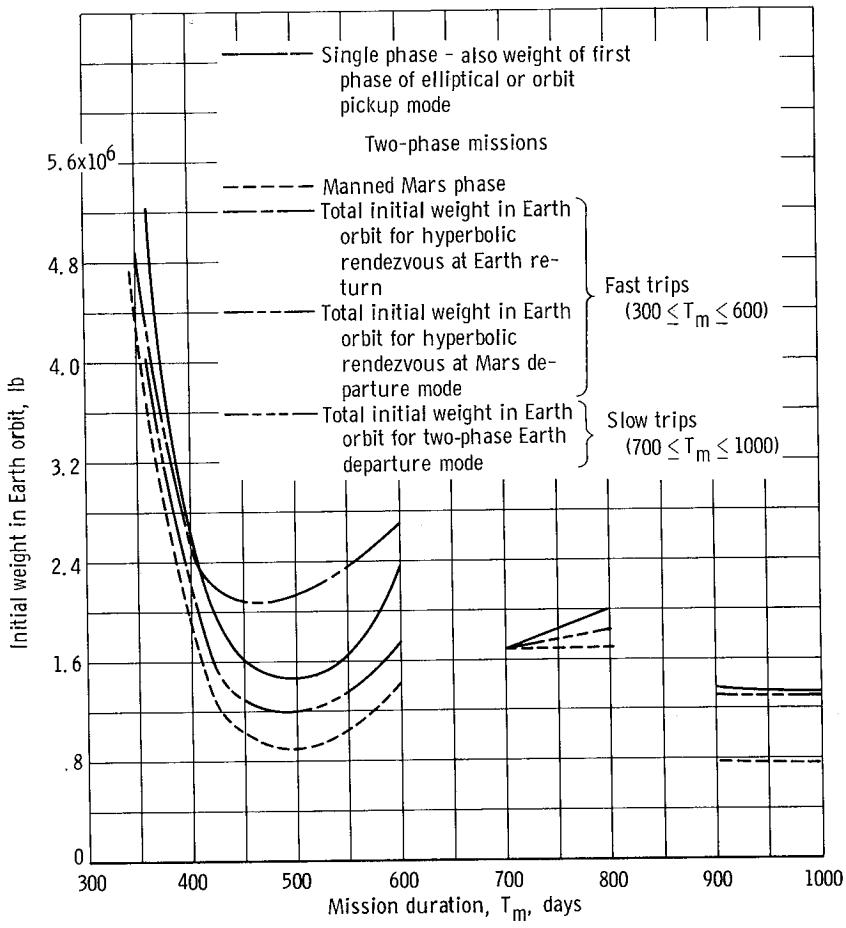

Figure 31. - Initial weight in Earth orbit for two-phase mission profiles. Inert shielding; atmospheric braking at Earth from 52 000 fps; Mars parking orbit at 1.1 radii; nuclear space propulsion.

manned Mars mission phase of a two-phase mission using hyperbolic rendezvous at Earth return. The dash-dot curve is the sum of the weights for the mission and the recovery phases of the two-phase mission. For the 420-day trip, the IWIEO for the manned mission phase is reduced from 1.96 to 1.3 million pounds for the single-phase mission, while the total IWIEO for the two phases of the mission is increased to 2.2 million pounds. The weight represented by the difference between the dashed and the dash-dot lines is the recovery system weight, which is launched near the end of the manned portion of the mission.

The primary advantage of this profile is to reduce the IWIEO required at mission launch. It has the disadvantages of increasing the total launch weight and decreasing the overall mission reliability because of the rendezvous maneuver that must be performed within close time limits at Earth return.

Hyperbolic rendezvous at Earth return has been discussed when inert shielding is assumed. If propellant shielding is used this profile reduces, in the limit, to the elliptic orbit pickup mode.

Because of the nonfailsafe nature of this trajectory, it may be undesirable for the primary mission mode. The hyperbolic rendezvous at Earth, however, could serve as a rescue mode of operation for one of the other mission profiles.

Hyperbolic rendezvous at Mars departure. - The trajectories associated with the hyperbolic rendezvous at Mars departure are shown in figure 30(b). The manned phase trajectory can be one of the fast trip trajectories previously used for the fast missions. Perhaps 30 days after the Earth departure of the manned phase, an unmanned phase, for which the payload is the Earth deceleration stage, is launched from Earth orbit. The trajectory for the unmanned phase is of the nonstop round-trip type and uses a propulsion gravity turn at Mars to match the inbound leg of the manned phase. The rendezvous between the two mission phases can take place anywhere on the inbound leg between Mars and Earth. The required ΔV's and launch dates for these mission profiles are also given in table VII (p. 23) (columns 6 and 7). It is noted that the ΔV's (column 7) for the unmanned Earth deceleration system are much less than they were for the previous case of hyperbolic rendezvous at Earth (column 5) and are also less than for the manned stopover trajectory (column 2).

The IWIEO for this profile are also given in figure 31 for the fast trips ($T_m < 600$ days). The weight of the manned phase is again the lower curve (dashed). The dash double-dot curve is the total IWIEO, which includes the recovery system. This mode of operation yields lower IWIEO than the single-phase mission (solid line). For this mission profile, two weights each substantially less than that for a single-phase mission are launched from Earth at dates from 20 to 40 days apart for trip durations of 360 to 500 days.

Two-phase Earth departure. - While the previous two-phase profiles were primarily of interest for the fast trips, the two-phase mission to be discussed now is of interest for both fast and slow trips. The slow trips have a long stay time at Mars and a correspondingly large weight is used for surface exploration (see fig. 16(b), p. 37). In the two-phase Earth departure profile the surface exploration weight is sent ahead of the manned phase (several months or a synodic period ahead) and is landed directly on the Mars surface by atmospheric braking. The IWIEO for the system are also shown in figure 31 (dash triple-dot line) for the slow trips ($T_m > 700$ days). The total weight is little different from that for the single-phase mission profile (solid line); however, the required weight may now be launched from Earth orbit in two about equal "packages" at times separated by about a month or a synodic period. The separation time between launches can be made more flexible for an increase in system weight.

The launch of a separate phase to deliver the Mars surface exploration weights to Mars can also be applied to the fast trips and yields a weight reduction for trips faster than about 420 days.

The discussion of two-phase mission profiles is now summarized. The elliptical orbit pickup mode is of particular interest because it eliminates the requirement for

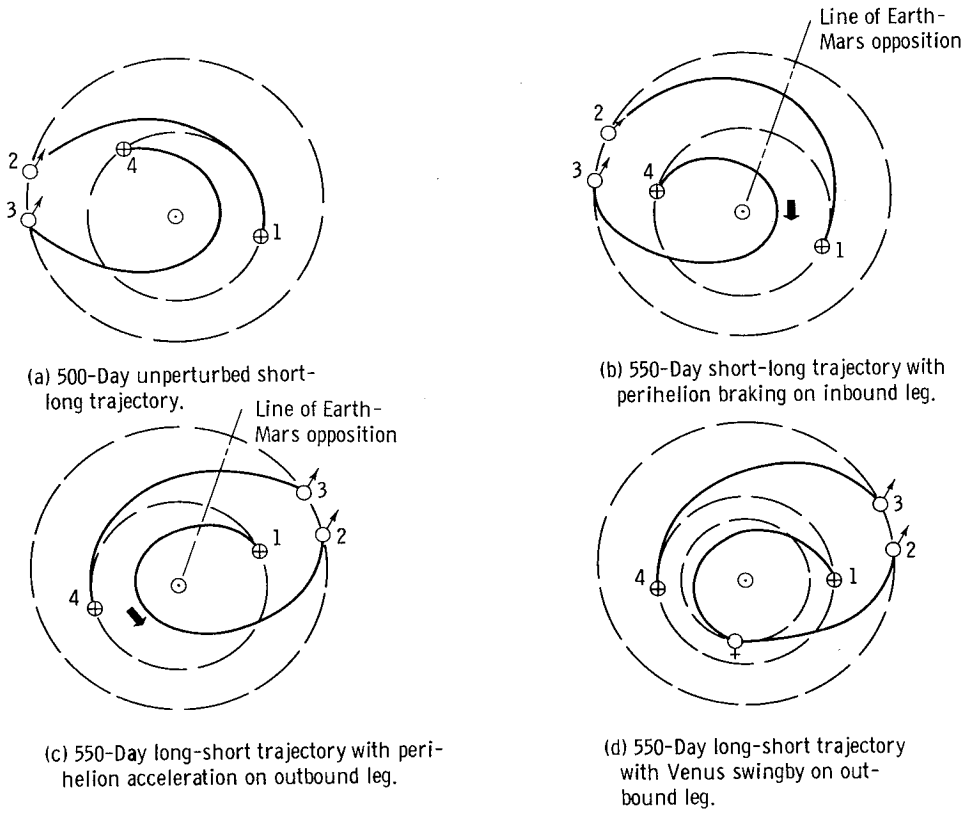

Figure 32. - Types of perturbed Mars stopover round-trip trajectories.

Earth entry velocities above 37 000 fps. The hyperbolic rendezvous at Earth return is probably of interest only as an emergency recovery mode. The hyperbolic rendezvous after Mars departure offers a reduction in IWIEO. The use of a separate phase to send ahead the Mars exploration equipment reduces the weight to be launched at any one date for slow and fast trips and can reduce the total IWIEO for very fast trips.

Perturbed Trajectories

In this section single-phase missions are again considered. The single-phase interplanetary trajectories considered previously consisted of a single conic section (with the Sun as one focus) for the outbound leg and another for the inbound leg. Another class of trajectories occurs when one leg of the trajectory is made up of segments of two different conic sections pieced together. Such a trajectory occurs when the trajectory of one leg is perturbed in transit by a force. The result of the perturbation can be to reduce the mission propulsive velocity increments and possibly the IWIEO for a given mission duration.

The source of the perturbation may be a midcourse propulsion usually near the mission perihelion, a close pass to Venus (Venus swingby), or a lunar swingby. The first two possibilities mentioned will be compared with an unperturbed trajectory and each other to

bring out their common features. Sketches of a typical set of perturbed trajectories are shown in figure 32. The corresponding ΔV's and leg travel times and angles are given in table VIII (p. 24). The unperturbed trajectory is considered first. It has a 500-day duration and yields close to minimum $\sum_{1}^{4} \Delta V$ as a function of trip duration. The outbound leg is short. The inbound leg is long, has a heliocentric travel angle of about 300°, and passes through a perihelion of 0.4 astronomical unit. It is this inbound leg that is a candidate for replacement by a two-segment conic, one kind of perturbed trajectory.

Perihelion propulsion. - The term perihelion propulsion is used to refer to those trajectories that use thrusting at or near the trajectory perihelion in addition to propulsion at the planet termini. Figure 32(b) illustrates the kind of perihelion propulsion trajectory considered. It consists of two semiellipses that are cotangential with each other at their common perihelion. The first of these semiellipses is also cotangential with the orbit of Mars at Mars departure, and the second is cotangential with the orbit of Earth at Earth arrival. The total heliocentric travel angle is 360°. The difference in velocity between the two semiellipses at their perihelions is made up by impulsive tangential thrusting. When this type of trajectory is used for the inbound leg, the perihelion propulsion is in the retrograde direction, or a braking. (Ehricke in reports subsequent to ref. 8 has suggested using a solar-heated hydrogen expansion rocket for the perihelion propulsion.) The analysis of a more general class of double conic trajectories is reported in reference 38. There the location of the midcourse impulse is not restricted to the trajectory perihelion but is selected to minimize the total ΔV. This class of trajectories gives lower total ΔV's than do the present perihelion propulsion trajectories. However, the present trajectories are expected to give an indication of the merits of such a midcourse impulse.

The characteristics of two perihelion propulsion trajectories that yield near minimum total ΔV and of an unperturbed trajectory are given in table VIII (p. 24). (The labels to the left of the double line apply to the columns to the left of the double line and the labels on the right to the columns on the right. The trips outlined on the left proceed from top to bottom while those on the right proceed from the bottom upward. With this arrangement numbers in a given row are to be compared.) Compared with the unperturbed trajectory, perihelion braking on the inbound leg yields a slightly reduced ΔV to leave Mars and an Earth arrival ΔV that is reduced from 8.3 to 3.6 or by 4.7 miles per second. A ΔV of 1.7 miles per second is required at perihelion, which is at about 0.38 astronomical unit. The total mission ΔV has been reduced from 16.2 to 13.8 miles per second. If the ΔV at Earth return is assumed absorbed by atmospheric braking and hence omitted from the ΔV summation, the remaining ΔV sum is less for the unperturbed trajectory. Also for atmospheric braking at Mars and Earth the ΔV summation is less for the unperturbed trajectory. Figure 9 (p. 17) shows the total ΔV sum for unperturbed trajectories and for trajectories using perihelion braking for a range of total

trip times. The perihelion propulsion trajectories give comparatively low $\sum \Delta V$'s in the range of trip times from 480 to 650 days, which is the region between the fast and intermediate trips.

The previous discussion has dealt with perihelion braking on the inbound leg of a short-long trajectory (fig. 32(b), p. 64). An alternative is to use perihelion acceleration on the outbound leg of a long-short trajectory (fig. 32(c)). This trajectory is approximately a reflection of the short-long trajectory in the line of the Earth-Mars opposition. In the ideal situation (coplanar orbits with the line of opposition and the line of apoapsis of both planetary orbits concident) ΔV_1 becomes ΔV_4, ΔV_2 becomes ΔV_3, etc. The extent to which this ΔV interchange holds in the actual situation may be seen by comparing the characteristics of the two perihelion thrusting trajectories in table VIII (p. 24). The two perihelion thrusting trajectories are very nearly mirror images.

The total ΔV for the two trajectories is about the same. The ΔV that can be absorbed by atmospheric braking, however, differs because of the interchange of ΔV's mentioned previously. With atmospheric braking at Earth only, the ΔV sum is less for the perihelion braking on the inbound leg of a short-long trajectory because of the higher Earth approach ΔV for this case. With atmospheric braking at both Earth and Mars the ΔV sum is less for perihelion thrusting on the outbound leg of a short-long trajectory because of the higher Mars arrival ΔV's. These ΔV's will of course be reflected in the IWIEO's.

The individual propulsive ΔV's for trips of several durations are given in table IX (p. 25) for perihelion propulsion on the inbound leg and in table X (p. 26) for perihelion propulsion on the outbound leg. To determine the IWIEO, estimates were made of the

TABLE XII. - EARTH RETURN MISSION PAYLOAD WEIGHTS

	Perihelion thrusting			
	Inbound leg, lb			Outbound leg, lb
Mission duration, days	476	556	596	500 to 650
Command module, living module exclusive of shielding, plus space power and fixed part of life support system	27 000	27 000	27 000	27 000
Radiation shielding	19 400	27 000	48 000	11 000
Earth entry vehicle	11 750	11 750	11 750	11 750
Total	58 150	65 750	86 750	49 750

fixed weights carried to but not through the Earth deceleration maneuver (table XII). The weight of the first group of items is the same as that used in the previous calculations. For thrusting on the inbound leg, where the mission perihelion occurs on the inbound leg, the shield weights were taken as those to give 100 mea-rem (see fig. 19, p. 42). The mission perihelion (i. e., the lower of the two-leg perihelions) is the same each trip of this group but the shield weight to maintain a given dose increases with increasing trip time to offset the effect of the increased exposure time. The combination of a low perihelion, 0. 375 astronomical unit, which gives a large flux from the flare assumed to occur at perihelion, and the long trip times, which give large total background flux, make the shielded weights sensitive to changes in trip time. (The propellant for perihelion thrusting could be used for radiation shielding prior to the thrusting to reduce the dose.)

The Earth atmospheric entry velocities can be below 37 000 fps if the radiation shield weight is also retropropellant. Hence, an entry vehicle weight of 11 750 pounds was used.

For thrusting on the outbound leg, the mission perihelion occurs on the outbound leg. The perihelion of the inbound leg is 1 astronomical unit and only 11 000 pounds of shield is required on the inbound leg according to the curve of 100 mea-rem (fig. 19, p. 42). Again the Earth entry velocities can be below parabolic, if the shielding is also propellant, so the entry vehicle weight is 11 750 pounds. At the mission perihelion, which occurs on the outbound leg, radiation shielding in addition to the 11 000 pounds carried to the end of the mission is required, for instance, about 48 000 pounds for a 100 mea-rem at 600 days. This shielding is assumed to be provided by the chemical propellants on board the spaceship. (The Mars landing system weights are the same as those used previously.)

The IWIEO's for the perihelion propulsion mission profiles are given in figure 33 for atmospheric braking at Earth and propellant shielding. The bars of figure 33(a) compare the IWIEO's for perihelion thrusting on the inbound leg of the short-long trajectory with perihelion propulsion on the outbound leg of a long-short trajectory for several mission profiles. Generally perihelion propulsion on the inbound leg gives the lower weights. An exception occurs when atmospheric braking to a low circular parking orbit is used at Mars. For this case perihelion propulsion on the outbound leg gives a slightly lower weight.

In figure 33(b) the weight for perihelion propulsion on the inbound leg is compared with several single conic mission profiles. If the atmospheric entry velocity at Earth is limited to 37 000 fps, the perihelion propulsion trajectory gives a slightly lower weight than the conventional single conic trajectory (the first bar). If entry velocities of 52 000 fps are allowed, the single conic trajectory gives the lower weight. These results are consistent with ΔV summations of table VIII (p. 24). The last result means that if a 52 000 fps Earth atmospheric entry velocity is permissible, a zero midcourse impulse is best.

In figure 33(c) the variation of the weight with mission duration for perihelion propul-

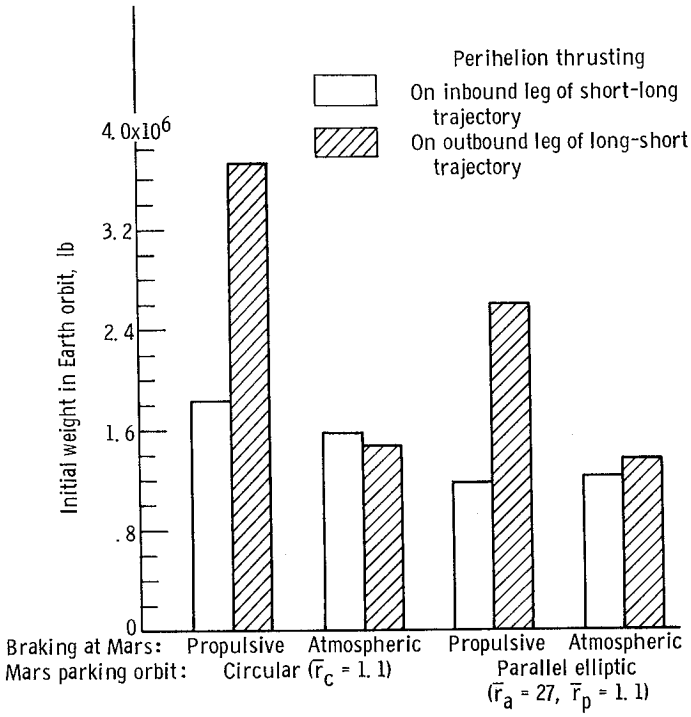

(a) Comparison of inbound and outbound perihelion propulsion. Mission duration, 550 days; atmospheric entry velocity at Earth, ≤ 37 000 fps.

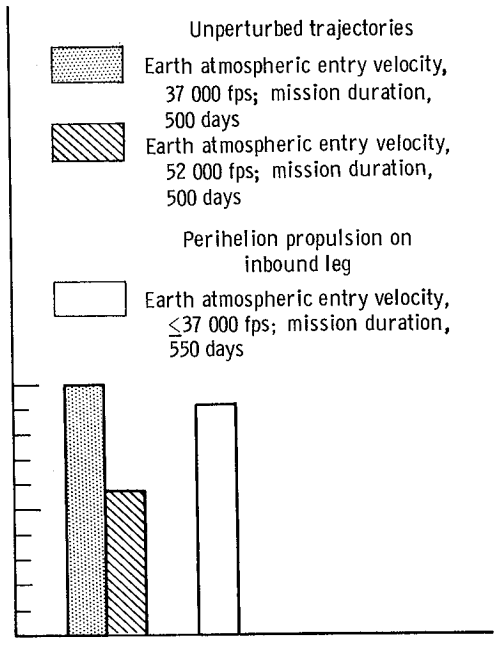

(b) Comparison with unperturbed trajectory profiles. Propulsive braking to a circular parking orbit at 1.1 Mars radii.

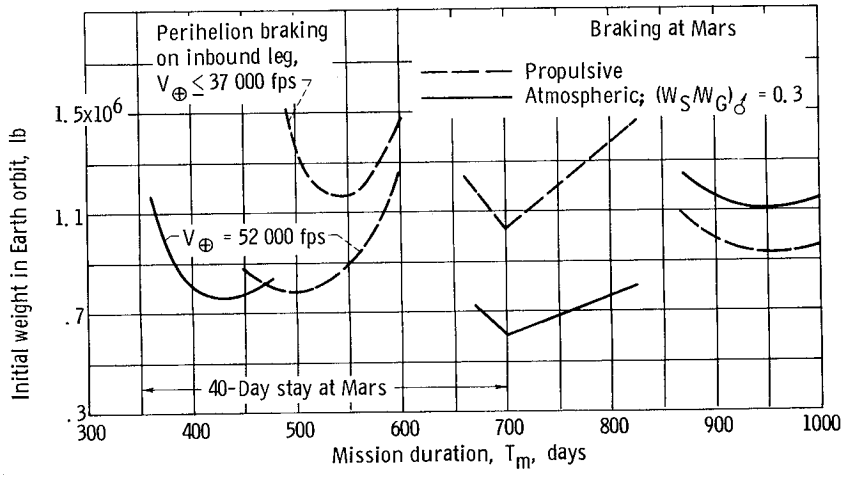

(c) Effect of mission duration for parallel elliptic parking orbit.

Figure 33. - Effect of perihelion propulsion on initial weight. Atmospheric braking at Earth; propellant shielding; nuclear space propulsion.

sion on the inbound leg is compared with that for single conic trajectories previously discussed.

Perihelion propulsion appears of interest primarily in the vicinity of a 550-day trip duration, which was the time selected for figures 33(a) and (b). For shorter trip times the weight increases primarily because the $\sum \Delta V$ increases. For longer trips the weight increases both because, as discussed earlier, the radiation shielding weight increases, and because for trips longer than about 580 days the $\sum \Delta V$ increases.

Propulsion at Mercury. - A variation of the perihelion propulsion trajectory was briefly considered. The perihelion of these trajectories is about 0.38 astronomical unit or less. The orbit of the planet Mercury is about 0.39 astronomical unit. The efficiency of adding the perihelion ΔV can be improved if it occurs within the gravitational field of Mercury. The period of Mercury is about 80 days and timing the trajectory to intercept Mercury is not difficult. On the other hand, Mercury has a small mass and a correspondingly small gravitational field. The reduction in ΔV for thrusting at 1.1 Mercury radii is 0.12 mile per second as compared with a total mission ΔV of 7 to 14 miles per second (table VIII, p. 24). The reduction in IWIEO for perihelion thrusting at Mercury compared with perihelion thrusting alone is small, perhaps several percent if the penalties for guidance and timing are neglected.

Venus swingby. - Venus in addition to Mars is a close neighbor of the Earth and an object of scientific curiosity. One of the advantages of a Mars stopover mission using a Venus swingby is that it offers the opportunity for a close observation of Venus. A second advantage of a Venus swingby, and the one of primary concern here, is that it can reduce the ΔV's for the Mars mission. The trajectory for a Venus swingby on the outbound leg and for a total trip time of 550 days is shown in figure 32(d). It is geometrically similar to the trajectory for perihelion thrusting on the outbound leg in that the heliocentric travel angle between Earth and Mars exceeds 360° by only 10°. The travel angle between Earth and Venus exceeds 180°, and the pass at Venus is on the dark side.

The ΔV's, leg times, and travel angles for trips of several durations are given in tables VIII and XI (pp. 24 and 27). The trajectory for a 550-day Venus swingby on the outbound leg (table VIII) is similar in terms of ΔV's to that for perihelion thrusting on the outbound leg with two exceptions: First, the perihelion propulsion is eliminated, and second, the ΔV to leave Earth is reduced. The $\sum_{1}^{4} \Delta V$ and $\Delta V_1 + \Delta V_3$ for the 550-day Venus swingby mode are lower by 2 to 4 miles per second than the corresponding values for either the unperturbed or perihelion propulsion trajectories. The $\sum_{1}^{3} \Delta V$ is about the same for the Venus swingby and unperturbed trajectories.

The Earth return mission weights for the Venus swingby are the same as those given in table XII (p. 66) for perihelion propulsion on the outbound leg and for the same reasons.

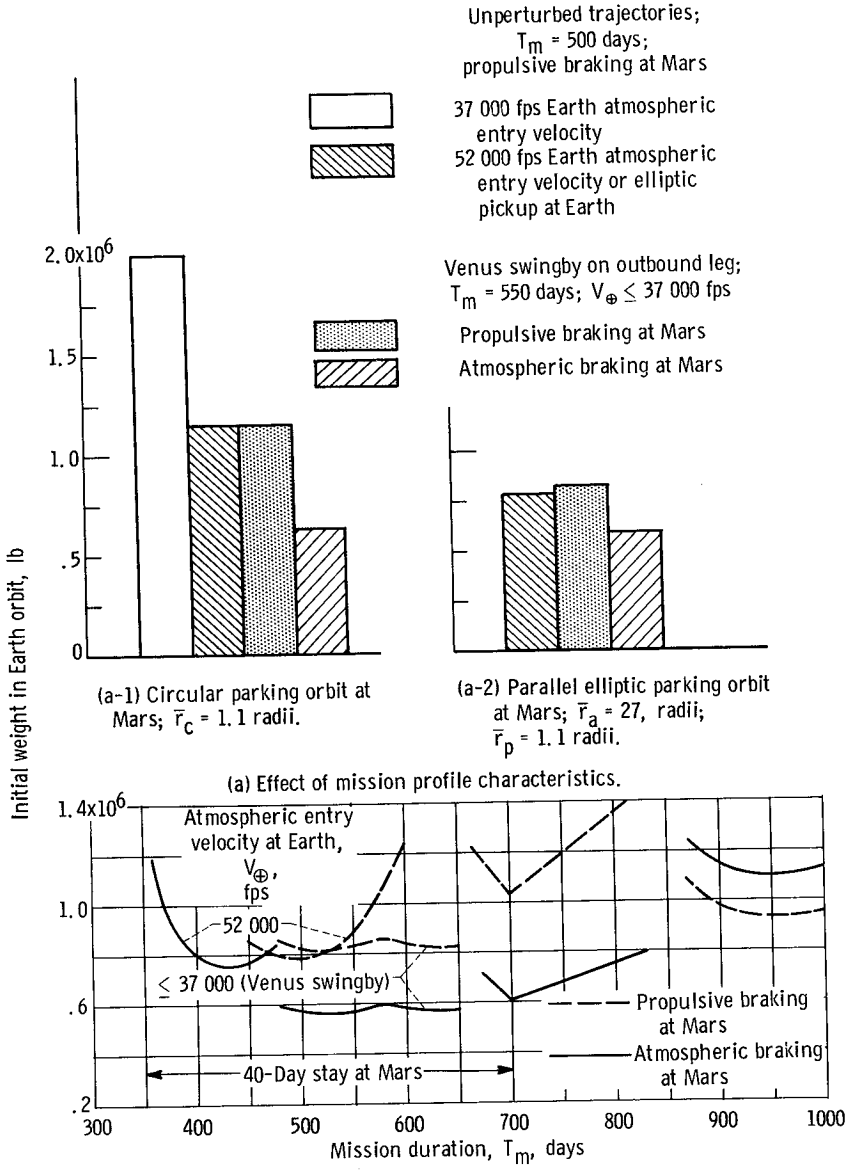

(b) Effect of mission duration on initial weight in Earth orbit for parallel elliptic parking orbit; $\bar{r}_p$ = 1.1 radii; $\bar{r}_a$ = 27 radii.

Figure 34. - Effect of Venus swingby (on outbound leg). Atmospheric braking at Earth; propellant shielding; nuclear space propulsion; $(W_S/W_G)_{\sigma'}$ = 0.3 when atmospheric braking at Mars is used.

The Mars landing systems are also the same. An additional 300 fps of guidance ΔV to be provided by the chemical midcourse correction system is assumed to assure the correct passage at Venus.

The IWIEO for the Venus swingby are presented in figure 34. The bar graph of figure 34(a) compares several mission profiles. The Venus swingby profile yields the lightest weights when atmospheric braking is used at Mars. Atmospheric braking at Mars is very beneficial because the Mars approach velocity is comparatively high, about 30 000 fps. (The approach velocities of the other trajectories were given in fig. 28, p. 56).

If propulsive braking is used at Mars, the Venus swingby profile, which has an Earth atmospheric entry velocity of 37 000 fps or less, gives weights comparable to the conventional single conic trajectories with 52 000 fps entry velocities. Table VIII (p. 24) shows that the Earth approach velocities for the Venus swingby are sufficiently low so that by using the propellant as radiation shielding the entry velocities can be less than 37 000 fps. In this instance, the effect of the Venus swingby has been to eliminate the desirability, from a weight saving viewpoint, of developing a high velocity (e. g., 52 000 fps) Earth atmospheric entry capability.

Figure 34(b) indicates the range of mission durations over which the Venus swingby mode is applicable. Low weights occur for trip durations of 480 to 650 days. Table XI (p. 27), however, shows that for the 480-day trip the Earth approach velocity is much higher than for the 550-day trip but still significantly lower than those for the unperturbed 500-day trajectory. At 700-day trip time the unperturbed intermediate class of trips with atmospheric braking at Mars yields weights about the same as the 650-day Venus swingby also with atmospheric braking at Mars. When the factors of solar radiation, trip time, IWIEO, and low Earth approach velocities are considered, the most attractive Venus swingby trips occur for 500- to 550-day trips.

The preceding discussion applies to a Venus swingby in 1978-80. A favorable swingby depends on the appropriate configuration of the planets Mars, Earth, and Venus. As a consequence, a swingby on the outbound leg is not possible or not favorable in all synodic periods. In some synodic periods a swingby on the inbound leg will be favorable. By analogy with the cases of perihelion thrusting, such a trip will be approximately a mirror image of the one in 1978-80. Since for the 550-day Venus swingby (table XI, p. 27) both ΔV_1 and ΔV_4 are low, low Earth entry velocities will occur for a swingby on either the outbound or inbound leg. However, for a swingby on the inbound leg the Mars approach velocity will be significantly reduced because ΔV_2 and ΔV_3 become interchanged. In this case the pronounced weight reduction for using atmospheric braking at Mars will be much reduced or eliminated.

In summary, in the 1979-80 synodic period, missions based on a Venus swingby trajectory can yield IWIEO's with Earth atmospheric entry velocities of about 37 000 fps

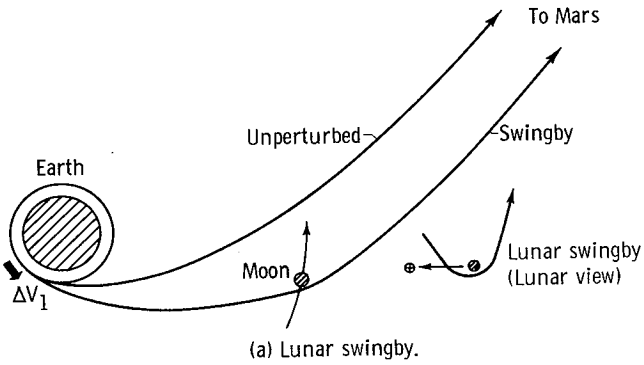

(a) Lunar swingby.

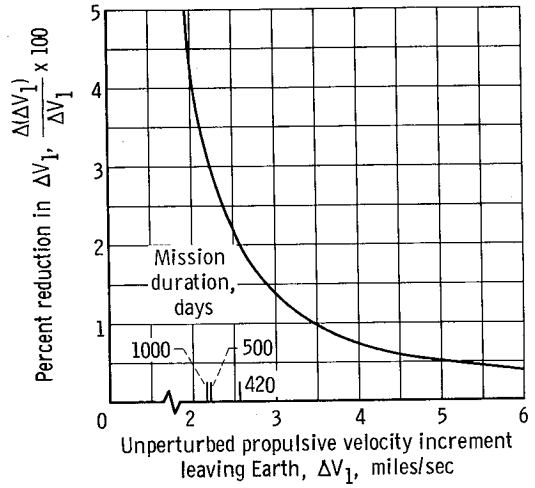

(b) Reduction in propulsive velocity increment leaving Earth for lunar swingby at minimum altitude.

Figure 35. - Effect of lunar swingby at Earth departure on propulsive velocity increment.

comparable to the weights of missions based on unperturbed trajectories with Earth entry velocities of 52 000 fps. In some synodic periods, those when a Venus swingby on the outbound leg is favorable (e. g., 1978-80), the Venus swingby with atmospheric braking at Mars will yield an IWIEO 25 to 40 percent less than unperturbed trajectories or Venus swingby trajectories with propulsive braking at Mars. In other synodic periods atmospheric braking at Mars will be of little benefit. Trip durations of 500 to 550 days are of primary interest.

Lunar swingby. - The effect of a lunar swingby is considered in figure 35. The propulsion to leave Earth can be so timed that the trajectory to Mars passes near the Moon (fig. 35(a)). Because of the Moon's gravity and motion a pass on the appropriate side of the Moon will increase the vehicle velocity with respect to the Earth, thus reducing the required propulsion to leave Earth. Figure 35(b) presents the percent reduction in the unperturbed ΔV to leave Earth against the unperturbed value. The total trip time associated with several of the ΔV's are also noted on the abscissa. The percent reduction in ΔV is greatest for the lowest unperturbed ΔV's. The greatest reduction also occurs for the closest practical perilune. The values shown are for the limiting case of a pass at the lunar surface. For the trip times of interest, the reduction in ΔV_1 is 3 percent or less.

Table XIII presents the interchange ratio between the percent change in ΔV_1 and the percent change in IWIEO. This ratio has a value of about 0. 7 for nuclear systems, but is generally higher for chemical systems (1. 0 to 1. 3). The lunar swingby thus offers the greatest weight savings for chemical systems. By combining the percent ΔV reduction with weight exchange ratio, it is seen that a lunar swingby at Earth departure offers a potential weight reduction of about 3 percent.

The use of a lunar swingby at Earth return will be less favorable than at Earth

TABLE XIII. - EXCHANGE RATIO BETWEEN WEIGHT AND

PROPULSIVE VELOCITY INCREMENT

Propulsion system	Specific impulse, I, sec	Mission duration, T, days	
		420	1000
		[a]Ratio of percent change in initial weight in Earth orbit to percent change in ΔV_1, $\Delta W_G/W_G / \Delta V_1/V_1$	
Nuclear	850	0.74	0.70
Chemical	460	1.3	1.0

[a]Propulsive deceleration at Mars.

departure because the approach velocities are generally higher than those at departure and because of the lower stage weights. In general, a lunar swingby is of small or no importance in the reduction of the IWIEO.

Other Mission Profiles

While many mission profiles have been considered, there are many more than can be conceived. Several other mission profiles or variations of the previously described profiles are briefly discussed here.

Two option stay time. - The mission profiles considered up to this point had for their objective either a short (40 days) or a long stay (100 to 450 days) at Mars. By sending ahead to Mars the weight for a long Mars exploration time, as discussed for the two-phase mission profiles, any of the fast trips then offer the crew the options of staying for the short time and returning to Earth or of staying the long time and performing a thorough exploration of Mars before returning to Earth. Because of its flexibility, this concept may be of interest for planning now when little is definitely known about mission objectives and what stay times and mission times are feasible or desirable.

Phobos or Diemos landing. - There may be an advantage to parking the spaceship on one of the moons of Mars, Phobos or Diemos, and conducting the Mars landing from there. The very least advantage this may offer is the manned exploration of that moon. The previous discussion of operations at Mars (figs. 21 to 26, pp. 45 to 52) is applicable with some degree of approximation to the possibility of a moon landing because the orbital planes of the moons are near the requisite parking orbit planes and the gravity of the moons is small so that a landing would involve little propulsive weight.

When a circular parking orbit is selected that is the same as the orbit of one of the moons, a landing on that moon could be accomplished, providing of course that the timing is appropriate. The radii of the orbits of Phobos and Diemos are, respectively, 2.8 and 7.0 Mars radii and their direction of rotation is direct. Either direct or retrograde

parking orbits are possible at Mars for the same magnitudes of the propulsive velocity increments and hence the same system weights.

The previous results are reviewed as they apply to a Mars moon landing. From figure 23(b) (p. 48) a direct entry in the orbits of the moons will increase the system weight as compared with that for using a low circular parking orbit at Mars. Because of the comparatively low altitudes of the Mars moons ($\overline{r}$ = 2.8 and 7.0), entering their orbit by means of semiellipses will yield an IWIEO at best only slightly less than the low circular parking orbit. Thus, the potential weight reduction of using a high circular parking orbit (e.g., $\overline{r}_c$ = 27) or of using an elliptic parking orbit would be sacrificed if a landing of the spaceship on a Mars moon is undertaken.

If an important objective of the Mars trip is the exploration of one of its moons, the spaceship could be parked in a favorable parking orbit and an excursion vehicle sent to a moon.

Convoy mode. - Another possible variation in mission profile is the convoy mode (ref. 8). In this mode, the spaceship on its outbound leg consists of two or more independent units, for instance a passenger and two or more freight phases, with interchangeable parts. This mode reduces the number of rendezvous required in Earth orbit but substitutes rendezvous on the outbound leg or at Mars. Although the convoy mode is not expected to reduce the IWIEO, it does improve the probability of a safe return for the crew.

Chemical Space Propulsion

The previous sections have all presumed the use of nuclear rocket space propulsion. However, nuclear rockets of the assumed characteristics have not yet been developed. It is therefore of interest to examine the performance attainable with conventional chemical rockets. For this study hydrogen-fluorine propellants with a specific impulse of 460 seconds are assumed for the space propulsion. A specific impulse of 430 seconds is still used for the deceleration at Earth return and for midcourse corrections.

The IWIEO for several mission profiles is shown in figure 36. The general trends of the curves with mission time and with changes in mission profile are similar to the changes already discussed for nuclear propulsion so only some general comments will be made. The weight for a chemical system for the less sophisticated profiles considered, for instance as characterized by 37 000 fps Earth entry velocity, inert radiation shielding, and low circular parking orbits at Mars as shown by the upper curve on the left side of figure 36, is 7.5 million compared with 2.5 million pounds for the nuclear system for a 500-day trip. If the Earth atmosphere entry velocity were 26 000 fps, the chemical system would be seven times heavier than the corresponding nuclear system. The weights

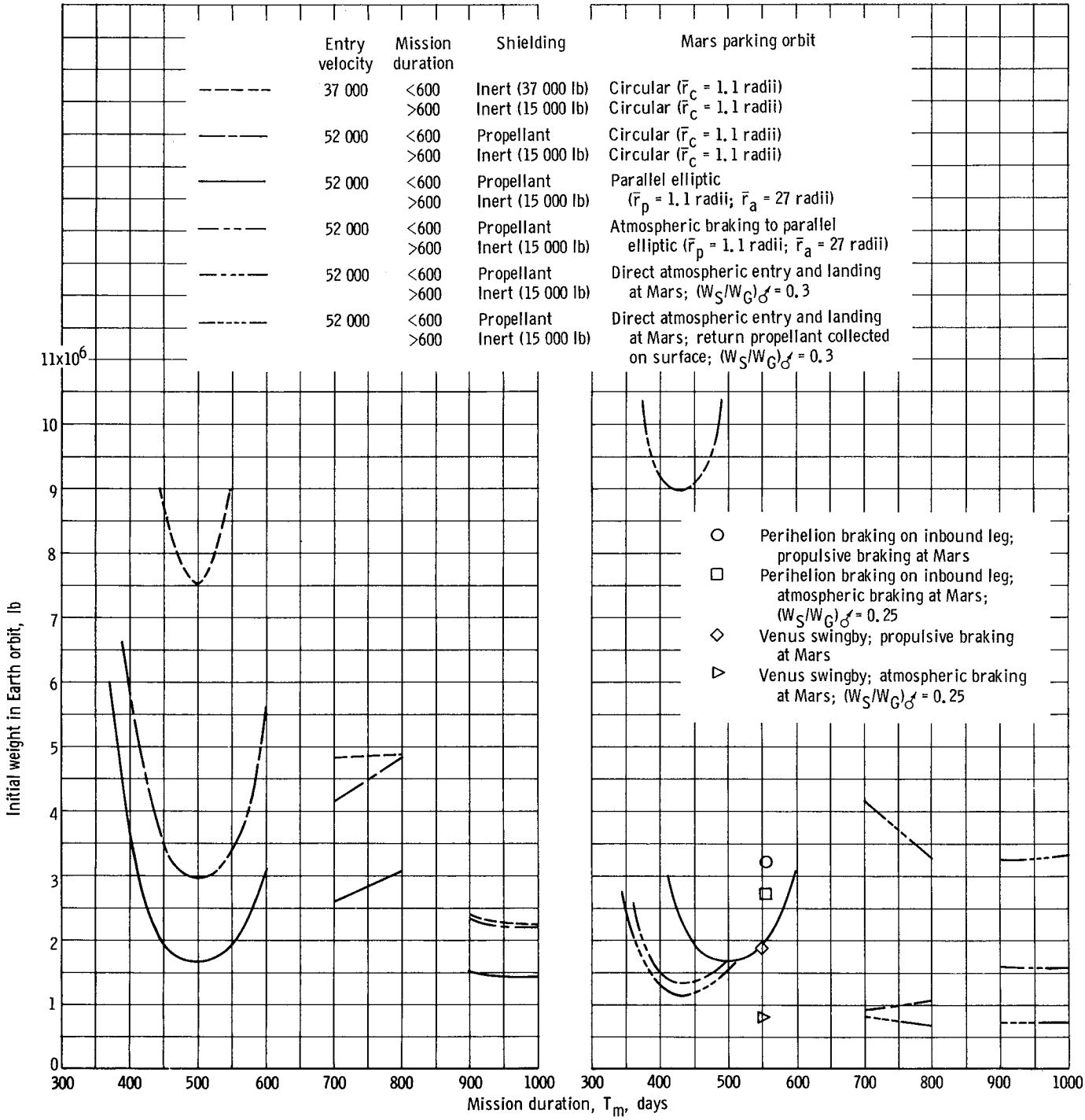

Figure 36. - Effect of profile on initial weight in Earth orbit for chemical space propulsion. Specific impulse, 460 seconds.

for the 900- to 1000-day trips are about 2.3 million compared with 1.2 million pounds for the nuclear system. Thus chemical systems can be much heavier than nuclear systems. However, the weight of the chemical systems is markedly reduced by refinements in mission profile. For example, with a 52 000 fps Earth atmospheric entry velocity, propellant shielding, and an elliptic parking orbit at Mars (solid line), the weight of the chemical systems is down to 1.7 million pounds for a 500-day mission, about twice that of the nuclear system. The 900- to 1000-day missions have weights of about 1.5 million pounds. Systems using a direct landing with chemical propellant collection at Mars and the perturbed trajectories, particularly the Venus swingby with atmosphere braking at Mars, also yield attractive weights. In general, the chemical systems with sophisticated mission profiles can yield attractive weights.

Except for the Earth deceleration stage, consideration has been given to interplanetary propulsion that is either all nuclear or all chemical. In some circumstances it may be desirable to use combinations of nuclear and chemical propulsion. For instance, if the payload to be accelerated are smaller than or comparable in weight to the nuclear engine weight, then nuclear propulsion does not yield an efficient stage. (It is recalled that the nuclear propulsion was in some cases less efficient than chemical propulsion for the Earth deceleration stage because of the relative weights of the payload and engine). If, contrary to the indications of the many studies, hydrogen storage in space for long periods of time or near Mars proves impractical, the use of nuclear rockets for some stages may be excluded. The IWIEO of systems using a combination of chemical and nuclear propulsion will be intermediate between the weights for all the nuclear and all chemical systems.

Aborts

Providing for the safe return of the crew to Earth in case of an emergency is of paramount importance for a manned mission. Examples of emergencies requiring an abort are the severe but noncatastrophic damage to the spaceship as might result from a meteoroid hit or a serious malfunction of part of the spaceship like excessive propellant boil-off. Several aspects of the abort problem will be considered here.

One way to approach the abort problem is to design the interplanetary trajectory to assure a return to Earth. The outbound leg of the stopover trajectory can be the same as that of a nonstop round trip. Three kinds of nonstop round trips were analyzed in reference 35. They are catagorized by the type of maneuver used at Mars: (1) a gravity turn, which as its name implies uses only the gravity of Mars to change the trajectory; (2) a propulsion gravity turn, which uses propulsion to supplement the turning due to gravity and also to change the energy of the trajectory; and (3) an atmospheric turn, where aerodynamic forces generated by an aerodynamic vehicle flying in the Mars atmosphere are

used to both deflect the trajectory and change its energy. The appropriate type of nonstop round trip depends on the stopover mission profile.

Appropriate to all stopover mission profiles is an abort based on a gravity turn at Mars; these are sometimes referred to as stopover trajectories with a "free return." In this case the outbound leg of the stopover trajectory would be the same as that of a nonstop gravity-turn round trip. Figure 25 (p. 51) presented such nonstop round trips. In 1979 they occur for nonstop mission times of 380, 520 to 580, near 720, and near 1095 days. Stopover missions having an outbound leg the same as the outbound leg of the shorter of these nonstop missions are of interest. As was pointed out in the section entitled "Possibility of attaining parallel elliptic parking orbit performance," these same nonstop round trips can also be a basis for short-stay-time (perhaps 5 days) stopover trajectories with parallel elliptic parking orbit. The combined advantages of a free return abort capability and a parallel elliptic parking orbit make these trips attractive.

A comparison is made between the trajectories for a 540-day trip with minimum propulsive requirements and one with gravity-turn abort capability in table XIV (p. 78, columns 1 to 4). The conclusion to be drawn from these data is that for the 540-day trip the difference between the minimum ΔV trajectory and the trajectory with abort capability is small. The launch date is 5 days earlier and the $\sum \Delta V$ is increased from 9.67 to 9.79 or 1.2 percent for the case of full atmospheric braking at Earth (i.e., $\sum_{1}^{3} \Delta V$).

A much greater degree of freedom in selecting outbound leg times exists if some propulsion is permitted at Mars so that the nonstop propulsion-gravity-turn round trip can be used for abort. A comparison between the trajectory for minimum propulsion ΔV and one with propulsion-gravity-turn abort capability for 420- and 500-day trips is also made in the table XIV (last six columns). For the 420-day trip the two trajectories coincide. For the 500-day trip the launch date occurs 50 days earlier and the $\sum_{1}^{3} \Delta V$ is increased from 7.91 to 8.57 or 8.3 percent when full atmospheric braking at Earth is assumed.

For the propulsion-gravity-turn abort, either stage two or three may provide the propulsion (noted in table XIV) for the turn at Mars. Stage three will provide adequate ΔV whether a low circular or elliptic parking orbit is used at Mars. If stage two is to be used for the turn at Mars, stage three and the Mars payloads would be jettisoned, then stage two would produce about twice the mission ΔV_2. This ΔV is larger than that required for the propulsion gravity turn. Thus, for both trip times (420 and 500 days) and for either a low circular or elliptic parking orbit at Mars, either stage two or three (Mars arrival and departure stages, respectively) yield more than the ΔV required for an abort by means of a propulsion gravity turn. In general, it seems reasonable to conclude that stopover trajectories with propulsion-gravity-turn abort capability are possible for small penalties in $\sum \Delta V$ in the range of trip times from 420 to 500 days.

TABLE XIV. - COMPARISON OF PROPULSION REQUIREMENTS FOR STOPOVER ROUND TRIPS WITH MINIMUM PROPULSIVE VELOCITY INCREMENT AND WITH ABORT CAPABILITY

[Stay time at Mars, 40 days.]

	Nonstop gravity turn abort			Nonstop propulsive gravity turn abort					
	Mission duration, 540 days			Mission duration, 420 days			Mission duration, 500 days		
	Stopover round trip		Abort trajectory	Stopover round trip		Abort trajectory	Stopover roundtrip		Abort trajectory
	Minimum $\sum_{1}^{4} \Delta V$	With abort capability		Minimum $\sum_{1}^{4} \Delta V$	With abort capability		Minimum $\sum_{1}^{4} \Delta V$	With abort capability	
Earth departure date, Julian day, 2444 -	060	055	055	220	220	220	190	140	140
Outbound leg time, days	260	260	260	180	180	180	260	260	260
Propulsive velocity increment, ΔV, miles/sec:									
Leaving Earth	4.75	4.91	4.91	2.56	2.56	2.56	2.21	2.70	2.70
[a]Arriving Mars	2.34	2.33	0	2.58	2.58	[b]2.37	1.50	2.12	[b]1.64
[c]Arriving Mars	1.42	1.41	----	1.76	1.76	----	0.68	1.30	----
[a]Leaving Mars	2.58	2.55	----	3.75	3.75	----	4.20	3.75	----
[c]Leaving Mars	1.66	1.63	----	2.93	2.93	----	3.38	2.93	----
Arriving Earth	6.80	6.70	6.77	7.82	7.82	7.75	8.30	7.82	7.75
[a] $\sum_{1}^{4} \Delta V$, miles/sec	16.47	16.49	11.68	16.8	16.8	12.68	16.2	16.4	12.09
[a] $\sum_{1}^{3} \Delta V$, miles/sec	9.67	9.79	4.91	8.89	8.89	4.93	7.91	8.57	4.34

[a]Circular parking orbit at Mars, $\bar{r}_c = 1.1$ radii.

[b]For propulsive gravity turn at Mars, used at sphere of influence leaving Mars.

[c]Parallel elliptic parking orbit at Mars, $\bar{r}_a = 27$ radii, $\bar{r}_p = 1.1$ radii.

For stopover mission profiles using atmospheric braking at Mars it is appropriate to consider nonstop atmospheric-turn round trips as a basis for an abort.

In addition to aborts in the vicinity of Mars there are two other classes of aborts, near Earth and on the outbound leg. There is little that can be done to improve the return trajectory once the spaceship has left Mars, so no consideration has been given to aborting from the return leg.

If the abort occurs near Earth, the abort ΔV requirement would be no more than the hyperbolic excess velocity, which for a 420-day mission is about 3.1 miles per second. This is within the propulsion capability of each of the remaining propulsion stages, that is, either the arrive Mars stage, the depart Mars stages, or the Earth deceleration stage for the fast trips.

Aborts on the outbound leg are illustrated in figure 37(a), where the positions of the spacecraft at various times along the way are noted. The minimum ΔV abort trajectory if an abort were initiated at 90 days is shown by the broken line. The spacecraft arrives back at Earth before the planned return time.

The results of a study of a family of minimum ΔV trajectories are summarized in figures 37(b) and (c). Abort ΔV and mission time are plotted against the time of abort initiation. The lowest abort ΔV occurs in the early part of the trip; thereafter, the abort ΔV requirement increases steadily in time until the vicinity of Mars is reached where a propulsion gravity turn at Mars yields a reduced ΔV requirement. As before for an abort during the outbound leg of the journey, the propulsive capability of stage two or three is available to change the trajectory. If stage two were damaged, the full ΔV capability of stage three (3.75 miles/sec for a low circular parking orbit at Mars or 2.93 for a parallel elliptic parking orbit) is available. If stage three were damaged, it would be jettisoned, and in the abort application stage two will provide about 5 miles per second (or 3.5 miles/sec from a parallel elliptic orbit), which is about twice the planned ΔV. The ΔV's available for abort in general exceed the ΔV's required, except for a period up to 70 days prior to Mars arrival. At Mars the propulsion gravity turn is within the available propulsive capability.

There is a sharp rise in abort trip time after the vehicle leaves the Earth's sphere of influence, as indicated by figure 37(c). The abort mission times are generally less than planned trip times except for aborts occurring within about 40 days of Mars arrival.

A propulsive abort with one stage out, which satisfies the same constraints as the original trajectory, is possible at any point of the outbound leg of the trip. Although only the 420-day trip in 1979 was investigated in detail, a preliminary analysis of other trip times and launch years indicates that the previous result is valid for most fast trips of the short-long category.

The possibility of aborting with one stage out when one of the available propulsive

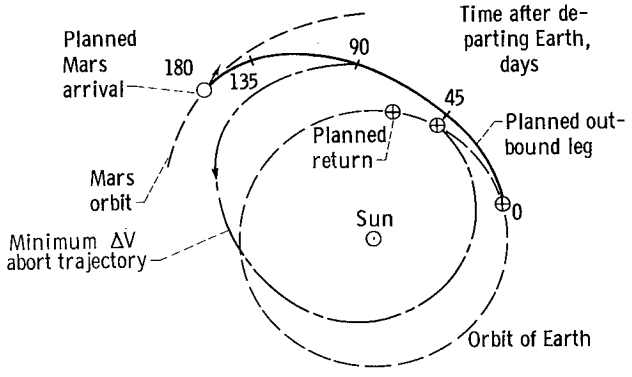

(a) Typical abort trajectory.

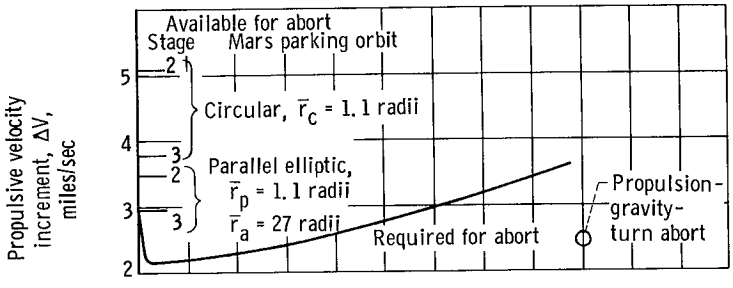

(b) Propulsion requirements.

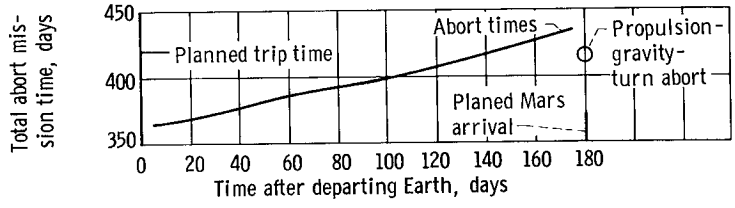

(c) Travel times.

Figure 37. - Aborts from outbound leg of a planned 420-day Mars trip with a 40-day stay, 1979-80.

stages is the stage for decelerating at Mars is an argument against using atmospheric braking at Mars.

To summarize, the fast mission profiles can be designed to include abort capability for little or no weight penalty.

Sensitivity of Initial Weight in Earth Orbit to Inputs

In the previous section, the initial weight in Earth orbit was estimated for a number of mission times. The estimated gross weights depend on the inputs of interplanetary vehicle payloads and on the propulsion system characteristics. Although an effort was made to make realistic estimates of the values for these inputs, there is a considerable variation in the estimates of values for the inputs between different investigators. Thus

it is informative to study the sensitivity of the initial gross weight to arbitrary variations in the inputs. That study is the purpose of this section.

Effect of mission payloads. - For this study, two 420-day single-phase mission profiles, each giving a high (H) and an intermediate (I) gross weight, were selected. The distinctive characteristics of each of the mission profiles are as follows: for case H, atmospheric braking from 37 000 fps at Earth return, 37 000 pounds of inert radiation shielding, and a low circular parking orbit at Mars; and for case I, atmospheric braking from twice circular velocity at Earth, propellant radiation shielding, and a low circular parking orbit at Mars. The sensitivity of the other mission profiles and mission times may be judged from these.

The effect of the interplanetary vehicle payload weights on the IWIEO is presented in figure 38. It is noted that the curves are all linear; the circled points correspond to the values assumed in the calculations prior to this sensitivity section, while the square symbol corresponds to twice these values. For reference, it is observed that if all the mission payloads were doubled simultaneously the IWIEO would at most double. Thus the effect of varying any one of the mission payloads individually must have less than a one-to-one effect on the IWIEO.

Figure 38(a) shows the effect of the Earth atmospheric entry vehicle weight. This weight undergoes all the interplanetary propulsive ΔV's. For case H, doubling this weight increases the IWIEO 36 percent. The percent increase would have been larger but for the large fixed weight of the nuclear engine used in the propulsive stage, which supplements the atmospheric braking, and does not scale up with an increase in stage weight.

For case I, chemical propulsion is used to supplement the atmospheric braking, and doubling the Earth entry vehicle weight increases the IWIEO about 47 percent. In this case, the advantage for decreasing the Earth entry vehicle weight is not the same as the penalty for increases in weight (i. e., the slopes of the curves differ for weight increases and decreases from the circled value). This behavior results from the hypothesized coincidence in the weight required for radiation shielding and for the weight of propellant required for partial rocket braking at Earth, at an Earth entry vehicle weight of 13 850 pounds. If the entry vehicle weight is increased, the chemical propellant must be correspondingly increased to provide the same propulsive deceleration. A propellant weight in excess of the radiation-shielding weight requirement then exists. If the entry vehicle weight is reduced, however, there can be no corresponding reduction in the propellant-shielding weight because the shielding requirements must be satisfied. Part of the shielding could, however, now be solid rather than propellant.

Figure 38(b) shows the effect of the weight jettisoned just prior to the deceleration at Earth. For the H mission profile this weight consists of the command module, the living module, the power supply, the fixed part of the food-air system, and the solar radiation shielding. For the I profile the solar flare shielding is not included because this weight

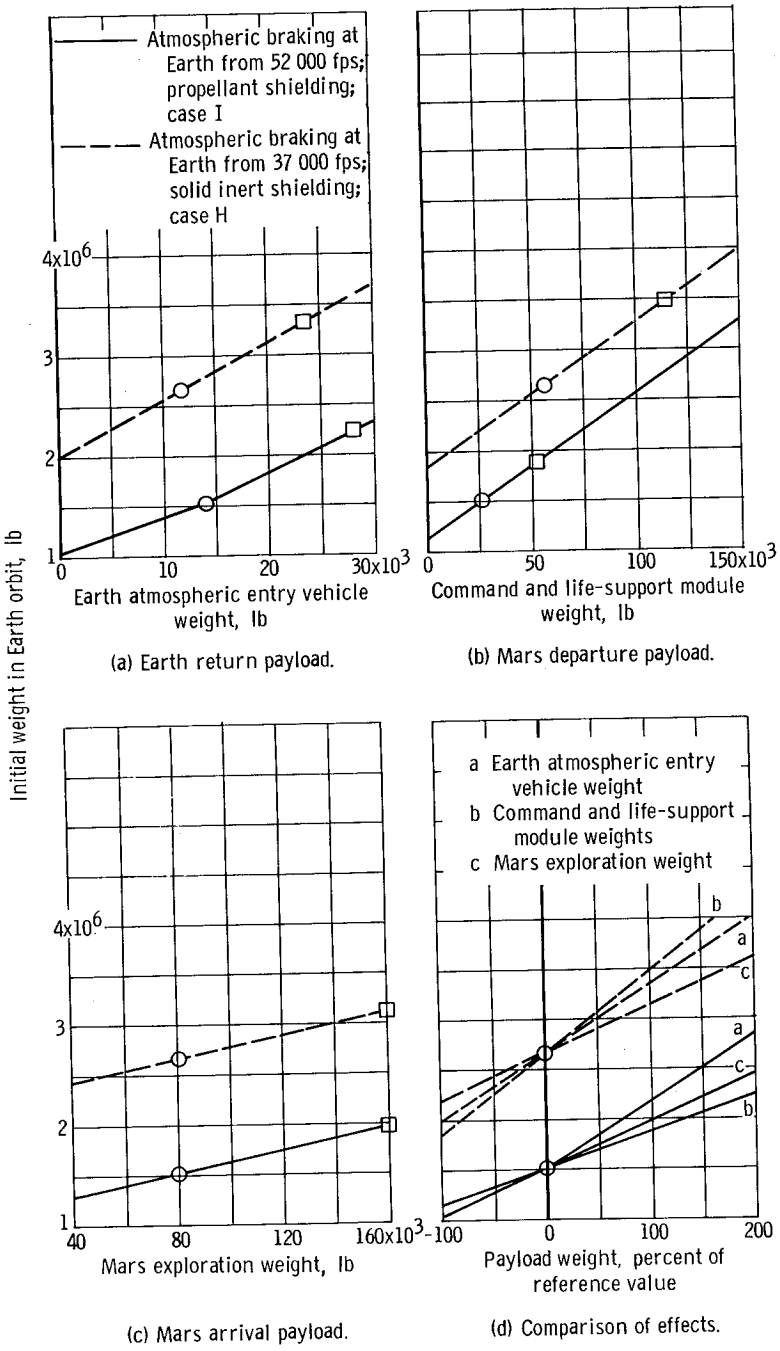

Figure 38. - Effect of mission payloads on initial weight in Earth orbit for a 420-day mission with a 40-day stay. Circular parking orbits at 1.1 Mars radii; nuclear space propulsion.

serves also as propellant for the propulsive part of the deceleration at Earth. The slopes of the two curves are the same, but because for the H profile this weight item is larger, the IWIEO is more sensitive to doubling this weight. The IWIEO is changed 32 percent compared with 22 percent for the I profile.

Figure 38(c) shows the effect of the Mars exploration weight, that is, landing systems plus probes and orbital observation equipment. The slopes of the two curves are the same, as are the weights of the exploration systems. Because the H profile has a higher IWIEO, it is less sensitive to doubling the weight of the Mars exploration system. In this case the weight increases 18 percent as compared with 29 percent for the I profile.

For the I profile the percent increase in IWIEO for simultaneously doubling all the mission payloads is 100 percent as expected. For the H profile the increase is 78 percent. This result occurs for the H profile because the nuclear engine for the Earth deceleration is a minimum (fixed) size and does not scale with the gross weight of that stage.

The abscissa of the previous variations have been normalized to a percent of the nominal or the circled value, and a comparison of the sensitivity of the initial weight to the interplanetary vehicle weights is made on this basis in figure 38(d). Both mission profiles are slightly more sensitive to a given percent change in the Earth entry vehicle weight (curve a) than to the Mars exploration weight (curve c). The importance of the weight jettisoned at Earth return (curve b) depends largely on whether this weight group includes inert radiation shielding or not. When inert shielding is carried, this weight group is more important than the other mission payloads (profile H). If propellant shielding is used and the radiation shield weight is not included in the life-support group, then the life-support weights are less important than the other mission payloads (profile I).

If the highest values shown in table I (p. 3) (the b values) had been used for each component of the mission payloads, the IWIEO's would have been about 70 percent higher than those for the reference points (circled points).

Because the mission payload weights vary from profile to profile, the sensitivities of the IWIEO to variations in the mission payloads will be different for the different mission profiles. The previous discussion has illustrated some factors affecting the sensitivities.

Effect of propulsion system performance. - Considered in figure 39 is the effect of engine specific impulse, engine weight, and effective propellant tank weight ratio. Again the circled point corresponds to the assumptions made in the mission profile analyses. Some specific examples are considered first. If the engine specific impulse is decreased from 850 to 750 seconds, then the IWIEO is increased from 1.55 to 2.05 million pounds or 32 percent. NERVA test performance, interpreted in terms of a 40:1 area ratio nozzle and a vacuum environment, has already attained a 750-second impulse (ref. 39). If, in addition, the engine weight is increased to give a corresponding reduction in the engine thrust-to-weight ratio from 8 to 4, the IWIEO is increased to 2.4 million pounds or

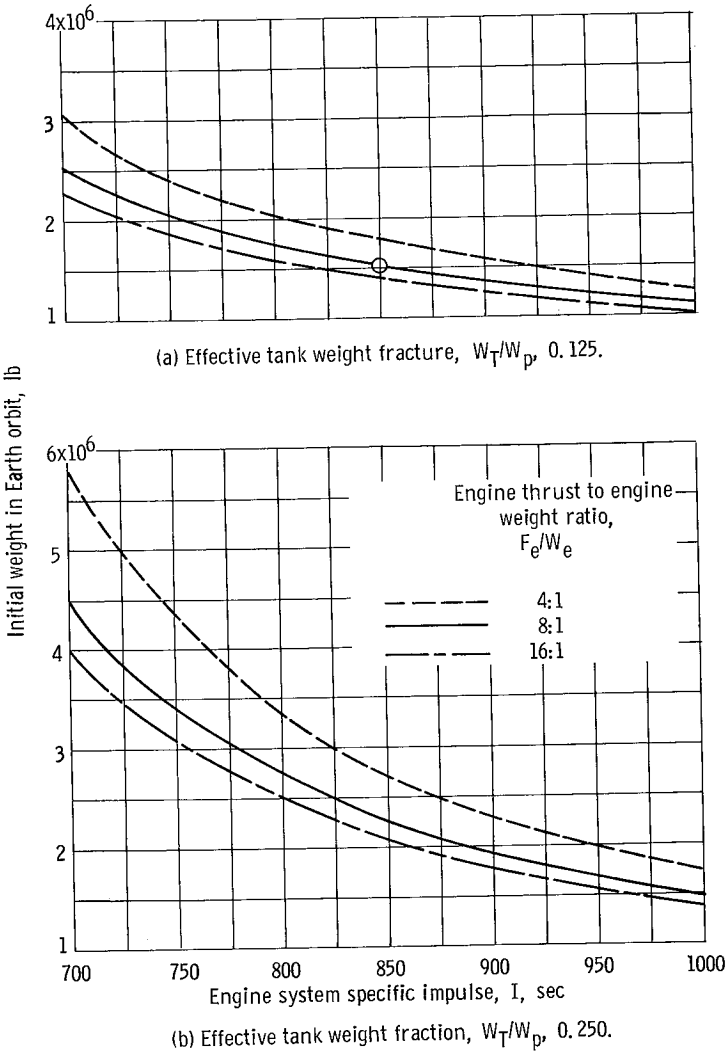

Figure 39. - Effect of propulsion system parameters on initial weight in Earth orbit. Mission duration, 420 days; stay time, 40 days; atmospheric braking at Earth from 52 000 fps; propellant shielding; circular parking orbits at 1.1 Mars radii; nuclear space propulsion.

another 17 percent. A thrust-to-weight ratio of 4 is about that of a 56 000-pound thrust NERVA; the ratio would increase for engines with a higher thrust (ref. 27). If, in addition, the effective tank weight fraction (see Mission Propulsion Systems for definition, p. 14) is increased from 0.125 to 0.25, the weight is increased to 4.35 million or another 81 percent. The percent increase in weight chargeable to each parameter depends on the order in which the incremental changes are calculated. Accumulated degradations in the performance of the three propulsion system parameters can result in large increases in the IWIEO (a factor of 2.7 in the present example).

A general observation to be made from the figure is that the sensitivity of the IWIEO to changes in propulsion performance is not linear; that is, the slopes of the curves are greatest at the highest values of IWIEO. This means it is important to achieve the performance levels assumed in the body of the report.

In figure 40 a number of mission profiles are compared for two sets of propulsion system inputs. The profiles with nuclear propulsion show that the IWIEO for the less sophisticated profiles, those with high propulsive ΔV's (profiles 1 and 2), are very sensitive to the performance of the propulsion system. The sophisticated profiles (profiles 3, 4, and 5) with low ΔV are much less sensitive to the performance of the propulsion system. It is for this reason that profiles 3, 4, and 5 can be accomplished for reasonable weights by using chemical propulsion as shown by the last three bars.

The chemical systems because of their higher weight tend also to be more sensitive to changes in performance. However, because chemical systems presently exist, there is less uncertainty in the values of some of the propulsion system parameters for chemical systems than for nuclear systems. For example, a specific impulse of 425 seconds

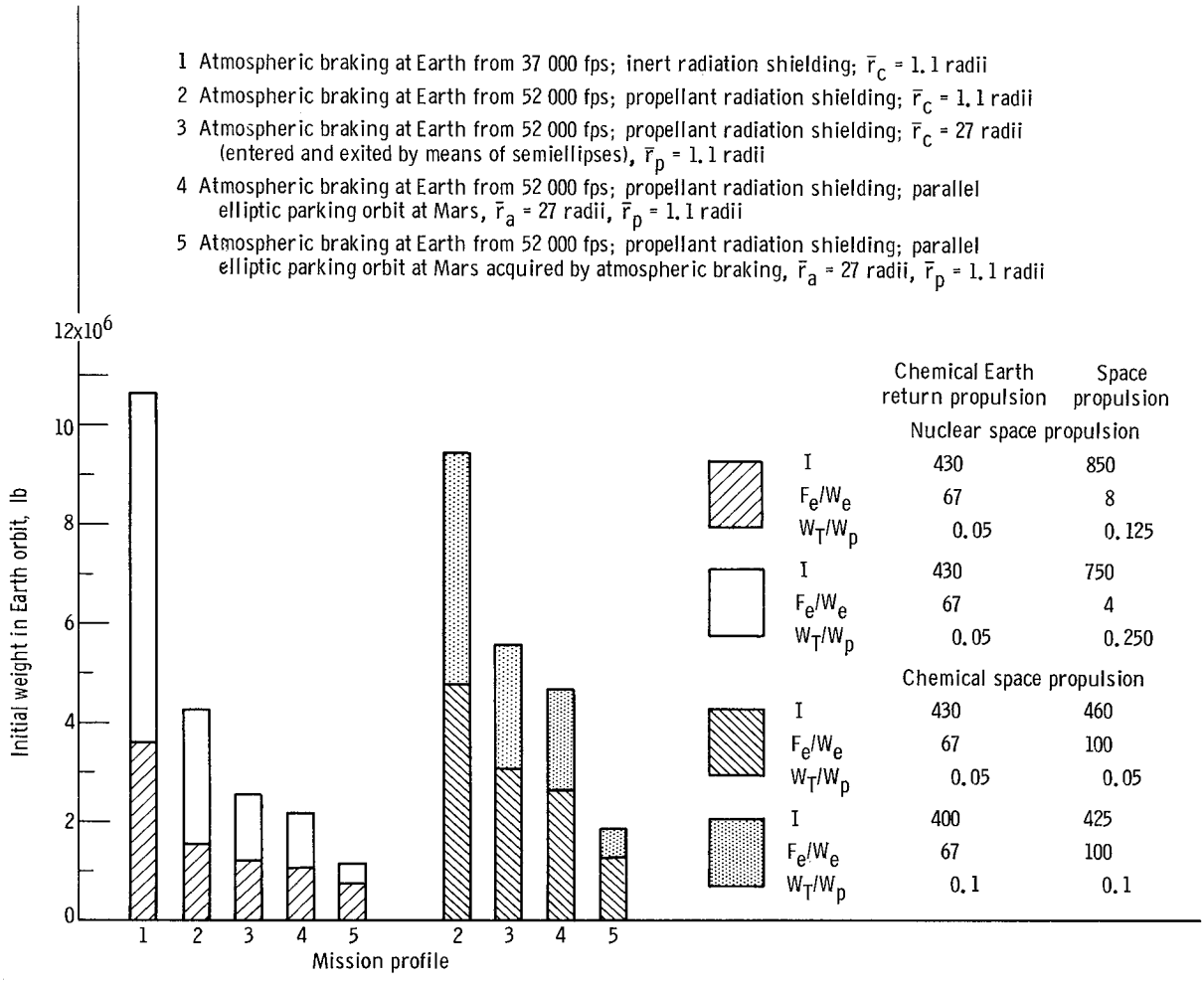

Figure 40. - Sensitivity of various mission profiles to combined variations of propulsion system parameters. Mission duration, 420 days; stay time, 40 days.

is presently obtainable with hydrogen-oxygen propellants, and engines with thrust-to-weight ratios of 67 do exist. Techniques of improving the existing values are known. For example, specific impulse may be improved by using hydrogen-fluorine and higher pressure engines with larger expansion ratios. The tank fractions of both chemical and nuclear systems are not well known.

Another point made by comparing the open and cross-hatched bars of figure 40 is that optimistic propulsion system characteristics show the effect of profile changes in a conservative light. With regard to the previously discussed effect of profiles the effects shown would all have been larger had lower levels of propulsion system performance been assumed.

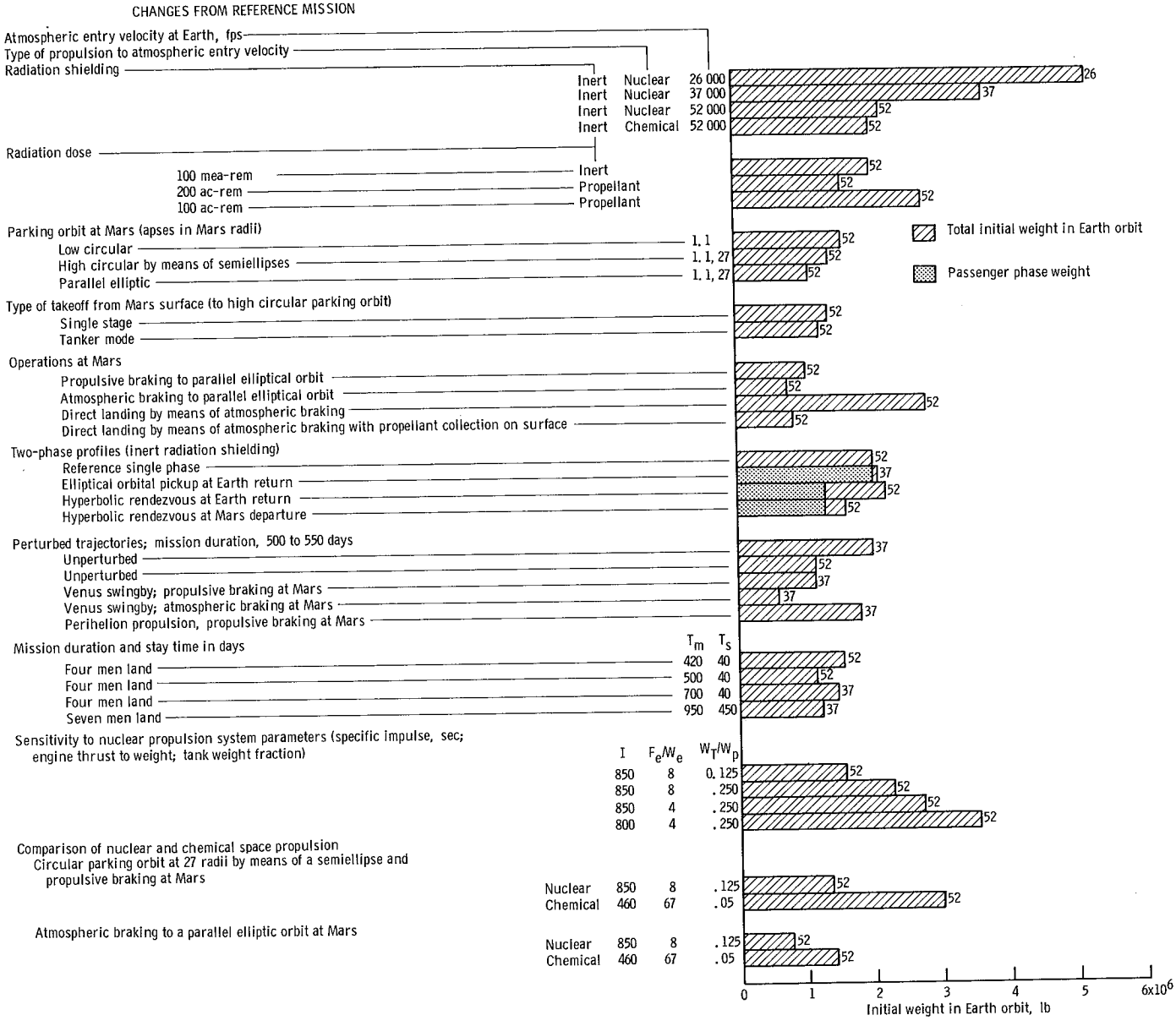

Figure 41. - Summary of effects of mission profile on initial weight in Earth orbit for seven-man Mars landing mission. Reference method has the following characteristics: nuclear space propulsion; mission duration, 420 days; stay time, 40 days; single phase; Mars parking orbit, 1.1 radii; single-stage takeoff from Mars surface; propellant for radiation shielding; dose, 100 mea-rem; seven-man crew, four men land. (Propulsion for deceleration at Earth return to atmospheric entry velocities noted at top of bars, 1000's fps.)

CONCLUDING REMARKS

A summary of the effects of mission profile on the initial weight in Earth orbit for a seven-man Mars landing mission is presented in figure 41.

Based on the insights gained from the mission analysis, the technical areas needing further research are pointed out, and a profile for an early mission is suggested.

Technical Areas for Research

The preceding analysis and discussion indicate that a final decision as to the best mission profile depends on increased information in the following areas:

1. Mission objectives: the desired length of stay time and the number of men desired on the surface, the surface mobility requirements, the number and location of landing sites, the scientific experiments to be performed
2. Rendezvous in planetary orbits and in solar orbits
3. Space environment: meteoroid and radiation fluxes from 0.30 to 1.5 astronomical units and in the vicinity of Earth and Mars
4. Man's capabilities: his physical reaction to acute and chronic proton and neutron radiation dose and his physiological and psychological reaction to long mission times and low g's
5. Explorability of the Mars surface and the Mars surface environment in terms of radiation, meteoroids, locomotion, and winds
6. Long-time life-support systems up to 1000 days
7. Earth atmospheric entry up to 52 000 fps or more
8. Performance of nuclear engines
9. Hydrogen tankage, including thermal and meteoroid protection, fuel transfer, and structural weights
10. High specific impulse, high density, and space storable, and Mars surface storable chemical propellants
11. Mars atmospheric entry from at least Mars parabolic speed (for landing from a Mars parking orbit)
12. Hyperbolic entry velocities at Mars
    (a) for the landing systems
    (b) for the entire spaceship
13. Feasibility of propellant generation at Mars

Criteria for Selecting a Mission Profile

To select a mission profile some criteria of merit must be adopted. Most criteria of merit are ultimately related to minimizing cost, that is, minimizing the required commitment of the national resources of material and manpower. The cost of fulfilling a number of objectives can be considered; for instance, one can consider minimizing the cost of a specific mission, the cost of the overall and continuing space program, which includes the above specific mission, or the cost per unit of information gained. While it is beyond the scope of this report to estimate actual costs, several factors related to cost can be considered.

Earth surface to orbit launch weight. - An important part of the cost of a mission is in the cost of delivering the space vehicle into orbit about the Earth. The IWIEO discussed in the preceding sections is a relative measure of this cost. Another factor influencing launch costs is the required launch rate. For the two-phase mission profiles, the launches occur in two periods separated by months or years.

Advanced development. - The cost of the research and development to reach the technology required to accomplish the mission is in part chargeable to the mission. This would include the development of new boosters or Earth orbital rendezvous techniques if they are required.

Compatibility with overall space program. - Perhaps more important than the cost of a specific mission is the cost of achieving the overall long-range space objectives. It is desirable to develop a technology that will be applicable to many missions. This technology in turn helps determine the desirable mission profile.

Data acquired. - The objective of the mission is to acquire data. Some mission profiles are more favorable in this respect than others, for instance, those with long stay times.

Timing. - The information to be acquired is presumably of value and so it is desirable to acquire this information as soon as practical.

Crew safety. - For manned missions the survival of the crew, even in the event the mission fails in some of its scientific aspects, is of paramount importance. This requires mission profiles that have abort capability from any point in the mission

Probability of mission success. - A high probability of mission success or a reliable mission is, of course, desirable. This suggests preferring simple operations, well established technologies, and a short mission duration.

Suggested Mission Profile

There are many attractive mission profiles to choose from, each with advantages and disadvantages. There is the 1000-day trip with its attractively long exploration

times and comparatively easy propulsion and atmospheric entry requirements, or there are the Venus swingby combined with atmospheric braking at Earth and Mars and the 700-day trip both with their very low weights. The profile to be described, however, seems to best fit all the criteria, although some of the reasons to be given for selecting this profile are matters of judgement rather than of facts.

The mission profile chosen for the 1980 time period is an unperturbed trajectory of 420 days in duration. This mission duration was chosen over the 1000-day missions on the basis of reliability and crew psychology, and because the 420-day trip offers abort possibilities that the 1000-day trip does not offer. It was chosen over the 500- to 550-day missions which includes perihelion propulsion and Venus swingby trajectories, to avoid the combination of low perihelions and long trip times that can result in high radiation doses or high shield weights. Trip times shorter than 420 days yield rapidly increasing IWIEO's.

Nuclear propulsion is used for all the space maneuvers except that of Earth approach because its potential offers lower weights than chemical propulsion. Chemical propulsion is used for the Earth deceleration and Mars landing and takeoff maneuvers because it is more efficient than nuclear propulsion for the light payloads associated with these maneuvers.

At Earth return the real mission payloads, the crew, samples, and data are decelerated to an elliptic orbit about Earth. These payloads are then picked up by a recovery vehicle launched from Earth at the end of the mission. This system was chosen over atmospheric braking at Earth return for several reasons:

1. The IWIEO for the two systems appear about equal, but propulsive braking should be cheaper to develop.

2. The propulsion system for the Earth deceleration is part of the system for aborting from orbit about Mars, as will be discussed subsequently.

3. The propulsive deceleration can be more reliable than the atmospheric braking system because of the dual nature of the deceleration system described next.

The Earth deceleration system is to consist of two potentially independent units. The first has the crew as its payload. The second has the samples and data as payload, which weighs about the same as the crew. Thrusting is initiated prior to perigee. In the event of a malfunction of the system with the crew, the samples and data are jettisoned and their propulsion system used to decelerate the crew. The samples and data may then make an atmospheric entry from the full hyperbolic approach velocity.

The Mars parking orbit is an elliptic orbit with its major axis nearly perpendicular to the plane of the interplanetary transfers. The elliptic orbits yield lighter weight than a low circular orbit. The plane chosen for the ellipse permits observation of all of the Mars surface and landing any place in one hemisphere with little weight penalty.

Propulsive deceleration is used at Mars. This can probably be developed to man-rated status cheaper and sooner than atmospheric braking, and atmospheric braking offers only a small weight advantage over propulsive braking when an elliptic parking orbit is used. Also, this propulsion stage is available for abort propulsion in the event of damage to the leave-Mars stage on the outbound leg of the trip.

The Mars landing system is viewed as consisting of three manned-type landers. (The mission analyses assumed two.) Each lander has the capability of landing two men and returning two men plus 500 pounds of samples or four men to orbit. The first lander is to be landed and returned to orbit by remote control (unmanned) to serve as a "proof test" vehicle. If the test is successful, the men land. If it is unsuccessful, the men do not land. A fourth lander is an equipment vehicle. It lands a roving laboratory that can be operated remotely from orbit or by the landed explorers.

The most difficult point from which to perform an abort (in terms of increased mission weight) is from the Mars parking orbit in the event of damage to or a malfunction of the leave-Mars stage. To achieve an abort capability from this situation, a separate life support and Earth deceleration system may be launched from Earth shortly after the mission launch on a hyperbolic-rendezvous-at-Mars departure trajectory. The crew then uses the Earth deceleration stage existing in the Mars parking orbit to rendezvous with this second Earth deceleration and life-support system. This appears to be the lightest method to achieve an abort capability from Mars orbit.

The purpose of the preceding example has been to review some of the more important concepts and ideas that have resulted from the present analysis such as the use of elliptic orbital pickup at Earth return, the dual use of chemical propellants for deceleration at Earth return and for radiation shielding, the elliptic parking orbits at Mars, the tanker mode of Mars takeoff operation, the possible critical importance of long mission times and low perihelions to crew radiation dose, and the mission profiles with abort capability from any place in the mission.

More generally the present analysis has shown there are a large number of potentially attractive mission profiles. This is important because it means that it is unlikely that technical obstacles in any one area will preclude doing the mission. As was mentioned earlier, the final choice of a preferred profile must await further definition of mission objectives, additional information on many technical areas, and further study that will hopefully reveal still more favorable mission profiles.

Lewis Research Center,
National Aeronautics and Space Administration,
Cleveland, Ohio, September 14, 1965.

APPENDIX A

SYMBOLS

e	parking orbit eccentricity
F_e/W_e	engine thrust to engine weight ratio (includes weight of thermal shielding - and biological shielding when required)
g	acceleration due to gravity at Earth's surface, ft/sec^2
I	propulsion system specific impulse, pounds of thrust per Earth pounds of fuel per second, sec
L/D	atmospheric entry vehicle lift-drag ratio
$\overline{r}_a$	apoapsis in Mars radii of elliptical parking orbit at Mars
$\overline{r}_c$	radius in Mars radii of circular parking orbit at Mars
$\overline{r}_p$	periapsis in Mars radii of elliptical parking orbit at Mars or of semiellipse used to depart from or arrive at a high circular parking orbit
$\overline{r}_\oplus$	radius in Earth radii of rendezvous with spaceship at Earth return (fig. 30(a), p. 61)
T_m	mission duration, days
T_s	stay time, days
$\Delta T_{1,2}$	transit time from Earth to Mars, days
$\Delta T_{2,3}$	stay time at Mars, days
$\Delta T_{3,4}$	transit time from Mars to Earth, days
V_H	velocity along trajectory in heliocentric coordinates
$V_\oplus$	atmospheric entry velocity at Earth, fps
$V_{\sigma'}$	atmospheric entry velocity at Mars, fps
ΔV	propulsive velocity increment, statute miles/sec
W_E	empty weight of stage
W_G	initial weight of stage
W_S/W_p	shield to propellant weight ratio
$(W_S/W_G)_{\sigma'}$	ratio of structure plus heat protection weight plus atmospheric approach guidance and control weight to entry vehicle gross weight for atmospheric braking from hyperbolic speeds at Mars
W_T/W_p	effective tank weight fraction

α angle between heliocentric trajectory and local horizontal (perpendicular to radius vector from Sun), deg

τ period of parking orbit at Mars, days

Subscripts:

a to establish elliptical rendezvous orbit at Earth (fig. 30(a), p. 61)

b to rendezvous with spaceship at Earth return from elliptical rendezvous orbit (fig. 30(a))

h at perihelion

mc midcourse correction

1 leaving Earth

2 arriving Mars

3 leaving Mars

4 arriving Earth

5 to perform landing at Mars from elliptic parking orbit

6 to perform landing at Mars from circular parking orbit

7 to transfer from high circular parking orbit at Mars to a cotangential ellipse with a periapsis at 1.1 Mars radii

8 to transfer from cotangential ellipse to circular orbit about Mars at 1.1 Mars radii

$\oplus$ Earth

σ Mars

APPENDIX B

BIOLOGICAL SHIELDING

Biological shielding requirements constitute one of the major factors affecting IWIEO. The purpose of this section is to discuss the radiation environment and to show how the shield weights were estimated as a function of mission time and mission trajectory.

Radiation Sources

The crew receives radiation from nuclear reactors, Van Allen belts, galactic sources, and solar flares. Radiation from the nuclear reactor has been discussed in the Mission Propulsion Systems section (p. 14).

The Van Allen belts consist of protons and electrons trapped in the Earth's magnetic field. The dose received during Earth departure is about 0.5 rem since the crew can be in the command module and the traversal time is on the order of 1 hour (ref. 40). For Earth return, however, the command module will be jettisoned prior to the Earth deceleration maneuver. The crew will pass through the belts in the Earth entry vehicle. Despite the small shielding density afforded by vehicle structure and heat protection material, the dose for Earth return is still only 4 rem because of the short traversal time. These doses are of minor importance compared to those from other sources.

Galactic radiation consists of highly energetic particles, which are mostly protons. Although the flux of these particles is very low, they exhibit significant variations with time that are related to solar activity. Because these particles have enormous penetrating power and due to the buildup of secondaries even in low Z-number materials, shielding may be impractical. The dose from this source will be discussed later along with that from small solar flares.

At irregular intervals, the Sun emits bursts of radiation that are classified according to the area of the visible disturbance of the Sun's surface. Class 1 and 2 flares occur almost continuously, but their accompanying radiation is believed to be low in energy. Class 3 flares, which occur less frequently, emit mostly protons of energies up to 500 million electron volts.

At rare intervals there occur giant major flares. These are large flares of the class 3+ type. During these events the flux of energetic particles may increase several thousand times the quiescent values. Typically, total intensities of big events are on the order of 10^4 particles per square centimeter per second of energy above 40 million electron volts.

Although it is well established that large solar flares will present a serious hazard

TABLE XV. - LARGE SOLAR FLARE FREQUENCY

[0.99 Probability of not exceeding specified number.]

Exposure time, days	Class of flare	
	3+ (1/2 envelope)	[a]Envelope
	Average frequency, yr	
	1	4
	Number of flares	
160 - 210	2	1
210 - 300	2	2
300 - 462	3	2
462 - 630	4	2
630 - 654	4	3
654 - 800	5	3
800 - 1000	6	4

[a]Envelope flare of reference 30.

to space flight, background sources consisting of galactic radiation and small solar flares may also contribute significantly, especially for missions of extended duration. Foelsche (ref. 41) estimates the free-space dose rate from galactic radiation to be about 0.45 rem per week during solar maximum years, and approximately twice this during solar minimum years. When major solar flares are neglected (ref. 32), it is estimated that the yearly average skin dose from solar protons, behind 6 to 8 pounds per square foot of shielding, is probably less than the maximum integrated yearly free-space dose estimated for galactic radiation.

When these estimates are used, the background dose rate is assumed to be 1.4 rem per week. Galactic radiation, which accounts for 0.9 rem per week, is typical of that for a solar minimum year. The crew is exposed to the solar proton dose rate of 0.5 rem per week in the living module where the shield density is about 6 pounds per square foot.

The dose from these sources is affected by the 11-year solar cycle. In solar maximum years the galactic dose rate decreases. The frequency of small flares, however, increases. Because of uncertainties involved in this area, the background dose rate is assumed to be constant with both time and distance from the Sun.

The dose from large solar flares is dependent strongly on the flare spectrum. For the giant major flare, the spectrum at 1 astronomical unit is taken to correspond to the envelope flare of reference 32 which is assumed to occur with an average frequency of once every four years. The other large class 3 flares are assumed to have an average frequency of one per year. For a given shield thickness, their dose is assumed arbitrarily to be one-half that of the giant major flare. It is further assumed that the flux of these flares varies inversely with the square of the distance from the Sun for closer distances (ref. 42 gives some discussion of this point).

The occurrence of large solar flares cannot be predicted at the present time except on statistical grounds. They are, therefore, assumed to occur at purely random intervals with the previously mentioned average frequency. The design number of flares is given in table XV where the probability is 0.99 of not exceeding the given number of each type. Correspondingly, the probability of not exceeding the radiation dose associated with the design number of flares is also 0.99.

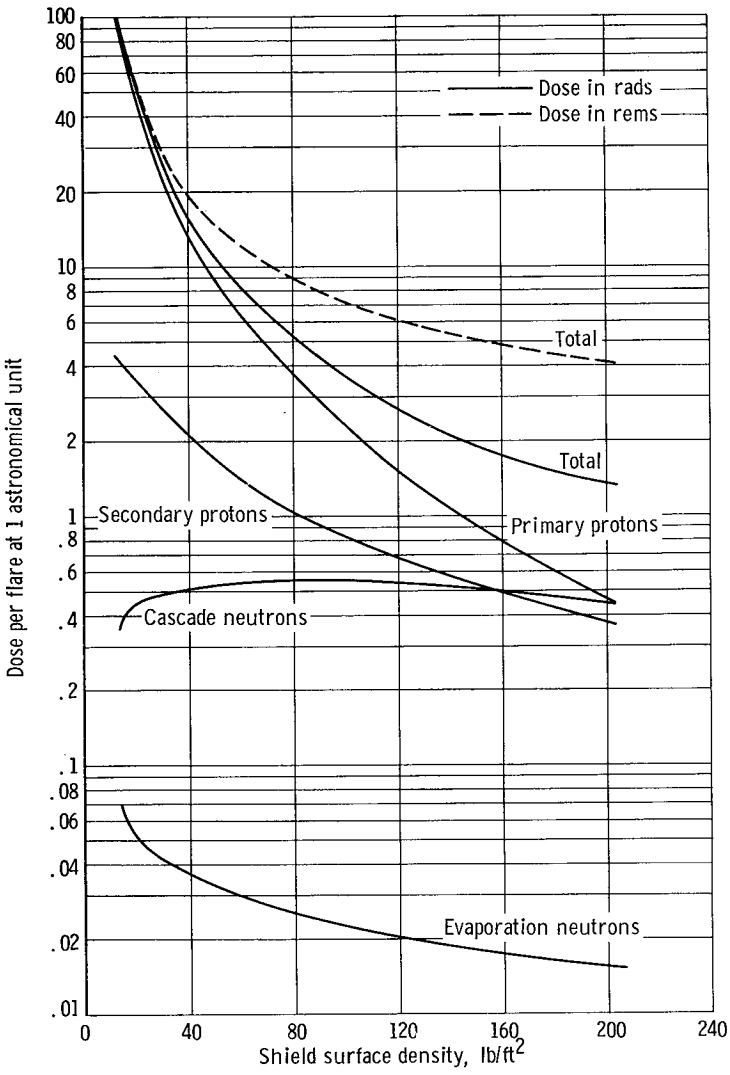

Figure 42. - Radiation dose from giant major flare at 1 astronomical unit.

Giant major flares are assumed to occur at the following points along the trajectory: the first at the point of closest approach to the Sun; the second at 1 astronomical unit just before final propulsive maneuver; the third just before leaving Mars; the fourth evenly distributed, in time, on the Earth-Mars trajectory. The other large class 3 flares are distributed with one at the perihelion and the others at 1 astronomical unit and evenly distributed, in time throughout the mission duration.

Shield Characteristics

The radiation dose received from these flares is also a function of the interposed shield surface density and the characteristics of the shield material. Figure 42 shows the variation in dose, imparted by a single giant major flare at 1 astronomical unit, with shield surface density (in lb/sq ft of surface area). The results were obtained by using the method of reference 43. The shield material is water, which is assumed to be representative of the shielding characteristics of $BeH + H_2O_2$ or $B_2H_6 + OF_2$ that are assumed in many of the mission calculations. The solid lines indicate the dose, in rads, from solar flare protons and secondary radiation produced by the interaction of these particles with the shield material. These secondary particles include protons in addition to cascade and evaporation neutrons. When a relative biological effectiveness (RBE) of 1 is assumed for both primary and secondary protons and an RBE of 7 for both cascade and evaporation neutrons, the total rem dose is indicated by the dashed line.

If adequate shielding is provided around the volume desired for normal living quarters, the shield weight is prohibitive. A solution to this problem exists because as previously mentioned large solar flares occur only infrequently and last for only short periods of time (e. g., a day). During these periods, the crew can be sheltered in a small volume

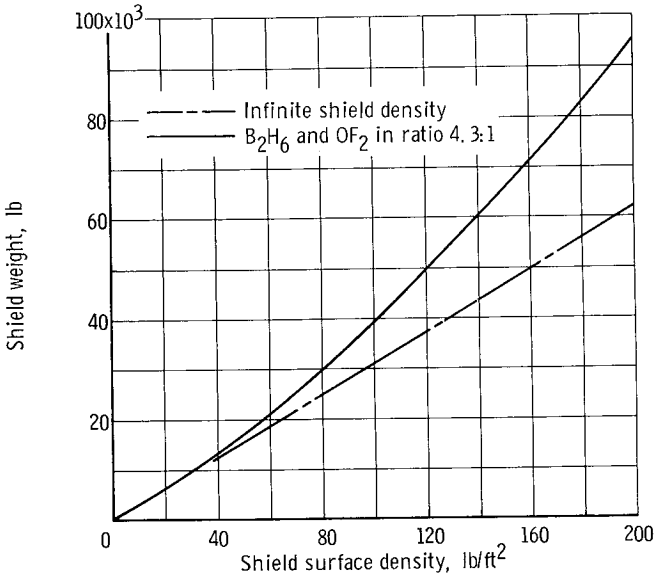

(a) Effect of shield surface density on shield weight.

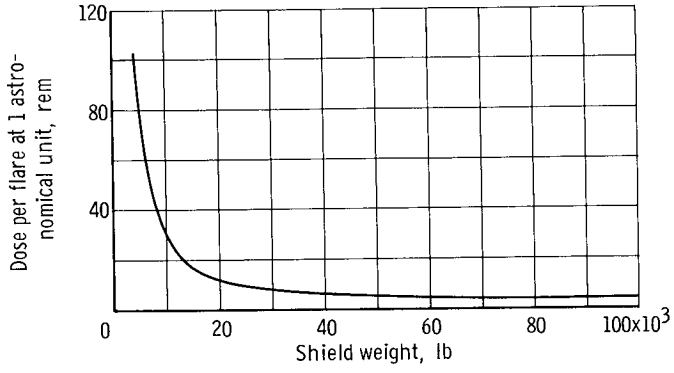

(b) Variation of water shield weight with dose.

Figure 43. - Command module shielding. Volume, 450 cubic feet.

to reduce shielding weight. This command module has a volume 450 cubic feet. From the shielded volume and shield surface density the shield weight may be calculated. Figure 43 shows the variation in shield weight with dose.

Allowable Dose

One of the many uncertainties concerning shielding calculations involves a definition of the permissible crew dose. The median lethal dose for man is considered to be about 500 rems (ref. 33). Reducing the dose to 200 rems is expected to cause vomiting and nausea for about one day, followed by other symptoms of radiation sickness in about 50 percent of the personnel. For still lower doses the immediate effects are reduced, so that only about 5 to 10 percent of the personnel exposed to 100 rems will experience any radiation sickness (ref. 33). No deaths are anticipated at either of these two levels. Since these symptoms are for acute radiation exposure, they do not include the influence of dose rate.

It is known that equal rem doses given over different exposure times result in different degrees of injury; that is, a considerably larger dose can be tolerated if it is received over a period of weeks or months rather than days. These observations lead to the hypothesis that the body recovers from radiation. Schaefer in reference 34 suggests a tentative quantitative model based on small animal (mice) data extrapolated to man. The effective injury is expressed in terms of an equivalent instantaneous dose. As an example, a dose rate of 1.14 rem per day for 1 year yields an accumulated dose of 416 rem, but with body recovery the net injury is the same as that from instantaneous dose of 100 rem. A recent report (ref. 44) shows a much slower rate of recovery for large animals (sheep and goats) than would be expected from the extrapolation of the data for small animals. Hence, the present results which assume body recovery may be optimistic. Thus, in attempting to assign limits to the radiation dose, one of the uncertainties derives from

the influence of the recovery phenomenon.

The approach used here is to assign limits to the crew dose depending on whether the recovery phenomenon was assumed. Doses of 100 and 200 rems were selected when assuming no recovery, while the dose assuming recovery was 100 rems. These doses are called accumulated dose and maximum equivalent acute dose, respectively. As mentioned before, the probability of not exceeding the specified doses is 0.99 corresponding to the probability of not exceeding the number of flares assumed.

Shield Weights

When the aforementioned data is used, the required shield weights can be found. Figure 19 (p. 42) shows the variation in shield weight with trip time for the three values of the crew dose. If the crew is limited to an accumulated dose of 100 rems, the shield weight increases rapidly with mission time. Since the dose from background radiation is assumed to be fully cumulative, the allowable dose from solar flares decreases. Consequently, the required shield thickness must be increased.

To increase the allowable dose for solar flares, the total accumulated dose can be increased. It is seen that a value of 200 rems results in a substantial weight reduction and a more gradual change in shield weight for mission times of less than about 500 days. Similar shield weights are required if the crew is limited to a maximum equivalent acute dose of 100 rems.

However, for the longer trips (i.e., 700 to 1000 days), a maximum equivalent acute dose of 100 rems results in much lower shield weights than the 200 ac-rem. Also for the same maximum equivalent dose, the shield weight is about as low or lower than that required for shorter trip times. Although more flares occur during the longer trip times, the vehicle does not approach as close to the Sun.

APPENDIX C

MARS LANDING AND TAKEOFF MANEUVERS

The Mars landing systems weight depends on the propulsive velocity increments for landing and takeoff. The landing and takeoff trajectories are shown schematically in figure 44 and the corresponding ΔV's are shown in figure 45. The purpose of the landing trajectories (figs. 44(a) and (b)) is to inject the lander into the Mars atmosphere where the primary deceleration takes place by atmosphere braking. (A terminal retrorocket is also used.) This general mode of operation is possible for even the lower estimates for the Mars atmosphere surface density. Trajectories are characterized by a 10^{o} path

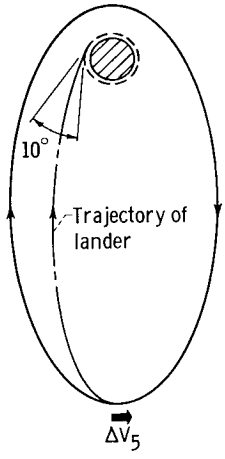

(a) Landing from elliptic orbit.

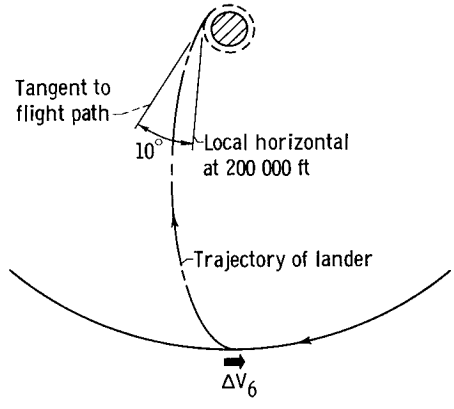

(b) Landing from circular orbit.

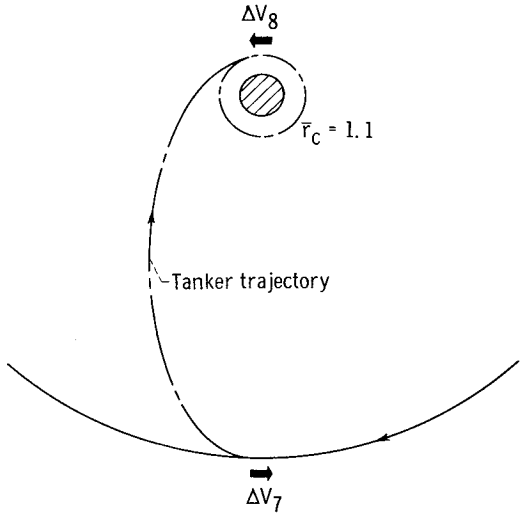

(c) Maneuvers for tanker and two-stage mode of operation.

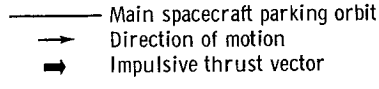

Figure 44. - Mars landing and takeoff maneuvers.

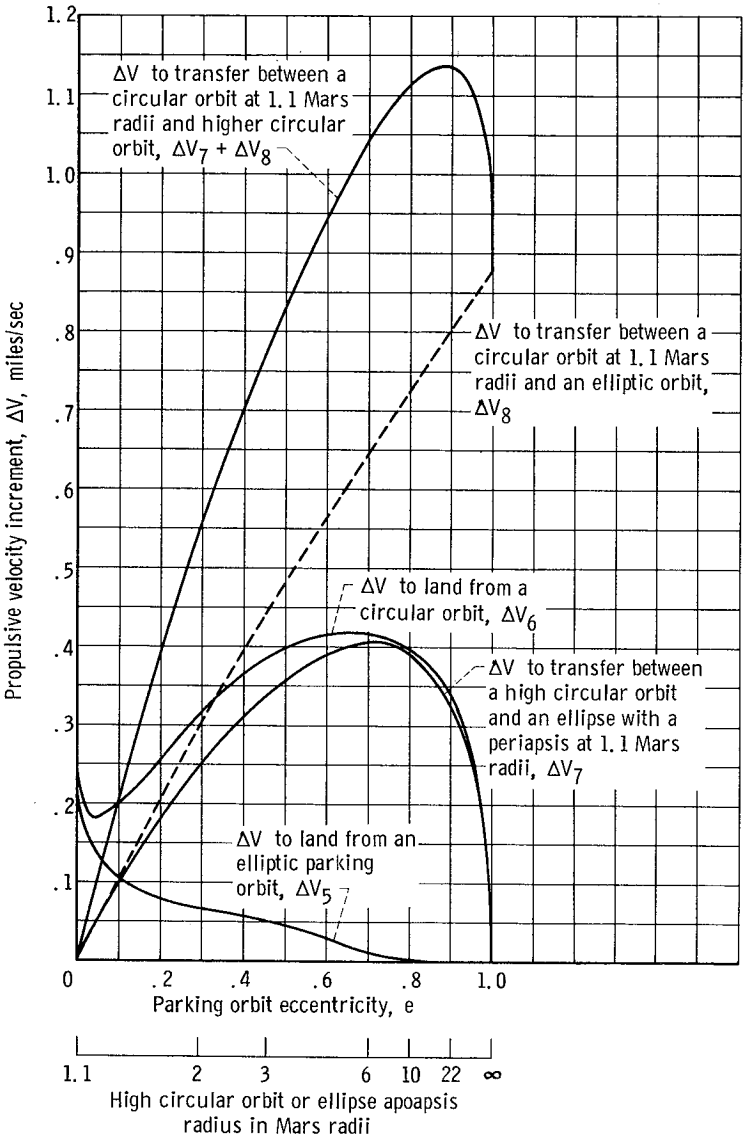

Figure 45. - Propulsive velocity increments for Mars landing and takeoff.

angle at 200 000 feet altitude within the atmosphere. The 10^{o} path angle is believed to give good landing accuracy with acceptable heating and g loads. The retro ΔV required at the apoapsis of a parking ellipse is designated ΔV_5. The parking ellipes have a periapsis of 1.1 Mars radii in every case. The retro ΔV for injection into the atmosphere from a circular parking orbit is ΔV_6. From figure 45 it is noted that a much larger ΔV is required to land from the circular parking orbit than from the elliptic parking orbit, and that the ΔV to land from the less eccentric ellipses is larger than for the highly eccentric ellipses.

One of the landing and takeoff profiles considered uses a tanker maneuvered into a circular orbit at 1.1 Mars radii (fig. 44(c)). For this case ΔV_7 is the increment to transfer from the high circular orbit to a cotangential ellipse with a periapsis at 1.1 Mars radii. The ΔV_8 is the increment used to establish the circular orbit at 1.1 radii. The total ΔV to establish a low circular orbit from a high circular orbit is $\Delta V_7 + \Delta V_8$. If the spaceship parking orbit is an elliptic orbit, then only ΔV_8 is required to establish the low circular orbit. It is noted that $\Delta V_7 + \Delta V_8$ can be substantially larger than ΔV_8.

For takeoff the same $\Delta V_7 + \Delta V_8$ is required to attain rendezvous at the high circular orbit from the low circular orbit, and ΔV_8 is needed to achieve an elliptic parking ellipse from a low circular orbit.

The takeoff from the Mars surface to achieve a low circular parking orbit was calculated by using an optimum thrusting program. The required total velocity increment to achieve a 1.1 radii orbit is 16 700 feet per second. This is 1.37 times the surface circular velocity. This factor is larger than is usually estimated for a comparable Earth launch.

REFERENCES

1. Ehricke, Krafft A.: A Systems Analysis of Fast Manned Flights to Venus and Mars. Pt. I: Mission Philosophy, Life Support, Scientific Reconnaissance and Prototype Vehicle Layout. Rept. No. AZM-072, Convair-Astronautics, Mar. 11, 1959.

2. Konecci, E. B.; Trapp, R. F.; and Hunter, M. W.: Manned Nuclear Space Systems. Pt. I - High-Thrust Nuclear Systems. Aero/Space Eng., vol. 19, no. 1, Jan. 1960, pp. 34-41.

3. Himmel, S. C.; Dugan, J. F., Jr.; Luidens, R. W.; and Weber, R. J.: A Study of Manned Nuclear-Rocket Missions to Mars. Aero/Space Eng., vol. 20, no. 7, July 1961, pp. 18-19; 51-58.

4. Ehricke, K. A.; Garber, D.; Robey, D.; D'Vincent, F.; and Evans, B., et al.: A Study of Early Manned Interplanetary Missions. NASA CR-51364, 1963.

5. Dixon, F. P.; Caldwell, M. H.; Johnson, D. P.; Nagorski, R. P.; and Onstead, E. W.: Empire - A Study of Early Manned Interplanetary Missions. NASA CR-51709, 1962.

6. Ragsac, R. V.; Ross, M. G.; Koehler, L. F.; Taulber, Z. A.; and McLaughlin, J. F., et al.: Early Manned Interplanetary Mission Study. Vol. 1. Summary Report. NASA CR-51297, 1963.

7. Anon: Manned Mars Exploration in the Unfavorable (1975-1985) Time Period. Vol. II. Summary. NASA CR-53911, 1964.

8. Ehricke, K. A.: A Study of Early Manned Interplanetary Missions (Empire Follow-On). NASA CR-60375, 1964.

9. Anon.: A Study of Manned Mars Exploration in the Unfavorable Time Period (1957-1985). Vol. III. NASA CR-53668, 1964.

10. Sohn, R. L.: Summary of Manned Mars Mission Study. Paper presented at Symposium on Manned Planetary Missions, 1963/1964 Status, NASA Marshall Space Flight Center, January 28-30, 1964. Rep. 8572-6009-RU-000, Thompson-Ramo-Wooldridge Space Technology Labs., 1964. (Also available as NASA TM X-53049, 1964, pp. 149-219.)

11. Widmer, Thomas F.: Application of Nuclear Rocket Propulsion to Manned Mars Spacecraft. Proc. AIAA and NASA Conf. on Eng. Problems of Manned Interplanetary Exploration, Palo Alto (Calif.), Sept. 30-Oct. 1, 1963, AIAA, pp. 85-101.

12. Ragsac, R. V., et al.: Manned Interplanetary Missions. Follow-on Study of Final Report. Vol. 1. Summary. NASA CR-56762, 1964.

13. Jones, A. L.; and McRae, W. V.: Manned Mars Landing and Return Mission Study. Vol. 1. Condensed Summary. NASA CR-57012, 1964.

14. Shapland, D. J.: Preliminary Design of a Mars-Mission Earth Reentry Module. NASA CR-56209, 1964.

15. Dixon, Franklin P., and Neuman, Temple W.: Study of a Manned Mars Excursion Module. Vol. I of III - Pt. I. NASA CR-56182, 1963.

16. Seiff, Alvin: Atmosphere Entry Problems of Manned Interplanetary Flight. Proc. AIAA and NASA Conf. on Eng. Problems of Manned Interplanetary Exploration, Palo Alto (Calif.), Sept. 30-Oct. 1, 1963, AIAA, pp. 19-33.

17. Luidens, Roger W.: Approximate Analysis of G Loads and Heating During Atmospheric Entries and Passes with Constant Aerodynamic Coefficients. NASA TN D-1280, 1962.

18. Luidens, Roger W.: Approximate Analysis of Atmospheric Entry Corridors and Angles. NASA TN D-590, 1961.

19. Friedlander, Alan L.; and Harry, David P., III: A Study of Statistical Data-Adjustment and Logic Techniques as Applied to the Interplanetary Midcourse Guidance Problem. NASA TR R-113, 1961.

20. Harry, David P., III; and Friedlander, Alan L.: An Analysis of Errors and Requirements of an Optical Guidance Technique for Approaches to Atmospheric Entry with Interplanetary Vehicles. NASA TR R-102, 1961.

21. Luidens, Roger W.: Flight-Path Characteristics for Decelerating from Supercircular Speed. NASA TN D-1091, 1961.

22. Popma, Dan C.: Life Support for Space Stations. Astronautics, vol. 7, no. 9, Sept. 1962, pp. 44-47.

23. Bernatowicz, D. T.; Guentert, D. C.; and Klann, J. L.: Space Powerplant Needs and Selection. Astronaut. and Aerospace Eng., vol. 1, no. 4, May 1963, pp. 22-26.

24. Davison, Elmer H.; and Winslow, Paul C., Jr.: Space Debris Hazard Evaluation. NASA TN D-1105, 1961.

25. Davison, Elmer H.; and Winslow, Paul C., Jr.: Direct Evaluation of Meteoroid Hazard. Aerospace Eng., vol. 21, no. 2, Feb. 1962, pp. 24-33.

26. Smolak, George R.; Knoll, Richard H.; and Wallner, Lewis E.: Analysis of Thermal-Protection Systems for Space-Vehicle Cryogenic-Propellant Tanks. NASA TR R-130, 1962.

27. Chovit, A. R.; Kylstra, C. D.; and Plebuch, R. K.: Performance Characteristics and Mission Capabilities of the Second Generation Nuclear Rocket Engine. Paper Presented at AAS Post-Apollo Space Exploration Meeting, Chicago (Ill.), May 4-6, 1965.

28. Smith, D. S.; and Mann, D. J.: OF_2 Looks Promising as Space-Storable Propellant. Space/Aeron., vol. 39, no. 1, Jan. 1963, pp. 103-108.

29. Knip, Gerald, Jr., and Zola, Charles L.: Three-Dimensional Sphere-of-Influence Analysis of Interplanetary Trajectories to Mars. NASA TN D-1199, 1962.

30. Moeckel, W. E.: Trajectories with Constant Tangential Thrust in Central Gravitational Fields. NASA TR R-53, 1959.

31. Strack, William C.; Dobson, Wilbur F.; and Huff, Vearl N.: The N-Body Code - A General Fortran Code for Solution of Problems in Space Mechanics by Numerical Methods. NASA TN D-1455, 1963.

32. McDonald, Frank B., ed. (contributions by C. E. Fichtel, D. E. Guss, H. H. Malitson, K. G. McCracken, K. W. Ogilvie, and W. R. Webber): Solar Proton Manual. NASA TR R-169, 1963.

33. Glasstone, Samuel, ed.: The Effects of Nuclear Weapons. (Pamphlet 39-3, Department of the Army, May 1957), Atomic Energy Commission, June 1957.

34. Schaefer, Hermann J.: Radiation Tolerance Criteria in Space Operations. ARS J., vol. 32, no. 5, May 1962, pp. 771-773.

35. Luidens, Roger W.; and Kappraff, Jay M.: Mars Nonstop Round-Trip Trajectories. NASA TN D-2605, 1965.

36. Koehler, Leighton F.: On the Orbital Perturbations of Martian Satellites. Rept. No. LMSD-703029, Lockheed Aircraft Corp., July 1960.

37. Demetriades, S. T.: Preliminary Study of Propulsive Fluid Accumulator Systems. J. British Interplanetary Soc., vol. 18, no. 10, July-Aug., 1962, pp. 392-402.

38. Willis, Edward A., Jr.: New Class of Optimal Interplanetary Trajectories with Specified Trip Time. AIAA J., no. 65-66, Jan. 1965 (NASA TM X-52072, 1965).

39. Finger, Harold B.: Nuclear Rocketry - Confidence Substantiated. Astronaut. Aeron., vol. 3, no. 6, June 1965, pp. 34-35.

40. Beck, Andrew J.; and Divita, Edward L.: Evaluation of Space Radiation Doses Received Within a Typical Spacecraft. ARS J., vol. 32, no. 11, Nov. 1962, pp. 1668-1676.

41. Foelsche, Trutz: Current Estimates of Radiation Doses in Space. NASA TN D-1267, 1962.

42. Hofman, David J.; and Winckler, John R.: Simultaneous Balloon Observations at Fort Churchill and Minneapolis During the Solar Cosmic Ray Events of July 1961. J. Geophys. Res., vol. 68, no. 8, Apr. 15, 1963, pp. 2067-2098.

43. Schofield, W. M.; Smith, E. C.; and Hill, C. W.: Shielding Problems in Manned Space Vehicles. Rep. ER-5997, Lockheed Nuclear Products, Lockheed-Georgia Co., Dec. 1962.

44. Leong, G. F.; Wisecup, W. G.; and Grisham, J. W.: Effects of Divided Doses of X-Ray on Mortality and Hematology of Small and Large Domestic Animals. Ann. N. Y. Acad. Sci., vol. 114, art. 1, Mar. 1964, pp. 138-149.